**Sudan University of Sciences and Technolog (SUST)**

**College of Graguate Studies**

**College of Computer Sciences and Information Technology**

# Flood Water Analysis Using LiDAR DEMs
## Study Area (Sudan - Khartoum- Azozab)

**تحليل الفيضان بإستخدام نموذج الإرتفاعات الرقمي المنتج عن طريق كشف الضوء والمدى**

**منطقة الدراسه (السودان – الخرطوم – العزوزاب)**

**Dissertation Submitted in Partial Fulfilment of the requirements for the degree of Doctor of Philosophy in Computer Sciences and Information Technology**

**By: Fatma Ibrahim Abdelmoutalib Siddiq**

**Supervised by: Prof. Dieter Fritsch**

**September 2022**

## Dedication

This research is dedicated to the soul of my brother/ Sami Ibrahim, my husband, my father, mother and sisters who have steadily encouraged and inspired me to go on conducting this research.

Moreover, I dedicate this research to Dr. Eng. / Yahya Hassan Altayeb for his sincere academic advice and guidance without which it would be difficult to complete this research.

**Acknowledgements**

First of all I would like to thank God for facilitating conducting this reseach and enabling me to overcome many difficulties which I have faced. I will keep on trusting God for the rest of my life.

I would like to acknowledge and express my warmst thanks my supervisor (Prof. Dieter ) who made this work possible. His guidance and advice have led me through all the stages of conducting the research.

My sincere gratefulness goes to Dr. Eng. Yahya Hassan for supporting me during all the stages of performing the research.

I would also like to thanks the college of Computer Sciences and information technology at Sudan University of Sciences and Technology.

I would also like to give special thanks to my husband and my family for their continuous support and understanding for the entire period while I have been conducting the research .

Moreover, I would like to thank the staff of surveying depart of Jabbal Awliya locality.

## Abstract

Flood is the deadliest type of severe weather. A flood is an overflow of water that submerges land that is usually dry. Floods can also come on quickly or build gradually. It is a well-known fact that the use of Geographic Information Systems (GIS) and Remote Sensing in Water Management is very helpful**.** This research was conducted in "Azozab", Khartoum statement, Sudan. Azozab is used to be exposed to severe floods frequently and the last incident of flood was in August 2020. The materials used for this research were Light Detection And Ranging (LiDAR DEM 1, 2020), aerial photograph 2018 with spatial resolution 0.3 m, a polylines shapefile containing flood extent lines in 1946, 1988, an existing protection bank, and field-collected GPS point coordinates. These materials were processed using ArcGIS 10.2 and Archydro to produce a 3-meters vertical interval contour map, 3D coordinates (X, Y, Z) of each of the flood extent lines 1946, 1988, and the existing protection bank, and the drainage system of the study area. The point coordinates of the mentioned lines were plotted as graphs. It was found that the flood line 1946 is 4.59 km long, flood line 1988 is 4.57 km long, and the protection bank is 3.5 km long, therefore, the protection bank should be extended so that its length becomes equal to the length of 1946 flood line, i.e. to be extended by 1.09 Km. Furthremore, the elevations of the protection bank were found lower than the elevations of the higher flood line (1946 ) for a distance of 3.060 km. This distance represents the length of the protection bank that requires increasing its elevations (i.e. the construction of a higher embankment). It was found that the average height increment of the protection bank embankment wall equals 1.37 m approximately. It was found that (11) services such as mosques, education, health and other services are located inside the flood extent line of 1946, thus they were affected by flood. Also, (8) educational services were threatened by flood, because they are located in the vicinity of (i.e. located within 200 meters away from) the 1946 flood extent line.

**المستخلص**

الفيضانات هي أخطر أنواع الطقس القاسي. الفيضان هو تدفق المياه الذي يغمر الأرض التي عادةً ما تكون جافةً. يُمكن أن تحدث الفيضانات أيضًا بسرعةٍ أو تتراكم تدريجياً. من الحقائق المعروفة أن استخدام نظم المعلومات الجغرافية (GIS) والإستشعار من بعدٍ في إدارة المياه مفيد للغاية. تم إجراء هذا البحث بمنطقة العزوزاب، ولاية الخرطوم، السودان، ظلت العزوزاب تتعرّض لفيضاناتٍ شديدة بشكلٍ متكررٍ وكانت آخر حادثة فيضان في أغسطس ٢٠٢١م. المواد المستخدمة في هذا البحث هي نموذج الإرتفاعات الرقمي المنتج عن طريق كشف الضوء والمدى(LiDARDEM1)، الصورة الجوية ٢٠١٨م ذات الدقة المكانية ٠,٣ م، ملف شكل متعدد الخطوط يحتوي على خطوط مدى الفيضان ١٩٤٦م، ١٩٨٨م، ترس الحماية الموجودة أصلاً، وإحداثيات نقاط تم الحصول عليها من الموقع بواسطة جهاز قراءة الإحدثيات الجغرافية GPS. تمت معالجة هذه المواد باستخدام ArcGIS 10.2 و Archydro لإنتاج خريطة كنتور بفاصلٍ رأسيٍ ٣ أمتار وإحداثيات ثلاثية الأبعاد (X, Y, Z) لكلٍ من خطوط الفيضان ١٩٤٦م، ١٩٨٨م، و ترس الحماية الموجودة أصلاً، ونظام تصريف المياه في منطقة الدراسة. تم رسم إحداثيات نقاط الخطوط المذكورة في شكل رسومٍ بيانيةٍ. وُجد أنّ طول خط الفيضان ١٩٤٦م يبلغ ٤,٥٩ كم وطول خط الفيضان ١٩٨٨م يبلغ ٤,٥٧ كم ويبلغ طول ترس الحماية ٣,٥ كم، لذا يجب تمديد ترس الحماية أفقياً لكي يساوي طولُه طول خط الفيضان في عام ١٩٤٦م أي يجب تمديده بمقدار ١,٠٩ كلم. علاوةً على ذلك، فقد وُجدت إرتفاعات ردمية الحماية أقل من إرتفاعات خط الفيضان الأعلى (١٩٤٦م) لمسافةٍ أفقيةٍ تُساوي ٣,٠٦٠ كم. هذه المسافة تمثل طول خط الحماية الذي يتطلب زيادة إرتفاعاته (بناء ترسٍ أعلى). وجد أنّ عدد وحدات الخدمة التي تقع بداخل خط إمتداد فيضانن ١٩٤٦م يساوي (١١) تتضمّن مساجد، مؤسسات تعليمية وصحية وخدمات أخرى. أيضاً هناك عدد (٨) مؤسسات تعليمية مهددة بالفيضان لأنها تقع بالقرب (أي على بعد ٢٠٠ متر) من خط إمتداد فيضان ١٩٤٦م.

.

## List of acronyms

| Acronym | Stands for |
|---|---|
| (ALOS) “DAICHI” | Advanced Land Observing Satellite “DAICHI” (ALOS) |
| ASTER | Advanced Space borne Thermal Emission and Reflection Radiometer |
| CSR | Completely Spatially Random |
| DEM | Digital Elevation Model |
| DLR | German Aerospace Agency |
| DSM | Digital Surface Model |
| DTM | Digital Terrain Model |
| EGM96 | Earth Gravitational Model 96 |
| FEMA | Federal Emergency Management Agency |
| FIRM | Flood Insurance Rate Maps |
| GCPs | Ground Control Points |
| GE | Google Earth |
| GECO | Global Energy and Climate Outlook |
| GECO | Geothermal Emission Control |
| GGM | Global Geopotential Model |
| GSD | Ground Sampling Distance |
| HEC-RAS | Hydrologic Engineering Center's River Analysis System |
| ISO | International Standards Organization |
| JAXA’s | Japan Aerospace Exploration Agency’s |
| KUSD | Kilo United States Dollars |
| LGN | Surveying Authority of Lower Saxony, Germany |
| LiDAR | Light Detection And Ranging |
| NASA | National Aeronautics and Space Administration |
| NGA | National Geospatial-Intelligence Agency |
| NHD | National Hydrography Dataset |
| OKXE | Organization for Cadastre and Mapping of Greece |
| PAUs | Public of Administration Units |

| **Acronym** | **Stands for** |
|---|---|
| PRISM | Panchromatic Remote-Sensing Instrument for Stereo Mapping (radiometer) |
| RSLUA | Laboratory of Remote Sensing and GIS at the University of the Aegean |
| SEAM project | Social, Education of Adults through Mobility project. |
| SIR-C | Space borne Imaging Radar |
| SRCS | Sudanese Red Crescent Society |
| SRTM | Shuttle Radar Topography Mission |
| UAV | Unmanned Aerial Vehicle |
| USGS | United States Geological Survey |
| VGS | Virtual Global Systems |
| X-SAR | X-band Synthetic Aperture Radar |

**Table of contents**

## List of tables

## List of Figures

# Chapter One

# Introduction

## 1-Introduction:

### 1-1- Overview:

Believe it or not, flooding is the deadliest type of severe weather. There's probably a lot about floods and flooding you don't know, such as what causes flooding?" and "Where does flooding occur?. A **flood** is an overflow of water that submerges land that is usually dry. Floods are an area of study in the discipline of hydrology. They are the most common and widespread natural severe weather events. Floods can look very different because the word "flooding" covers anything from a few inches of water to several feet. They can also come on quickly or build gradually. To better answer the question of "What is a flood?". The National Severe Storms Laboratory, categorized floods into five types, which include:

1. River Flood
2. Coastal Flood
3. Storm Surge
4. Inland Flooding
5. Flash Flood

As can be inferred from the list above, flooding can happen anywhere, including both coastal and inland locations. Details of these types of floods are given in chapter 2 of this thesis "Literature Review".

There are plenty of different causes of flooding. While different flood types typically have different causes, most floods are caused by one of the following activities:

1. Heavy rainfall is the simplest cause of flooding. When there is too much rain or it happens too fast, there just isn't a place for it to go. This can result in floods like flash flooding.
2. Overflowing rivers are another cause of floods. You don't necessarily need heavy rains though to experience river flooding. As mentioned before, river flooding can happen when there is debris in the river or dams that block the flow of the water.

3. Regarding dams, collapse dams are another cause of flooding. Older infrastructure can fail when heavy rains come and water levels rise. When dams break, they release flows of water on houses while their inhabitants do not take the necessary precautions. This is part of what happened when Hurricane Katrina hit New Orleans in 2005.
4. Storm surge and tsunamis also cause flooding. Storm surges from hurricanes and other tropical systems can cause sea levels to rise and cover normally dry coastal areas in several feet of water. Tsunamis on the other hand are giant waves caused by earthquakes or underwater volcanic eruptions. As these waves move inland, they build height and can push a lot of water inland in coastal areas.
5. Channels with steep banks are also to be blamed for flooding. Flooding often occurs when there is fast runoff into lakes, rivers, and other basins. This is often the case with rivers and other channels that feature steep sides.
6. A lack of vegetation can cause flooding. Vegetation can help slow runoff and prevent flooding. When there is a lack of vegetation, there is little to stop water from running off and overflowing river banks and streams.
7. Melting snow and ice is another common reason for flooding. When a large amount of snow and/or ice melts quickly, it often doesn't have somewhere to go except low-lying areas.

No matter what causes of a flood are, it can have devastating effects on communities. There are actually many dangerous flooding effects. Besides physical danger, floods also cause economic and social problems.

The severest effect of flooding is death. In fact, flooding is the number one severe weather killer. Floods have claimed thousands of lives throughout history. But how does flooding kill?

Floods kill by carrying people away in fast-moving water or drowning them. It only takes six inches of water to wash a person away. Floods can also kill people by destroying buildings and creating unsafe environments. One often-overlooked deadly effect of flooding comes from waterborne illnesses.

From 2010 to 2018, the National Weather Service recorded hundreds of flooding deaths across the United States. Texas witnessed most of those deaths, with the 8-year total sitting at 212 fatalities, figure (1-1).

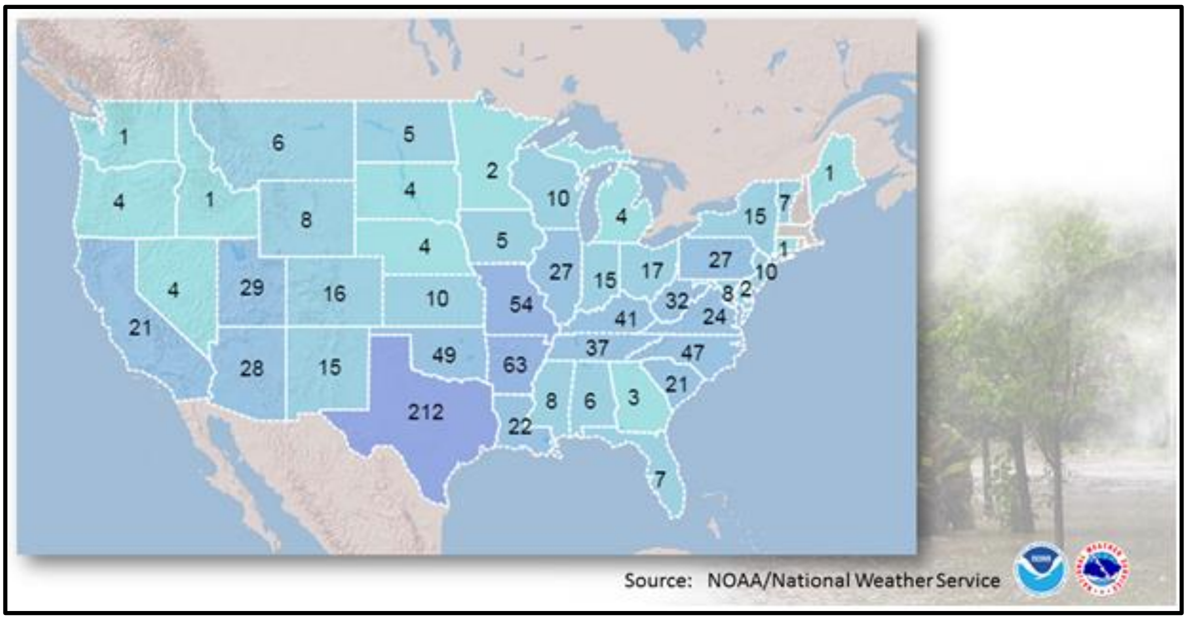


**Figure (1-1): 2010 – 2018 U.S. Flood Fatalities**

Since it only takes two feet of flood water to wash a car away, flooding can also cause great loss of property. Surely you've seen images of cars floating away in flood waters. This is why it is so important to avoid flooded areas when driving. You don't want to be in your car when it gets washed away in the flood!, fig. (1-2).

**Figure (1-2): Loss of Properties**

Flooding also causes property damage to buildings by blowing out windows, sweeping away doors, corroding walls and foundations, and sending debris into infrastructure at a fast pace. Not to mention the furniture and items inside a house or business those are damaged when flood water makes its way inside, figure (1-3).

**Figure (1-3): Collapse of buildings made of strong building materials**

The economic impact of flooding can be devastating to a community. This comes from damage and disruption to things like communication towers, power plants, roads, bridges, and vegetation. This brings business activities in an area to a standstill. Oftentimes, major flooding results in dislocation and dysfunction of normal life long after flood waters recede, figure (1-4).

**Figure (1-4): Palm trees destruction**

Flooding hinders economic growth and development because of the high cost of relief and recovery associated with floods. In frequently flooded areas, there is less likely to be any investment in infrastructure and other developed activities.

Flooding can also create lasting trauma for victims. The loss of loved ones or homes can take a steep emotional toll, especially on children. Displacement from one's home and loss of livelihood can cause continuing stress and produce lasting psychological impacts.

In Sudan, on August, 20, 2020 Gr., the state wise total of affected population was mapped in figure (1-5). The highest number of affected population was recorded in Gezira state which was 27,780 persons, followed by Kassala which was 27,225 persons.

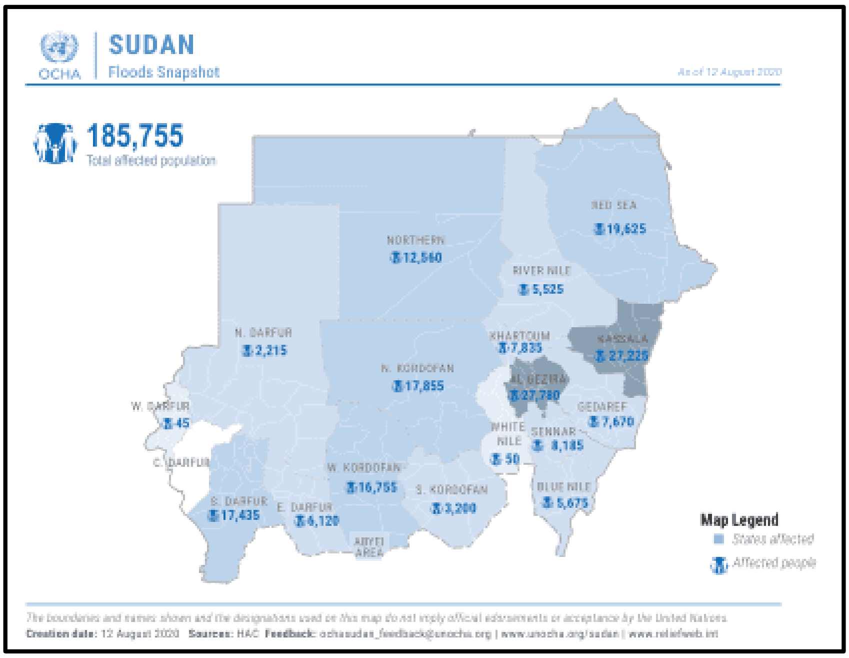


**Figure (1-5): Affected population in 2020 state wise**

## 1-2- Research Problem Statement:

The White Nile disastrous floods occur frequently in the study area (Azozab) in autumn leading to many devastating and serious effects on the community, such as loss of lives, property damage, economic effects, psychosocial effects, .. etc.

## 1-3- Research Question:

The main question that will be addressed in this research is: how GIS techniques and remotely sensed data can be used to design a protection bank to mitigate or prevent the flood water impact in Azozab area?

## 1-4- Research Objectives:

The objectives of this research include:

### 1-4-1- General Objective:

To study the floods in the study area (Azozab) utilizing the space technologies (remotely sensed data such as SRTM DEM30 and LiDAR DEM1) and geographical information systems' capabilities for mapping and analyzing flood extent.

### 1-4-2- Specific Objectives:

1. To produce topographic, surface water drainage systems and public administrative units (PAUs) maps …. etc. to obtain a clear picture of the flood extent in the study area, so that the right decision for avoiding or minimizing the adverse flood impacts can be taken.
2. To propose a method for enhancing the effectiveness and functionality of the existing flood protection bank in the study area.

## 1-5- The thesis structure:

This thesis is structured in five chapters: Chapter (1) which contains the introduction i.e. overview of the study, research problem, research question, which is research objectives, and the structure of the thesis. Chapter (2) the literature review, which covers the theoretical background of the research and relevant studies. Chapter (3) i.e. "materials and methods" which describes the materials used and the method adopted for performing the research. Chapter (4) i.e. "the results and discussions". Chapter (5) i.e. "conclusion and recommendations" Followed by the list of references and appendices.

# Chapter Two

# Literature Review

## 2- Literature review

### 2-1- Theoretical background

#### 2-1-1- Data types:

##### 2-1-1-1- Space Shuttle Radar Topography Mission (SRTM)

The Shuttle Radar Topography Mission (SRTM) is a partnership between NASA and the National Geospatial-Intelligence Agency (NGA) of USA, flown aboard the NASA Space Shuttle Endeavour (11-22 February 2000). SRTM fulfilled its mission to map the world in three dimensions. The USGS is under agreement with NGA and NASA's Jet Propulsion Laboratory to distribute the data. SRTM utilized dual Space borne Imaging Radar (SIR-C) and dual X-band Synthetic Aperture Radar (X-SAR) configured as a baseline interferometer to successfully collect data over 80 per cent of the Earth's land surface, everything between 60 degrees North and 56 degrees South latitudes.

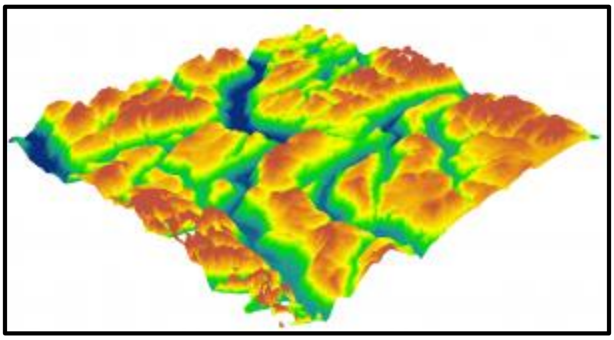

**Figure (2-1): Sample of the SRTM DEM**

(GIS Geography, 2021) In late 2014, the United States government released the highest resolution SRTM DEM to the public. This 1-arc second global digital elevation model has a spatial resolution of about 30 meters. Also, it covers most of the world with an absolute vertical height accuracy of less than 16m.

### 2-1-1-2- ASTER Global Digital Elevation Model

**Figure (2-2): ASTR DEM**

NASA and Japan's joint operation was the birth of Advanced Space borne Thermal Emission and Reflection Radiometer (ASTER). As part of this project emerged the ASTER Global Digital Elevation Model (GDEM).

ASTER GDEM produced a global resolution of 90 meters with a resolution of 30 meters in the United States. Despite its high-resolution and greater coverage (80% of the Earth), dissatisfied users expressed issues with its artifacts often in cloudy areas.

(Great Soviet Encyclopedia, 1979) ASTER GDEM used stereoscopic pairs and digital image correlation methods. Based on two images at different angles, it used stereo pairs and photogrammetry to measure elevation. However, the amount of cloud cover affected the accuracy of ASTER which wasn't the case for SRTM DEM. Because of how passive and active sensors work, this had the most significant effect on quality of DEM.

But over time, ASTER DEM data has improved its products with artifact corrections of their own. In October 2011, ASTER GDEM version 2 was publicly released, which was a considerable improvement.

Despite its experimental grade, ASTER GDEM-2 is considered a more accurate representation than the SRTM elevation model in rugged mountainous terrain.

Figure (2-3) shows how a stereoscopic model is constructed from two overlapping ASTER photographs.

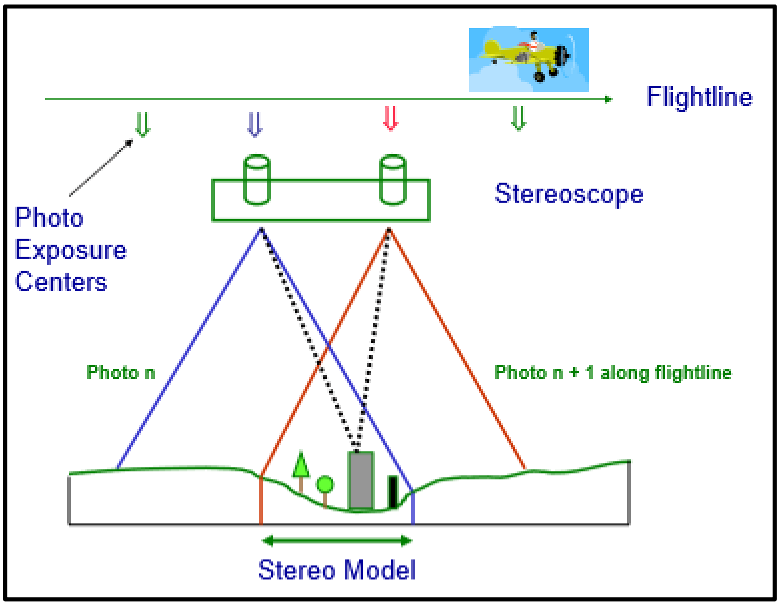


**Figure (2-3): Formation of Stereoscopic Model**

### 2-1-1-3- JAXA's Global ALOS 3D World

(GIS Geography, 2021) ALOS World 3D is a 30-meter resolution digital surface model (DSM) captured by the Japan Aerospace Exploration Agency's (JAXA). Recently, this DSM has been made available to the public.

The neat thing about it is that it is the most precise global-scale elevation data now. It uses the Advanced Land Observing Satellite "DAICHI" (ALOS) based on stereo mapping from PRISM, figure (2-4).

**Figure (2-4): JAXA's DEM**

### 2-1-1-4- Light Detection and Ranging (LiDAR)

(GIS Geography, 2021) You might think that finding LiDAR is a shot in the dark. But it's not anymore. Slowly and steadily, we are moving towards a global LiDAR map. With Open Topography topping the list at #1, a list of some of the 6 best

LiDAR data sources have been put together available online for free . These are: 1) Open Topography, 2) USGS Earth Explorer, 3) United States Inter-agency Elevation Inventory, 4) NOAA Digital Coast, 5) National Ecological Observatory Network (NEON), 6) LiDAR Data Online.

Because nothing is better than LiDAR, regarding the spatial accuracy - after the ground returns are filtered - an impressive DEM can be built from LiDAR, figure (2-5).

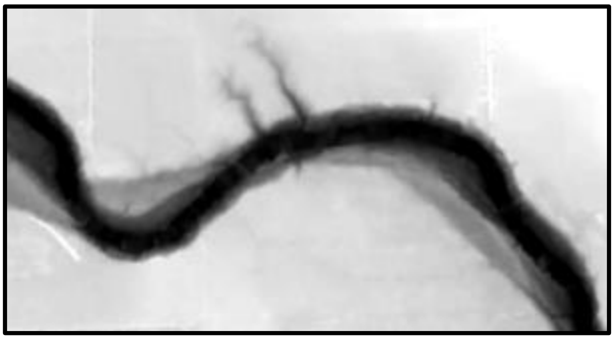

**Figure (2-5): Light Detection and Ranging (LiDAR)**

LiDAR data is usually collected with or without reference to ground control points using GPS/INS methods, which is called Integrated Sensor Orientation (ISO). This information delivers geo-centric locations and orientations of the LiDAR instrumentation as well as a geo- centric point cloud. Subsequently, the output coordinates are quite often ellipsoidal and can be transformed into any regional coordinate system, by coordinate transforms. A typical output of LiDAR is given in Figures (2-6) a and (2-6) b.

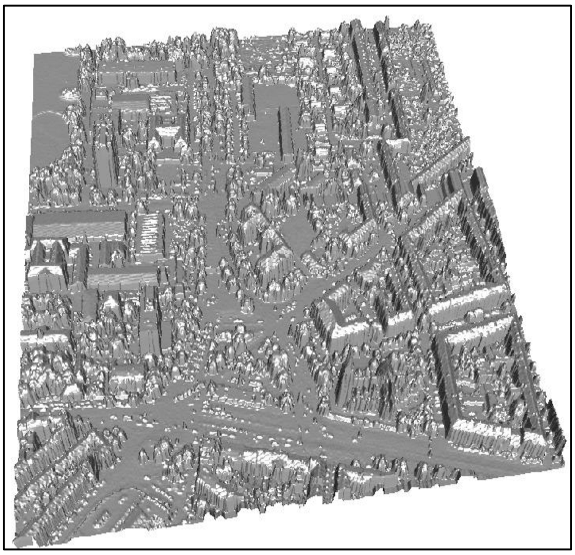

**Figure (2-6) a:** LiDAR DSM in an urban area – left: intensity image, right: DSM

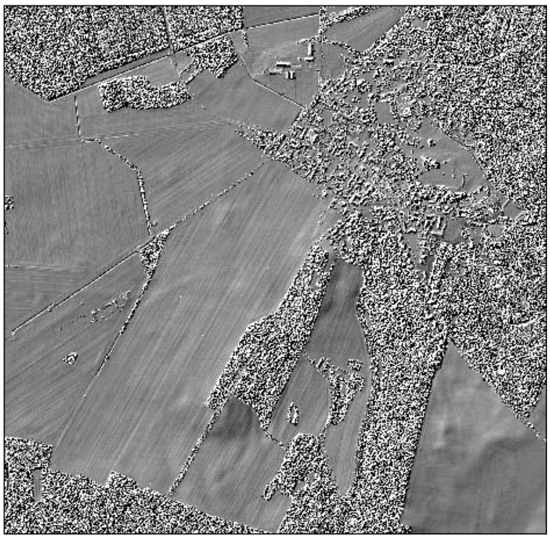

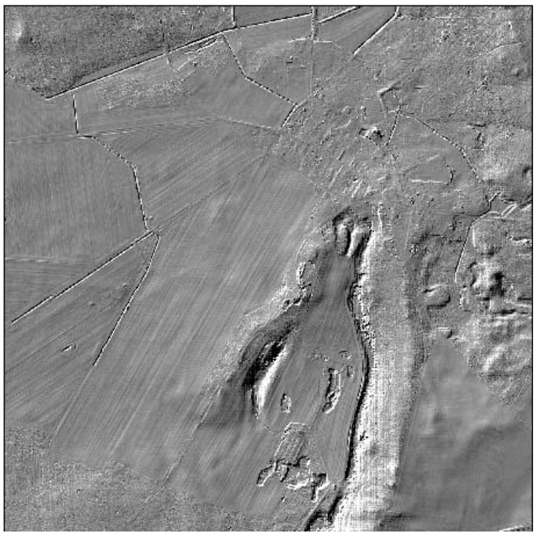

**Figure (2-6) b:** LiDAR SM in a rural area – left: with vegetation, right: without vegetation

In Europe, LiDAR is often used for flood water management systems, to allow for in situ flood water data collections, to monitor dyke infrastructures along coastlines, and to collect vegetation data to control the water flow, to name only few. The most recent developments in LiDAR technologies collect the full waveform of the echo, thus it is even easier to filter out the vegetation from the DSM to derive a final DTM. So far, we can conclude that a LiDAR DSM and/or DTM serve as a reference for any other data collection method to provide similar products. The point density of the LiDAR point cloud depends on some parameters to be chosen before data collection: flying height, flying speed, and the instrumentation parameters such as its architecture (rotating mirror, rotating prism, push broom, mutating mirror etc.). As an example: A LiDAR can deliver up to 40 points per sqm. from a flying height of about 500m, with a height accuracy of 0.1m.

**Table (2-1):** An overview of three LiDAR systems

| System | OPTECH ALTM 3100EA | RIEGL LMS-Q560 | TopoSys Falcon II |
|---|---|---|---|
| **Laser** | 1064nm | near IR | 1540 nm |
| **Flying height** | 80 – 3500m | 30 – 1500m | 60 – 1600 m |
| **Measurements** | Up to 4 pulses | full waveform | First and last return |
| **Scan frequency** | max. 70Hz | max. 160Hz | max. 630 Hz |
| **Scan angle** | max. 25° | max. 30° | 17° (fest) |
| **Pulse rate** | max. 100kHz | max. 100kHz<br>50 kHz @ 22,5° | 83 kHz |
| **Divergence** | 0.3mrad | 0.5mrad | 0.5 m rad |
| **Scan pattern** | Swinging mirror, saw tooth | Rotating prism, parallel pattern | Push broom, Parallel |

Today, there are 4-5 worldwide providers of LiDAR instrumentation, like Optech, Canada, Trimble, USA, Hexagon, Hong Kong and Switzerland, and Riegl, Austria. A typical system with ISO, costs around 500-1,000 KUSD, is therefore expensive.

### 2-1-1-5- Interferometric SAR

Airbus Defense and Spaces launched a 1.2 ton radar satellite TerraSAR-X on 15 June 2007 and provided Earth observation data of unprecedented quality, with a resolution of up to 1m in height, for scientific and increasingly diversified commercial applications.

TerraSAR-X will provide new features, which improve the Earth observation potential. Beside the typical advantages of SAR systems like all-weather as well as day and night observation capability, special mission services support the monitoring and mapping also of urban areas. This includes short revisit times, the ±250 m orbital tube and an operation of ortho- rectification service. High resolution data will enable very detailed studies, the consideration of texture measures and will open new perspectives also to SAR interferometry. Polarimetric data can be used to distinguish between different back scatter mechanisms on ground.

TerraSAR-X carries a high frequency X-band Synthetic Aperture Radar (SAR) sensor that can be operated in different modes and polarization. The Spotlight- Stripmap- and ScanSAR-modes provide high resolution SAR images for detailed analysis as well as wide swath data, whenever a larger coverage is required. Imaging will be possible in single, dual and quad-polarization. TerraSAR-X is an operational SAR system for scientific and commercial applications (Fritsch, D., Rothermel, M.,Oblique, 2016). The resulting DTM is provided by the German Aerospace Agency (DLR) Oberpfaffenhofen, Germany, with an x/y resolution of 30m and height accuracies of close to 1m. For some applications DLR can provide DTMs with 10m GSD. Figure (2-7).

Figure (2-7): SAR image of TerraSAR-X (Northern Germany, Copyright DLR)

### 2-1-2- Spatial Analysis:

Spatial analysis can be defined as the analytical techniques associated with the study of geographic phenomena locations together with their spatial dimensions and their associated attributes (ESRI, 2001).

*(Yamada, 2009*) Spatial analysis inevitably concerns itself with a finite region, a small bounded segment of an infinite space. Because of this finiteness of a study region, a boundary always exists, while any spatial phenomenon such as spatial distribution, association, interaction, and diffusion observed within the study region is most likely to extend beyond its boundary. In addition, the majority of spatial statistical theories have been developed on the basis of the infinite space assumption. Therefore, analysis confined within a bounded study region may well be biased because of the ignorance of the outside of the study region as well as the inappropriateness of the theories. This problem of potential bias in spatial analysis is referred to as edge effects (or boundary effects). Edge effects are important for any type of spatial analysis, including analysis of point and areal data, because methods for spatial analysis always require that spatial relationships between observations be defined based on their proximity, adjacency, or other criteria, which may be biased due to unrecorded observations located outside the study region.

For point pattern analysis, there are a variety of analytical methods that are based on inter-point distances. When points distributed outside the study region are ignored, the nearest-neighbor distance for a particular point observed within the study region may be overestimated, which will in turn distort test statistics. For instance, by applying such methods to a completely spatially random (*CSR*) pattern without realizing edge effects, one might falsely conclude that it was a regular pattern because of the longer inter-point distances than expected for CSR.

Methods for areal data analysis often take into account neighbors of individual areal units because, for example, a crime rate observed in a particular area in a city tends to be influenced not only by characteristics of the area itself but also by those of its neighborhood. Because areal units lying along the boundary of a study region generally have their neighbors outside the study region too, such areal data analysis methods will also be affected by edge effects. If those external influences are simply ignored, results of spatial analysis will be less reliable for areal units close to the study-region boundary than for those well inside. The problem of edge effects is often called the boundary value problem in areal data analysis.

(C.R. Paramasivam, S. Venkatramanan, 2019) Spatial analysis can be done using various techniques with the aid of statistics and geographical information systems (GIS). A GIS facilitates attribute interaction with geographical data in order to enhance interpretation accuracy and prediction of spatial analysis (Gupta, 2005). The spatial analysis that is involved in GIS can build geographical data and the resulting information will be more informative than unorganized collected data. According to the requirement of the end user, a suitable geospatial technique is chosen to be implemented with GIS. This selection of the geospatial technique will define the classification and method of analysis to be used (Burrough, 2001).

The word "analysis" used alone refers to data querying and data manipulation. Whereas spatial analysis refers to statistical analysis based on patterns and underlying processes. It is a kind of geographical analysis that elucidates patterns of personal characteristics and spatial appearance in terms of geostatistics and geometrics, which are known as location analysis. It involves statistical and manipulation techniques, which could be attributed to a specific geographic database (Cucala et al., 2018; Burrough, 2001).

Suppose the assigned GIS task is to record sampling stations chosen in a selected study site with different patterns, then by implementing spatial techniques appropriate results can be obtained (Burrough, 2001). These results further show the sample location's characteristics, such as dispersed or clustered. Spatial information relates to the position, area, shape, and size of objects on Earth and this information is stored as coordinates and topology (Cucala *et al.*, 2018; Fischer *et al.*, 1997; Gupta, 2005).

(C.R. Paramasivam, S. Venkatramanan, 2019) The sampling stations were observed for only the area of interest in the entire domain. This area is derived applying quantitative and statistical techniques on the spatial attributes of GIS database (Figure 2-8).

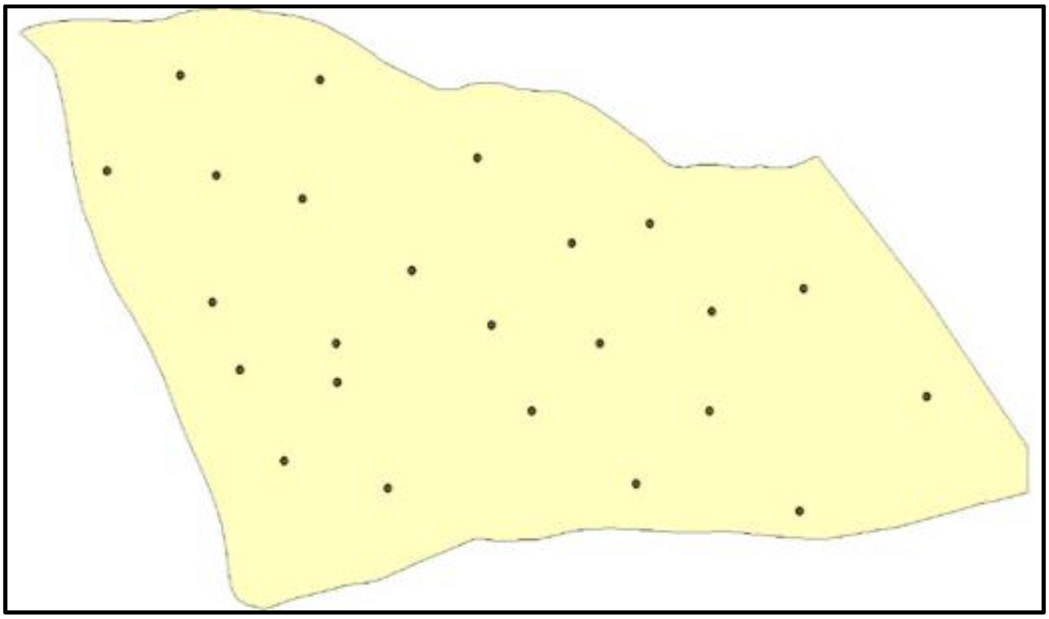

**Figure (2-8): Sampling locations distribution map**

**2-1-3- Interpolation methods:**

Geostatistics is a collection of methods that allow you to estimate values for locations where no samples have been taken and also to assess the uncertainty of these estimates. These functions are critical in many decision-making processes, as it is impossible in practice to take samples at every location in an area of interest.

It is important to remember, however, that these methods are a means that allows the construction of models of reality (that is, of the phenomenon of interest). It is up to the practitioner to build models that suit his specific needs and provide the information necessary to make informed and defensible decisions. A major part of building a good model is the understanding of the phenomenon, how the sample data was obtained and what it represents, and what is expected to be provided by the model. General steps in the process of building a model are described in 2-1-3-1" "The geostatistical workflow" and shown in figure (2-9).

Many interpolation methods exist. Some are quite flexible and can accommodate different aspects of the sample data. Others are more restrictive and require that the data meet specific conditions. Kriging methods, for example, are quite flexible, but within the kriging family there are varying degrees of conditions that must be met for the output to be valid. The geostatistical Analyst tool offers the following interpolation methods:

1. Global polynomial
2. Local polynomial
3. Inverse distance weighted
4. Radial basis functions
5. Diffusion kernel
6. Kernel smoothing
7. Ordinary kriging
8. Simple kriging
9. Universal kriging
10. Indicator kriging
11. Probability kriging
12. Disjunctive kriging
13. Gaussian geostatistical simulation
14. Areal interpolation
15. Empirical Bayesian kriging

Each of these methods has its own set of parameters, allowing it to be customized for a particular dataset and requirements on the output that it generates. To provide some guidance in selecting which to use, the methods have been classified according to several different criteria. After clearly defining the goal of developing an interpolation model and fully examining the sample data, the practitioner may be able to select an appropriate method.

**2-1-3-1- The geostatistical workflow:**

A generalized workflow for geostatistical studies is presented, and the main steps are explained. Geostatistics is a class of statistics used to analyze and predict the values associated with spatial or spatiotemporal phenomena. ArcGIS Geostatistical Analyst provides a set of tools that allow models that use spatial (and temporal) coordinates to be constructed. These models can be applied to a wide variety of scenarios and are typically used to generate predictions for unsampled locations, as well as measures of uncertainty for those predictions.

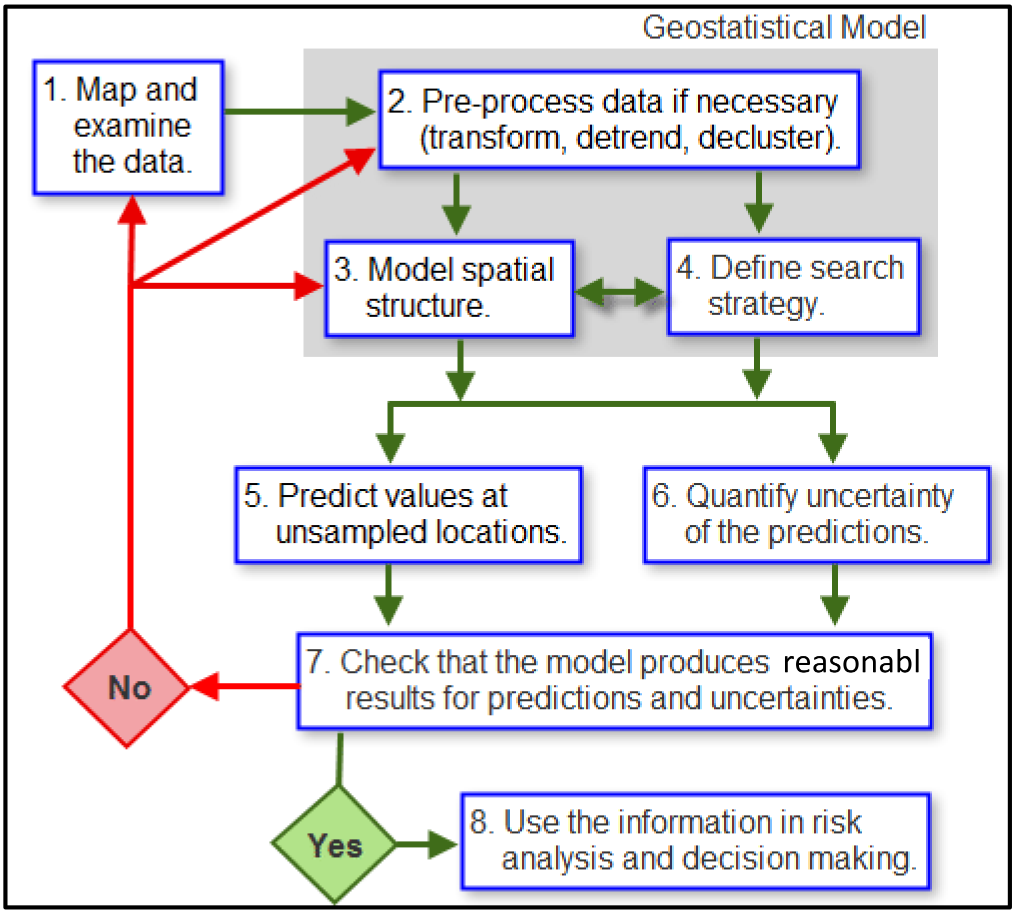


**Figure (2-9): The geostatistical workflow**

The first step, as in almost any data-driven study, is to closely examine the data. This typically starts by mapping the dataset, using a classification and color scheme that allow clear visualization of important characteristics that the dataset might present, for example, a strong increase in values from north to south (Trend); a mix of high and low values in no particular arrangement (possibly a sign that the data was taken at a scale that does not show spatial correlation); or zones that are more densely sampled (preferential sampling) and may lead to the decision to use declustering weights in the analysis of the data.

The second stage is to build the geostatistical model. This process can require several steps, depending on the objectives of the study (that is, the type(s) of information the model is supposed to provide) and the features of the dataset that have been deemed important enough to incorporate. At this stage, information collected during a rigorous exploration of the dataset and prior knowledge of the phenomenon determine how complex the model is and how good the interpolated values and measures of uncertainty will be. In figure (2-9), building the model can involve preprocessing the data to remove spatial trends, which are modeled separately and added back in the final step of the interpolation process; transforming the data so that it follows a Gaussian distribution more closely (required by some methods and model outputs); and declustering the dataset to compensate for preferential sampling. While a lot of information can be derived by examining the dataset, it is important to incorporate any knowledge you might have of the phenomenon. The modeler cannot rely solely on the dataset to show all the important features; those that do not appear can still be incorporated into the model by adjusting the parameter values to reflect an expected outcome. It is important that the model be as realistic as possible in order for the interpolated values and associated uncertainties to be accurate representations of the real phenomenon.

In addition to preprocessing the data, it may be necessary to model the spatial structure (spatial correlation) in the dataset. Some methods, like kriging, require this to be explicitly modeled using semivariogram or covariance functions; whereas other methods, like Inverse Distance Weighting, rely on an assumed degree of spatial structure, which the modeler must provide based on prior knowledge of the phenomenon.

A final component of the model is the search strategy. This defines how many data points are used to generate a value for an unsampled location. Their spatial configuration (location with respect to one another and to the unsampled location) can also be defined. Both factors affect the interpolated value and its associated uncertainty. For many methods, a search ellipse is defined, along with the number of sectors the ellipse is split into and how many points are taken from each sector to make a prediction.

Once the model has been completely defined, it can be used in conjunction with the dataset to generate interpolated values for all unsampled locations within an area of interest. The output is usually a map showing values of the variable being modeled. The effect of outliers can be investigated at this stage, as they will probably change the model's parameter values and thus the interpolated map. Depending on the interpolation method, the same model can also be used to generate measures of uncertainty for the interpolated values. Not all models have this capability, so it is important to define at the start if measures of uncertainty are needed. This determines which of the models are suitable.

As with all modeling endeavors, the model's output should be checked, that is, make sure that the interpolated values and associated measures of uncertainty are reasonable and match your expectations.

Once the model has been satisfactorily built, adjusted, and its output checked, the results can be used in risk analyses and decision making.

**2-1-3-2- Understanding interpolation analysis:**

Interpolation predicts values for cells in a raster from a limited number of sample data points. It can be used to predict unknown values for any geographic point data, such as elevation, rainfall, chemical concentrations, and noise levels.

**Why interpolate to raster?**

The assumption that makes interpolation a viable option is that spatially distributed objects are spatially correlated; in other words, things that are close together tend to have similar characteristics. For instance, if it is raining on one side of the street, you can predict with a high level of confidence that it is raining on the other side of the street. You would be less certain if it was raining across town and less confident still about the state of the weather in the next county.

Using the above analogy, it is easy to see that the values of points close to sampled points are more likely to be similar than those that are farther apart. This is the basis of interpolation. A typical use for point interpolation is to create an elevation surface from a set of sample measurements. The geostatistical Analyst tool also provides an extensive collection of interpolation methods.

**2-1-3-3- Examples of interpolation applications:**

Some typical examples of applications for the interpolation tools follow. The accompanying illustrations show the distribution and values of sample points and the raster generated from them.

### 1- Interpolating a rainfall surface

The input here is a point dataset of known rainfall-level values, shown by the illustration on the left. The illustration on the right shows a raster interpolated from these points. The unknown values are predicted with a mathematical formula that uses the values of nearby known points.

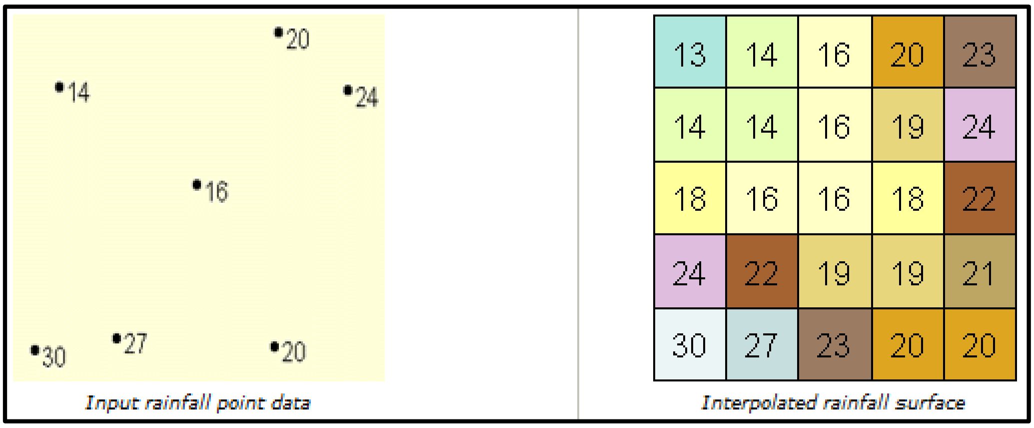


**Figure (2-10): Interpolating a rainfall surface**

### 2- Interpolating an elevation surface

A typical use for point interpolation is to create an elevation surface from a set of sample measurements. In figure (2-11), each point in the point layer represents a location where the elevation has been measured. By interpolation, the values for each cell between these input points are predicted.

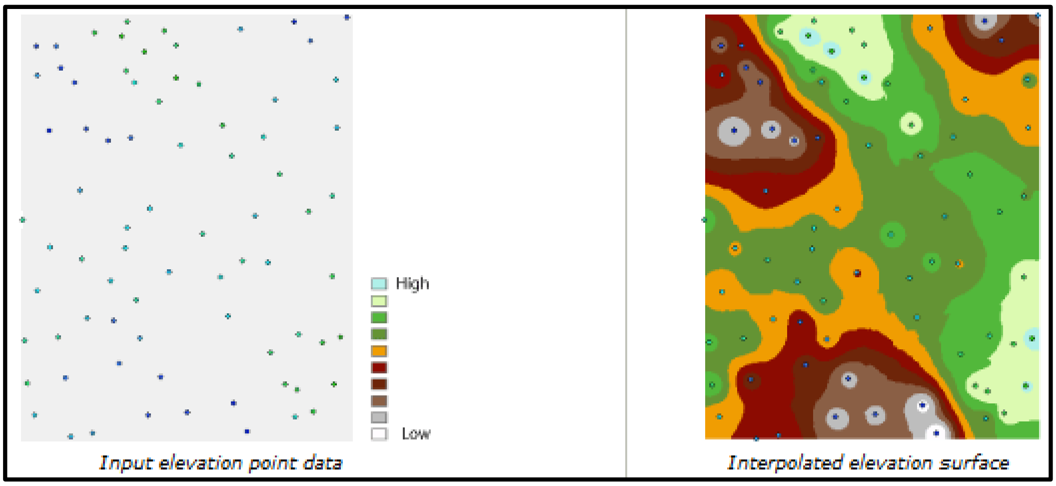


**Figure (2-11): Interpolating an elevation surface**

### 3- Interpolating a concentration surface

In the example below, the interpolation tools were used to study the correlation of the ozone concentration on lung disease in California. The image on the left shows the locations of the ozone monitoring stations. The image on the right displays the interpolated surface, providing predictions for each location in California. The surface was derived using kriging.

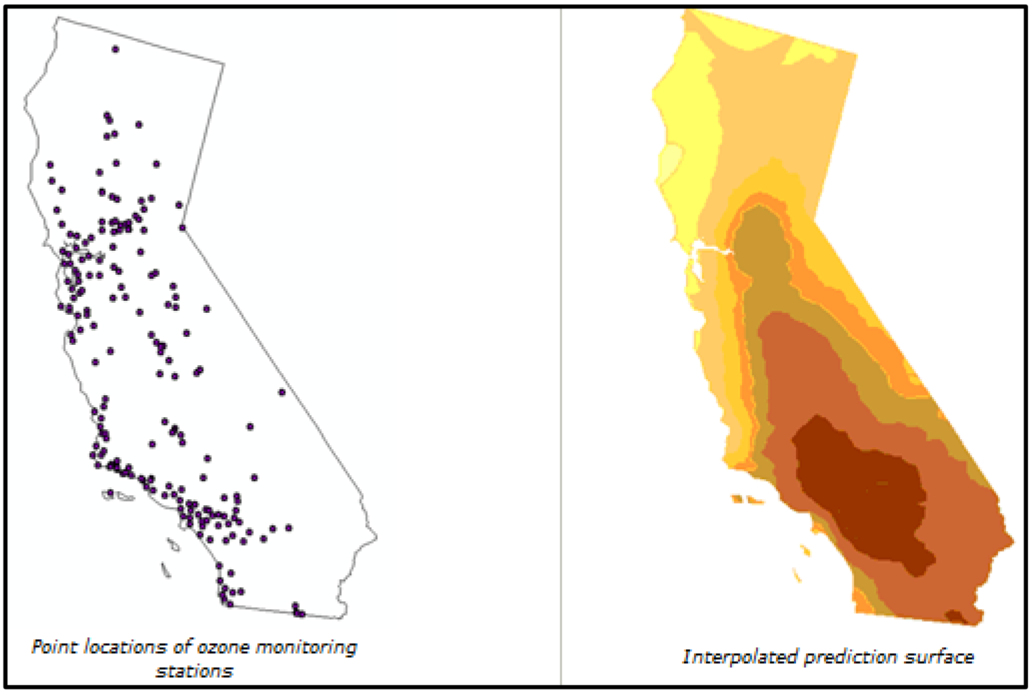


**Figure (2-12): Interpolating a concentration surface**

### 2-1-3-4- Inverse Distance Weighted (IDW) Interpolation Method:

(Geomatics, 2019) Many definitions have been formulated with regard to the concept of interpolation (e.g. Burrough 1986; McCullagh 1988; Robinson 1994). According to Burrough (1986): interpolation is the procedure of estimating the value of properties at unsampled sites within the area covered by existing point observations / data.

There is a great range of methods, models and techniques available for data interpolation, based on parameters that affect the quality of the result. Many of these methods and techniques are well established and are commonly used because they provide acceptable results. At the same time, research continues with the aim to evaluate their effectiveness and improve the quality of the results (Oswald and Raetzsch 1984; Gold 1988). The accuracy of a DEM that is produced with an interpolation procedure is related to the density and the distribution of the reference altitudes, as well as the selection of the interpolation procedure used (Schut 1976). Even the simplest interpolation method may be useful if the density of the reference altitudes is high and their distribution is ideal.

The Inverse Distance Weighted (IDW) method is widely recognized as the basic method in most systems that create and manage DEMs (Burrough 1986; Schut 1976). The main characteristic of this method is that all the points on the earth's surface are considered to be interdependent, on the basis of distance. Therefore, the calculation of altitudes in an area depends on the altitudes of the data points in the vicinity.

The basic IDW interpolation formula is given in equation (1). Where x* is an unknown value at a location (P), $w_i$ is the weight, and $x_i$ is known point value, $d_i$ is the distances of the known points from point P; n is the number of the known points used in the interpolation procedure for estimating the elevation of point P. The weight is inverse distance of the point (P) to each known point value ($w_i$) that is used in the calculation. Simply the weight can be calculated using equation (2).

$$x^* = \frac{w_1 x_1 + w_2 x_2 + w_3 x_3 + \ldots + w_n x_n}{w_1 + w_2 + w_3 + \ldots + w_n}$$ ------------------------------------Equation (1)

$$w_i = \frac{1}{d_{ix^*}^P}$$ -------------------------------------------------------------------Equation (2)

In case of contour maps, the points are the vertices of the digitized lines and interpolation is effected on this basis. Sometimes, it is possible to select a subset of these points, when for example there are more points than the minimum required to define the geometry of the contour. This involves a process of contour generalization.

### 2-1-3-5- Spatial analysis:

*(P.J. Mason, 2005)* Spatial analysis of individual maps and layers involves two-dimensional processing and geo-statistical methods, such as reclassification and thresholding, neighbourhood functions using spatial filters, distance, and buffer calculations, 2D spatial transformations and, importantly, gridding or interpolation.

Geo-statistical methods, involving the application of probabilistic methods to geographically related phenomena, can be used to highlight spatial correlation within a data layer. This idea is based on the assumption that points located close to one another, should also be close in value. Existing data are then used to interpolate into areas where no data exists.

The spatial analysis can be refined and made interactive, i.e., transformation, manipulation of maps, and applied simple mathematical facts (Bourgault and Marcotte, 1991). The spatial data can be derived from large databases providing detailed information and trends (Higgs *et al*., 1998). For example, multivariable or factor analysis allows changes in variables.

A GIS database computes spatial location, distribution, and relationship. Fundamentally, spatial analysis is a set of methods producing refined results with spatial correlation. A spatial link is observed between geometric and thematic data and attributes in the data components are identified. Nowadays all GIS software has modules designed to handle spatial data. Positions are connected with other features and details either spatial or nonspatial characters (Burrough, 2001).

The range of methods deployed for spatial analysis varies with respect to the type of the data model used. Measurement of length, perimeter and area of the features is a very common requirement in spatial analysis (Parasiewicz *et al.,* 2018; Clark and Evans, 1954). However different methods are used to make measurements based on the type of data used i.e. vector or raster. Invariably, the measurements will not be exact, as digitized feature on map may not be entirely similar to the features on the ground, and moreover in the case of raster, the features are approximated using a grid cell representation (Oliver and Webster, 2007).

Many methods can be linked with GIS software, such as inverse distance weighted, natural neighbor inverse distance weighted, spline, kriging, and topo to raster methods. The suite of analyses should be incorporated into a GIS package, ensuring that a user can still intervene to choose the most appropriate form of analysis (Cucala *et al*., 2018; Fischer *et al.*, 1997).

**2-1-4-Understanding Drainage Systems:**

The area upon which waterfalls and the network through which it travels to an outlet are referred to as a drainage system. The flow of water through a drainage system is only a subset of what is commonly referred to as the hydrologic cycle, which also includes precipitation, evapotranspiration, and groundwater flow. The hydrology tools focus on the movement of water across a surface.

A drainage basin is an area that drains water and other substances to a common outlet. Other common terms for a drainage basin are watershed, basin, catchment, or contributing area. This area is normally defined as the total area flowing to a given outlet, or pour point. A pour point is the point at which water flows out of an area. This is usually the lowest point along the boundary of the drainage basin.

The boundary between two basins is referred to as a drainage divide or watershed boundary. Figure (2-13) shows the components of the drainage basin.

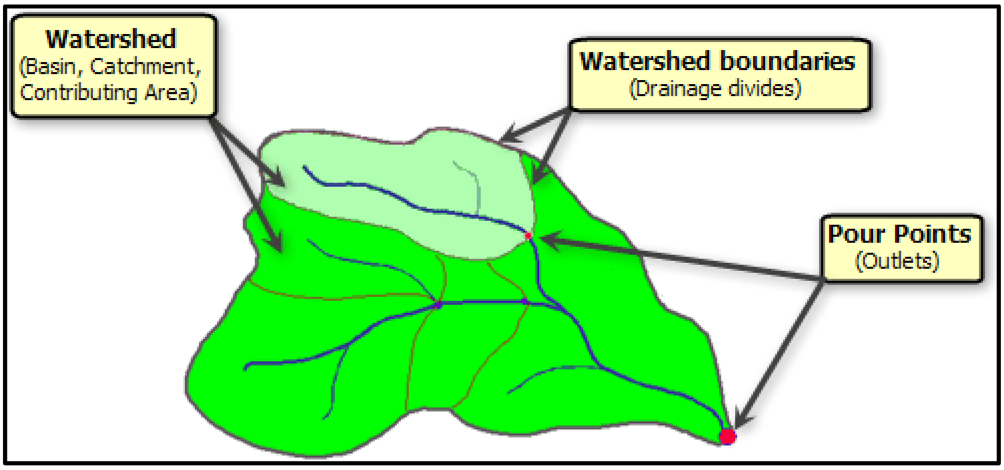


**Figure (2-13): Components of drainage basin**

The network through which water travels to the outlet can be visualized as a tree, with the base of the tree being the outlet. The branches of the tree are stream channels. The intersection of two stream channels is referred to as a node or junction. The sections of a stream channel connecting two successive junctions or a junction and the outlet are referred to as stream links.

### 2-1-5- Hydrologic analysis sample applications:

The hydrologic modeling tools in the ArcGIS Spatial Analyst extension toolbox provide methods for describing the physical components of a surface. The hydrologic tools allow you to identify sinks, determine flow direction, calculate flow accumulation, delineate watersheds, and create stream networks. Figure (2-14) is of a resulting stream network derived from an elevation model:

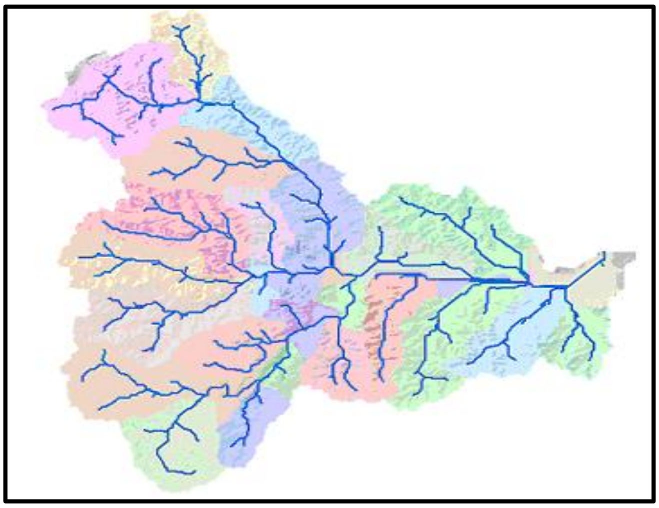

**Figure (2-14): Stream network derived from elevation model**

### 2-1-6- Deriving runoff characteristics:

When delineating watersheds or defining stream networks, you proceed through a series of steps. Some steps are required, while others are optional depending on the characteristics of the input data. Flow across a surface will always be in the steepest downslope direction. Once the direction of flow out of each cell is known, it is possible to determine which and how many cells flow into any given cell. This information can be used to define watershed boundaries and stream networks. The following flowchart shows the process of extracting hydrologic information, such as watershed boundaries and stream networks, from a digital elevation model (DEM).

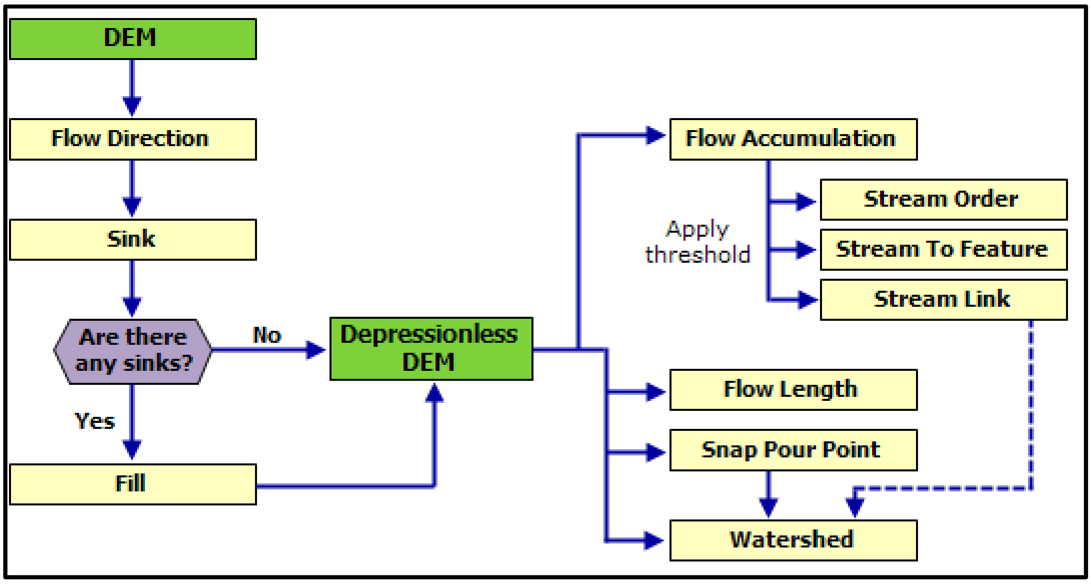


**Figure (2-15): Hydrological modeling flowchart**

Regardless of your goal, start with an elevation model. The elevation model is used to determine which cells flow into other cells (the flow direction). However, if there are errors in the elevation model or if you are modeling karst geology, there may be some cell locations that are lower than the surrounding cells. If this is the case, all water traveling into the cell will not travel out. These depressions are called sinks. The hydrologic analysis tools allow you to identify the sinks and give you tools to fill them. The result is a depression less elevation model. You can then determine the flow direction on this depression less elevation model.

If you are delineating watersheds, you need to identify pour points (locations for which you want to know the contributing watershed). Usually these locations are mouths of streams or other hydrologic points of interest, such as a gauging station. Using the hydrologic analysis tools, you can specify the pour points, or you can use the stream network as the pour points. This creates watersheds for each stream segment between stream junctions. To create the stream network, you must first calculate the flow accumulation for each cell location.

If you are defining stream networks, you not only need to know the direction water flows from cell to cell but also how much water flows through a cell, or how many cells flow into another cell. When enough water flows through a cell, the location is considered to have a stream passing through it.

### 2-1-7- Orthometric height vs. ellipsoidal height:

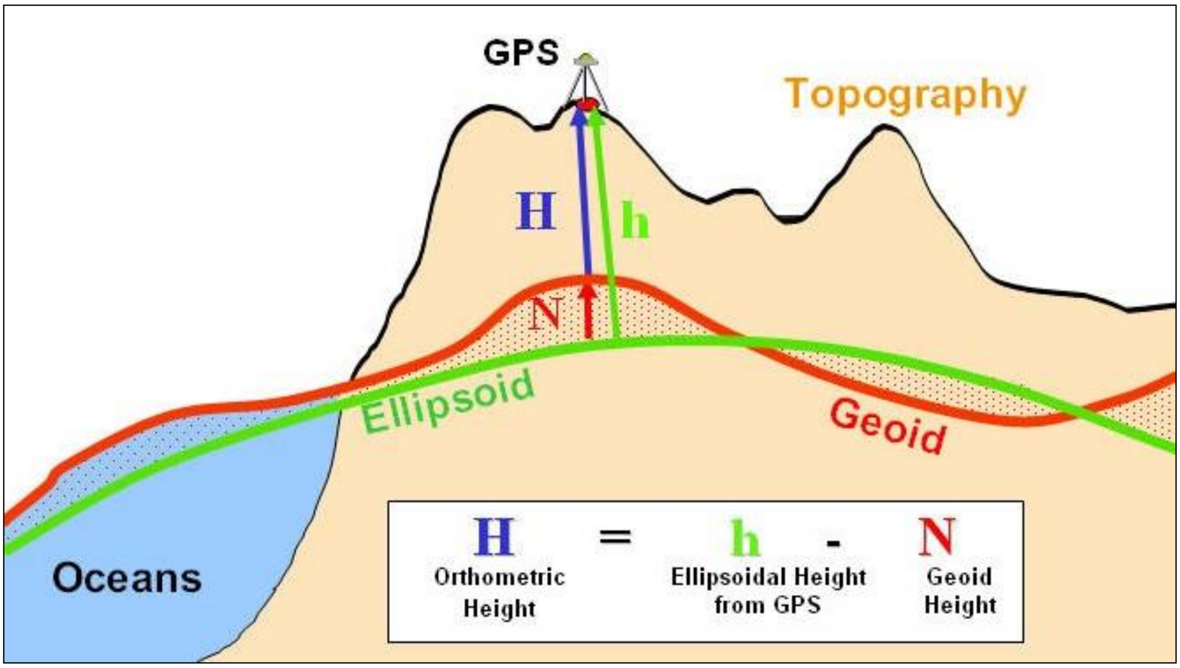


**Figure (2-16): Orthometric height vs. ellipsoidal height**

(Ssengendo R., 2015) Orthometric (geoidal) height H is **the height on the surface above the geoid**. ... Note that in this picture the geoid is shown above the ellipsoid. In the continental United States, the geoid is actually below the ellipsoid, so the value of the geoid height is negative

The ellipsoidal height of a point of the Earth Surface is **the distance h from the point to the ellipsoid**. The geoid height above the ellipsoid (N) is the difference between the ellipsoidal height and orthometric (geoid) height

### 2-1-8- Accuracy and precision:

In the fields of engineering, industry and statistics, the accuracy of a measurement system is the degree of closeness of measurements of a quantity to its actual (true) value. The precision of a measurement system, also called reproducibility or repeatability, is the degree to which repeated measurements under unchanged conditions show the same results (John Robert Taylor,1999). Although the two words can be synonymous in colloquial use, they are deliberately contrasted in the context of scientific method.

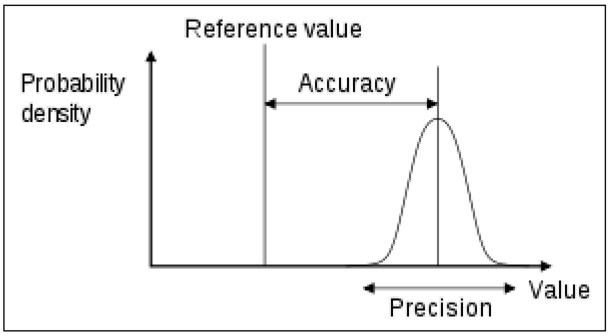


**Figure (2.17) : Illustration of precision and accuracy**

A measurement system can be accurate but not precise, precise but not accurate, neither, or both. For example, if an experiment contains a systematic error, then increasing the sample size generally increases precision but does not improve accuracy. Eliminating the systematic error improves accuracy but does not change precision.

The terminology is also applied to indirect measurements, that is, values obtained by a computational procedure from observed data such as coordinates obtained using a GPS device.

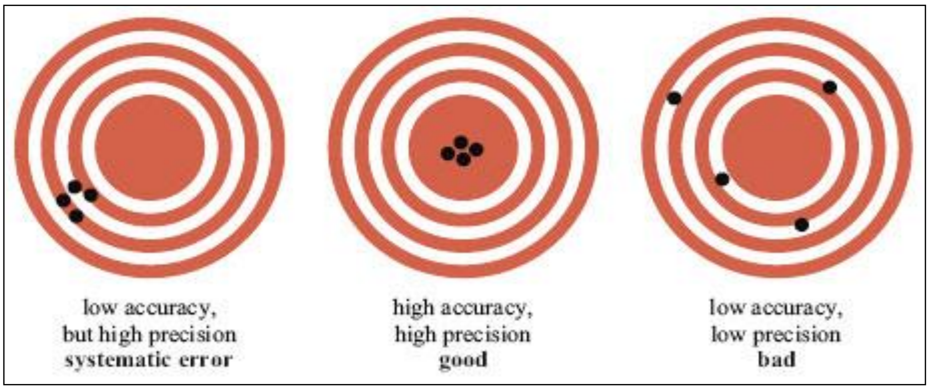


**Figure (2.18) : Bull's eye analogy (accuracy vs. precision)**

When measurements are repeated and averaged, the term standard error is properly applied; the precision of the average is equal to the known standard deviation of the process divided by the square root of the number of measurements averaged. Further, the central limit theorem shows that the probability distribution of the averaged measurements will be closer to a normal distribution than that of individual measurements.

With regard to accuracy we can distinguish the difference between the mean of the measurements and the reference value, the bias. Establishing and correcting for bias is necessary for calibration.

A common convention in science and engineering is to express accuracy and/or precision implicitly by means of significant figures. Here, when not explicitly stated, the margin of error is understood to be one-half the value of the last significant place. For instance, a recording of 843.6 m, or 843.0 m, or 800.0 m would imply a margin of 0.05 m (the last significant place is the tenths place), while a recording of 8,436 m would imply a margin of error of 0.5 m (the last significant digits are the units).

**2-1-8-1- Median, Mean, and Standard Deviation:**

The median is known as a measure of location; that is, it tells us where the data are. We do not need to know all the exact values to calculate the median; if we make the smallest value even smaller or the largest value even larger, it will not change the value of the median. Thus the median does not use all the information in the data and so it can be shown to be less efficient than the mean or average, which does use all values of the data. To calculate the mean we add up the observed values and divide by the number of them.

$$\boldsymbol{Mean} = \frac{\Sigma \boldsymbol{xi}}{\boldsymbol{n}} \quad \text{------------------------------------------------------} \quad \text{Equation (3)}$$

Where xi is each of the values; n is the number of these values. A major disadvantage of the mean is that it is sensitive to outlying points.

The standard deviation (SD) is an indication of the spread of observations about the mean. The theoretical basis of the standard deviation is complex and need not trouble the ordinary user. A practical point to note here is that, when the populations from which the data arise have a distribution that is approximately “Normal” (or Gaussian), then the standard deviation provides a useful basis for interpreting the data in terms of probability.

The Normal distribution is represented by a family of curves defined uniquely by two parameters, which are the mean and the standard deviation of the population. The curves are always symmetrically bell shaped, but the extent to which the bell is compressed or flattened out depends on the standard deviation of the population. However, the mere fact that a curve is bell shaped does not mean that it represents a Normal distribution, because other distributions may have a similar sort of shape.

The reason why the standard deviation is such a useful measure of the scatter of the observations is this: if the observations follow a Normal distribution, a range covered by one standard deviation above the mean and one standard deviation below it $\bar{x} \pm 1SD$ includes about 68% of the observations; a range of two standard deviations above and two below ($\bar{x} \pm 2SD$) about 95% of the observations; and of three standard deviations above and three below ($\bar{x} \pm 3SD$) about 99.7% of the observations. Consequently, if we know the mean and standard deviation of a set of observations, we can obtain some useful information by simple arithmetic. By putting one, two, or three standard deviations above and below the mean we can estimate the ranges that would be expected to include about 68%, 95%, and 99.7% of the observations.

**2-1-8-2- Standard deviation from ungrouped data:**

(Mullee M A., 1995) The standard deviation is a summary measure of the differences of each observation from the mean. If the differences themselves were added up, the positive would exactly balance the negative and so their sum would be zero. Consequently the squares of the differences are added. The sum of the squares is then divided by the number of observations minus one to give the mean of the squares, and the square root is taken to bring the measurements back to the units we started with. (The division by the number of observations minus one instead of the number of observations itself to obtain the mean square is because "degrees of freedom" must be used. In these circumstances they are one less than the total. The theoretical justification for this need not trouble the user in practice, but to gain an intuitive feel for degrees of freedom, consider choosing a chocolate from a box of n chocolates. Every time we come to choose a chocolate we have a choice, until we come to the last one (normally one with a nut in it!), and then we have no choice. Thus we have n-1 choices, or “degrees of freedom”.

Standard deviation in statistics, typically denoted by **σ**, is a measure of variation or dispersion (refers to a distribution's extent of stretching or squeezing) between values in a set of data. The lower the standard deviation, the closer the data points tend to be to the mean (or expected value), **μ**. Conversely, a higher standard deviation indicates a wider range of values. Similar to other mathematical and statistical concepts, there are many different situations in which standard deviation can be used, and thus many different equations. In addition to expressing population variability, the standard deviation is also often used to measure statistical results such as the margin of error. When used in this manner, standard deviation is often called the standard error of the mean, or standard error of the estimate with regard to a mean.

**2-1-8-3- Population Standard Deviation:**

The population standard deviation, the standard definition of **σ**, is used when an entire population can be measured, and is the square root of the variance of a given data set. In cases where every member of a population can be sampled, the following equation can be used to find the standard deviation of the entire population:

$$\sigma = \sqrt{\frac{1}{N}\sum_{i=1}^{N}(x_i - \mu)^2}. \qquad \text{---------------------------------------} \qquad \text{Equation (4)}$$

Where

$\mathbf{x_i}$ is an individual value

**μ** is the mean/expected value

**N** is the total number of values

### 2-1-8-4- Sample Standard Deviation:

In many cases, it is not possible to sample every member within a population, requiring that the above equation be modified so that the standard deviation can be measured through a random sample of the population being studied. A common estimator for **σ** is the sample standard deviation, typically denoted by **s**. It is worth noting that there exist many different equations for calculating sample standard deviation since, unlike sample mean, sample standard deviation does not have any single estimator that is unbiased, efficient, and has a maximum likelihood. Equation (3) provided below is the "corrected sample standard deviation." It is a corrected version of the equation obtained from modifying the population standard deviation equation by using the sample size as the size of the population, which removes some of the bias in the equation. Unbiased estimation of standard deviation, however, is highly involved and varies depending on the distribution. As such, the "corrected sample standard deviation" is the most commonly used estimator for population standard deviation, and is generally referred to as simply the "sample standard deviation." It is a much better estimate than its uncorrected version, but still has a significant bias for small sample sizes (N<10).

$$s = \sqrt{\frac{1}{N-1}\sum_{i=1}^{N}(x_i - \overline{x})^2}, \qquad \text{--------------------------------} \qquad \text{Equation (5)}$$

Where

$\mathbf{x_i}$ is one sample value

$\bar{\mathbf{x}}$ is the sample mean

**N** is the sample size

### 2-1-8-5- Applications of Standard Deviation

Standard deviation is widely used in experimental and industrial settings to test models against real-world data. An example of this in industrial applications is quality control for some products. Standard deviation can be used to calculate a minimum and maximum value within which some aspect of the product should fall some high percentage of the time. In cases where values fall outside the calculated range, it may be necessary to make changes to the production process to ensure quality control.

Standard deviation is also used in weather to determine differences in regional climate. Imagine two cities, one on the coast and one deep inland, that have the same mean temperature of 75°F. While this may prompt the belief that the temperatures of these two cities are virtually the same, the reality could be masked if only the mean is addressed and the standard deviation ignored. Coastal cities tend to have far more stable temperatures due to regulation by large bodies of water, since water has a higher heat capacity than land; essentially, this makes water far less susceptible to changes in temperature, and coastal areas remain warmer in winter, and cooler in summer due to the amount of energy required to change the temperature of the water. Hence, while the coastal city may have temperature ranges between 60°F and 85°F over a given period of time to result in a mean of 75°F, an inland city could have temperatures ranging from 30°F to 110°F to result in the same mean.

**2-1-8-6- Q-Q Plot:**

In statistics, a Q–Q (quantile-quantile) plot is a probability plot, which is a graphical method for comparing two probability distributions by plotting their quantiles against each other. First, the set of intervals for the quantiles is chosen. A point (x, y) on the plot corresponds to one of the quantiles of the second distribution (y-coordinate) plotted against the same quantile of the first distribution (x-coordinate). Thus the line is a parametric curve with the parameter which is the number of the interval for the quantile.

If the two distributions being compared are similar, the points in the Q–Q plot will approximately lie on the line $y = x$. If the distributions are linearly related, the points in the Q–Q plot will approximately lie on a line, but not necessarily on the line $y = x$.

## 2-2- Relevant studies:

### 2-2-1- Overview:

The literature review chapter has provided an opportunity for the researcher to show that she has understood the body of the academic work that has already been done in relation to the flood analysis topic and has surveyed scholarly articles, books, data, research papers, and other sources relevant to her particular area of research aiming to summarize and provide a critical analysis of the research arguments she has found in her readings. Conducting a literature review has established familiarity with and understanding of current research in this particular field for the student before carrying out her investigation, and enabled her to find out what research has already been done and identify what has not been unknown within her topic.

The literature review has enumerated, described, summarized, objectively evaluated and clarified some of the most relevant previous research. It has given a theoretical base for the research and helped the researcher determine the nature of her research. The literature review has acknowledged the work of previous researchers, and in so doing, it has to assure the reader that the researcher work has been well conceived. It is assumed that by mentioning a previous work in the field of study, that the researcher has read, evaluated, and assimilated that work into the work at hand. The literature review has generally followed a discussion of the study's goal or purposes. Conducting the literature review has helped the PhD. student to gain an understanding of the existing research and debates and build knowledge relevant to her area of study.

The researcher has reviewed many literature topics; she has divided the reviewed most relevant materials into two sections: section one was related to the materials and technologies used for flood studies and section two was related to flood monitoring and assessment.

### 2-2-2- Section one: Material and technologies used for flood studies

#### 2-2-2-1- Survey on Flood Monitoring and Alerting Systems - India:

(Priya S Patil, S Sanjeev, and Sanjeev N Jain, 2020) presented an overall survey on various flood monitoring and alerting systems in different flood prone areas around the world.

Spatial MultiCriteria Evaluation (SMCE) was implemented to identify the watershed of Omidieh and Bidboland 1,262.25 $Km^2$ area - Khuzestan. The causes of flood were investigated and found to include the slope, land use, geology, erosion rates, soil texture, average annual rainfall, drainage density and vegetation of the area. Based on the produced composite index map, an area equals to 466.025 $Km^2$, was found as a flooding-susceptible area i.e. about 62% of zonation area runs zero-risk while (36%) has a higher potential of flooding and 2% high-risk (M Arianpour and Ali Akbar Jamali, 2015). The investigation of the cause which was presented by the authors was suitable since they investigated many criteria such as slope, land use, geology, erosion rates, soil texture, average annual rainfall, drainage density and vegetation of the area.

This paper performs survey of environmental and flood disaster detection and monitoring systems and different communication technologies which help to improve upon the effective flood detection and flood warning problems. These systems with highly reliable sensors and effective Internet of Things (IoT) platforms will critically be used for large scale environment monitoring and disaster prevention.

#### 2-2-2-2- The Role of GIS in Earth Sciences:

(Akram J., 2006) reviewed the use of GIS in some earth sciences applications such as hazard zonation mapping and mapping earthquakes/Landslides disasters (Human deaths, property damage and injuries etc.), groundwater, project management, quality control and efficiency. In the end, the researcher explained that a comprehensive GIS database that incorporates cultural, geologic, geophysical, engineering, infrastructure and business-related data can support the analysis of different data types more effectively and enable gaining insights that are not otherwise apparent.

### 2-2-2-3- GIS Water Balance Approach to Support Surface Water Flood Risk Management - UK:

In his paper (Diaz J., 2012) stated that concern has arisen as to whether the lack of appropriate consideration to surface water in urban spatial planning is reducing our capacity to manage surface water flood risk. Appropriate tools are required that allow spatial planners to explore opportunities and solutions for surface water flooding at large spatial scales. An urban surface water balance model has been developed that screens large urban areas to identify flooded areas and which allows solutions to be explored. The model hypothesis is that key hydrological characteristics; storage volume and location, flow paths and surface water generation represent the key processes responsible for surface water flooding. The model uses a LiDAR DEM (light Detection and Ranging Digital Elevation Model) as the basis for determining surface water accumulation in catchments and has been developed so that it requires minimal inputs and computational resources.

The urban surface water balance approach is applied to Keighley in West Yorkshire where several instances of surface water flooding have been reported. Data for validating surface water flood risk models is sparse because such flooding events are of short duration, very localized and distributed across the catchment. This research used a postal questionnaire, followed with site visits to collect data on surface water flooding locations in Keighley. The validation exercise confirmed that the major processes responsible for flooding are largely well represented in the model for situations where interaction with the urban sewer network is well represented by the assumptions made in the model. A qualitative analysis based on field visits revealed that the degree of interaction with the sewer network varies spatially, and as the importance of the interaction of the sewer system increases, the accuracy of the model results becomes lower. It also highlighted that local detail not present in the DEM, the presence of urban drainage assets and the performance of the sewer system (which has not been represented in the model) can influence the accuracy of model results.

Model results were used as a basis to develop solutions to surface water flooding. A least cost path methodology was developed to identify managed flood routes. These routed were translated into model inputs in the form of a modified DEM. It was shown that the simple and fast representation of flood routes and surface storage is of considerable benefit for scenario analysis.

### 2-2-2-4- Accuracy Assessment of Contour Interpolation from 1:50,000 Topographical Maps and SRTM Data for 1:25,000 Topographical Mapping - Nigeria:

(A. P. Ozah a, *, O. Kufoniyib, 2008) stated that although free spatial data sources such as the Shuttle Radar Topographic Mission (SRTM) digital data provide excellent base data for extracting height data for topographic mapping, such datasets need to be adequately evaluated and subjected to further processing before extracting contours needed for topographical mapping. Extracting topographical data by contour interpolation from existing topographical maps and SRTM data therefore necessitates accuracy assessment of the interpolation result to ascertain its suitability for topographical mapping. This paper presents a framework for accuracy assessment of interpolating contours from 1:50,000 topographical maps and SRTM height data for topographical mapping at the scale of 1:25,000. Accuracy tests of contours interpolated from the two sources were performed for different terrain configurations and contexts to determine their suitability for topographical mapping in different scenarios. Using an on-going 1:25,000 topographical mapping project as a case study, the use of this contour interpolation accuracy assessment model for arriving at the best strategy for the mapping was also presented. The following findings were made from this study:

1) Both SRTM elevation data and elevation data from existing 1:50,000 topographic maps can be used to create a good representation of the terrain, because of their high positive correlation with the more accurate GPS height data of points.

2) The 90-m resolution SRTM DEM manifests artifacts and a prior processing of the data is recommended to achieve cartographic quality good for 1:25,000 topographical mapping.

### 2-2-2-5- Floodplain Modeling of Malaking-Ilog River in Philippines Using LiDAR Digital Elevation Model:

In their research (J. R. Ternate *et al.*, 2017) discussed the significance of the hydrologic model and the selection of return period in the design of various water related structures. They utilized river analysis software for designing a dike. The populations surrounding the river (who are directly affected when the river overflows) were identified. With the help of the hydrographs generated from the rainfall runoff model in this study, the design parameters of various water related structures are easily determined, leading to a more efficient design process.

This study can serve as a reference for water resources engineers and designers who decide to pursue construction of flood control facilities. With the knowledge on return periods considered for individual water structures, engineers could utilize the rainfall-runoff model developed by the researchers to determine the design discharge. Furthermore, the use of the river analysis software, Hydrologic Engineering Center's River Analysis System (HEC-RAS), is recommended for identifying the areas that need flood control measures and facilities.

### 2-2-2-6- Geographic Information Systems (GIS) in Water Management – Greece :

According to (Hatzopoulos J., 2002) the priorities in water management start with basic information, which, as stated in the USGS forum, is the creation of National Hydrography Dataset (NHD) and digital elevation datasets of 12 cm accuracy. Hydrologic Derivatives and Watershed Boundary Dataset can also be planned to be the next priority. Already Greece is facing many problems related to water shortage and it is necessary to start taking actions on that direction. The Athens Utility Company can play a very important role to make initiatives on those priorities so that other Utility companies can benefit as well. Parallel to that other Government services such as OKXE (Organization for Cadastre and Mapping of Greece) must get government support and also be staffed with qualified personnel to develop and deliver to the public the necessary mapping products which are necessary for any essential planning for development and which are so important for water management.

The production of basic data such as digital elevations and the access to the public will also help to develop know how on using the GIS technology in water management. The Laboratory of Remote Sensing and GIS (RSLUA) at the University of the Aegean has all necessary infrastructure to provide education (seminars, short courses, summer schools, workshops), and to do research on those areas and already cooperates with municipality of Drymalias of Naxos on a Social, Education of Adults through Mobility (SEAM) project.

#### 2-2-2-7- LiDAR DEM Data for Flood Mapping and Assessment; Opportunities and Challenges - Ethiopia:

According to (Wedajo, J., 2017) flood modeling, which is fully dependent on accurate and high-resolution DEM data, solves some of the limitations of Earth observation. As such, LiDAR system improved the performance of flood modeling via providing fine resolution DEM. The opportunities that LiDAR technology provided for flood mapping includes provision of accurate and high-resolution DEM data, relatively cost and time effective data collection system, capability of penetrating dense vegetation, improved flood model accuracy and fine scale flood modeling, adequate representation of man-made and topographic features, and capability of determining flood depth.

On the other hand, LiDAR system is challenged to be used for flood modeling. The major challenges include LiDAR data filtering (classification), data availability and accessibility, data file size, high computational time, unable to characterize channels bathymetry, and insufficiency of representing complex urban features. Therefore, multi-platform LiDAR data (i.e., ground-based, airborne and space borne) and data from additional sources such as echo soundings and electronic theodolite surveys should be integrated to increase the effectiveness of the LiDAR technology for flood modeling.

Moreover, flood modeling should be calibrated with gauge data and validated with remote sensing imagery. More importantly, further researches have to be conducted to improve LiDAR data filtering algorithm, particularly that best fits to urban areas.

### 2-2-2-8- Perspectives on Digital Elevation Model Simulation for Flood Modeling in the Absence of a High-Accuracy Open Access Global DEM – UK :

(Hawker L., *et al.*, 2018) stated that this article provides an overview of errors in some of the most widely used DEM data sets, along with the current advances in reducing these errors via the creation of new DEMs, editing DEMs and stochastic simulation of DEMs. They focused on a geostatistical approach to stochastically simulate floodplain DEMs from several open-access global DEMs based on the spatial error structure. This DEM simulation approach enables an ensemble of acceptable DEMs to be created, thus avoiding the spurious precision of using a single DEM and enabling the generation of probabilistic flood maps. Despite this encouraging step, an imprecise and outdated global DEM is still being used to simulate elevation. To fundamentally improve flood estimations, particularly in rapidly changing developing regions, a high-accuracy open-access global DEM is urgently needed, which in turn can be used in DEM simulation.

### 2-2-2-9- Practical use of SRTM data in the tropics: comparisons with digital elevation models generated from cartographic data - Colombia:

According to (Jarvis A., *et al.*, 2014) the most important message is that SRTM-derived DEMs provide greater accuracy than TOPO DEMs, but do not necessarily contain more detail. Cartography at scales of 1:25,000 and below (i.e., 1:10,000) contains topographic features not captured with the 3-arc second SRTM DEMs. However, if only cartography with scales above 1:25,000 (i.e., 1:50,000 and 1:100,000) is available, it is better to use the SRTM DEMs. This statement holds for use of SRTM DEMs for terrain derivatives (slope, aspect, landscape classifications, etc.) as well as pure elevation. For hydrological modeling, SRTM 3-arc second DEMs perform well, but are on the margin of usability. If good quality cartography of scale 1:25,000 and below is available, better results may be expected through digitizing and interpolating the cartographic data.

### 2-2-2-10- Quality Assessment and Validation of DSM Derived from SRTM – Germany:

(KOCH A., LOHMANN P., 2000) reported an attempt to check the quality and accuracy of the elevation data derived from the X-band instrument of SRTM. First of all possible error sources influencing the data quality and accuracy will be described and the effects of these errors will be demonstrated.

Reference data of a well-known test site will be used to assess the data and to derive quality measures. The area with a size of 50x50 km² is situated in Germany a few kilometers south of Hanover. Reference data are being made available by the Surveying Authority of Lower Saxony, Germany (Landes vermessung und Geobasis information Niedersachsen, LGN Hannover). The Digital Terrain Model of LGN (ATKIS DGM5) is said to have an accuracy of about ±0.5 meters. Also Trigonometric Points, which are the base of the fundamental geodetic network of Germany, are being used as reference data.

The tool used for assessing the data is a spatial transformation. As a result, 7 parameters, which describe the position, orientation and a scale of the SRTM elevation data with respect to the reference data, were being obtained. To obtain influences of terrain slope, the orientation of the terrain with respect to the sensor position, vegetation, land use and land cover the test site was divided into several subareas. The accuracy and quality of the data as a function of these parameters will be calculated.

Unfortunately, up to this moment (March 2000) the SRTM ITED-2 elevation data are not yet available. Because of the repeated postponements of the mission, the space shuttle Endeavour launched late in February this year. The data has been recorded and after the landing the calibration phase started. When this part is finished the assessment and validation of the data will begin. For this reason no actual results can be presented in this paper. Only the processing steps to assess the data were explained. Possible error sources and their effects on the data quality and accuracy were described.

### 2-2-2-11- The Use of LiDAR and Volunteered imagery to Map Flood Extents and Inundation – Australia:

(McDougall K., Temple-Watts P, 2012) stated that in this study, approximately 20 images of flood damaged properties were utilized to identify the peak of the flood. Accurate position and height values were determined through the use of RTK GPS and conventional survey methods. This information was then utilized in conjunction with river gauge information to generate a digital flood surface. The LiDAR generated DEM was then intersected with the flood surface to reconstruct the area of inundation. The model-determined areas of inundation were then compared to the mapped flood extent from the high resolution digital imagery to assess the accuracy of the process. This paper concluded that accurate flood extent prediction or mapping is possible through this method, although its accuracy is dependent on the number and location of sampled points.

### 2-2-2-12- Challenges and Opportunities for UAV-Based DEM Generation for Flood-Risk Management: A Case of Princeville, North Carolina-USA:

In their research (Hashemi L., *et.al*., 2018) investigated the quality of an Unmanned Aerial Vehicle (UAV)-produced DEM for spatial flood assessment mapping and evaluating the extent of a flood event in Princeville, North Carolina during Hurricane Matthew. The challenges and problems of on-demand DEM production during a flooding event were discussed. An accuracy analysis was performed by comparing the water surface extracted from the UAV-derived DEM with the water surface obtained using the nearby US Geologic Survey (USGS) stream gauge station and LiDAR data.

To improve the DEM quality, and remove the water artifacts, a post-processing method was developed and performed. This method is based on a hydro flattening concept, assuming that the surfaces of water (lakes and, in our case, flooded areas) are flat. This method improved the water surface model by estimating a plane from the land/water interface in the point cloud, creating 3D breaklines, and a conflation methodology to remove water artifacts.

#### 2-2-2-13- DEM Generation and Hydrologic Modeling using LiDAR Data- Australia:

(Glen Robert Kilpatrick, 2015) reported that the aim of his research project was to use LiDAR data to perform hydrologic analysis of a catchment area and to assess the usefulness and reliability of LiDAR data for hydrologic analysis and other related applications. The author stated that there are several perceived benefits for this project: Firstly the results from the analysis can be used for future researches to better understand the catchment characteristics of East Creek, Australia. Secondly the results of this research highlight the capabilities and limitations of airborne LiDAR technology with respect to hydrologic modeling and other applications. Thirdly this research reveals some avenues for further research or investigation into new applications of airborne LiDAR technology.

#### 2-2-2-14- The contribution of GIS in urban flood management - UK:

According to (Arinabo D., 2017) the effectiveness of GIS and Virtual Global Systems (VGS) such as Google Earth (GE) usage and applicability in urban flood management depends on number of interlocking complexities such as urban planning, land use patterns, topography, soils, precipitation and climate change which must all be analyzed and fed into an integrated flood management plan for a particular city. GIS analysis of one component does not necessarily transpose into a stronger approach for urban inundations mitigation. Therefore, a lot is desired in developing a GIS system that encompasses all the interconnecting components of a conurbation in order to effectively control city floods and its impacts.

### 2-2-2-15- Calculation of Uncertainty in 30m Resolution Global Digital Elevation Models: SRTM v3.0 and ASTER v2 - Nigeria:

In their study (Olusina J., Okolie C., 2018) they evaluated the performance of 30-metre resolution SRTM version 3.0 and ASTER GDEM version 2 over Lagos, Nigeria. Both datasets were examined by direct comparison with 176 highly accurate Ground Control Points (GCPs) coordinated by Global Positioning System (GPS). The basis of comparison was on the elevation differences between the Digital Elevation Models (DEMs) and the GCPs at coincident points. The performance of both DEMs was visualized in 2D and 3D space by comparing pixel values and surface models. In the assessment, the absolute vertical uncertainty of SRTM v3.0 and ASTER v2 were 4.23m and 28.73m respectively. The accuracy of SRTM for the study site proved to be higher than the value of 16m presented in the original SRTM specification. ASTER did not meet up with its 17m overall accuracy specification.

### 2-2-2-16- Assessment of the most recent satellite based DEM of Egypt:

According to (Rabah, M., *et al.*, 2017), the Digital Elevation Model (DEM) is crucial to a wide range of surveying and civil engineering applications worldwide. Some of the DEMs such as ASTER, SRTM1 and SRTM3 are freely available open source products. In order to evaluate the three DEMs, the impact of EGM96 is removed and all DEMs heights are becoming ellipsoidal height. This step was done to avoid the errors occurred due to EGM96. A number of 601 points of observed ellipsoidal heights (GPS) compared with the three DEMs, the results showed that the SRTM1 is the most accurate one, that produces mean height difference and standard deviations equal 2.89 and ±8.65 m respectively. In order to increase the accuracy of SRTM1 in EGYPT, a precise Global Geopotential Model (GGM) is needed to convert the SRTM1 ellipsoidal height to orthometric height, so that, we quantify the precision of most-recent released GGM (five models). The results showed that, the Geothermal Emission Control (GECO) model is the best fit global model over Egypt, which produces a standard deviation of geoid undulation differences equals ±0.42 m over observed 17 High Accuracy Reference Network

(HARN) GPS/leveling stations. To confirm an enhanced DEM in EGYPT, the two orthometric height models (SRTM1 ellipsoidal height + EGM96) and (SRTM1 ellipsoidal height + GECO) were assessed with 17 GPS/leveling stations and 112 orthometric height stations, the results showed that the estimated height differences between the SRTM1 before and after improvement were at rate of 0.44 m and 0.06 m respectively. (the correct RMSE differences as shown in the graph below were "4.57-4.64 = -0.83" and "0.61-1.44= -0.83).

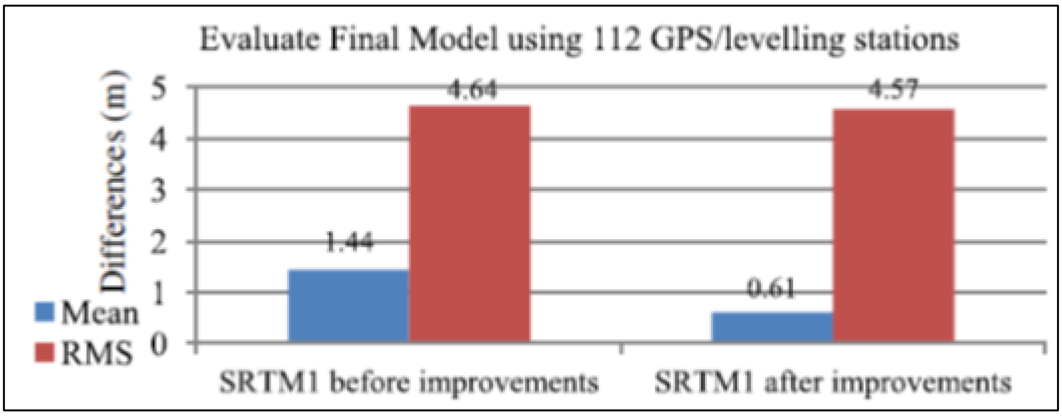


**Figure (2-19) : Height differences between 112 check points and SRTM1 before andafer improvement**

**2-2-3- Section two: Flood monitoring and assessment:**

**2-2-3-1- Flood monitoring and mitigation using low-cost space-related technologies – Sudan:**

(SRCS report, July, 2008) revealed that in Khartoum state alone a number of 15,003 houses were damaged, of which 6,500 were partially damaged and 8,503 were completely damaged (cited by Altayeb H. Yahya, 2014). This was due to the unusual heavy rain witnessed by Khartoum state that caused a rush of storm water floods upon Umdawwanban town and some villages within its vicinity. Since this town is already vulnerable because it has been built on a low land compared to its surroundings, it could not withstand the rushing floods and about 830 houses were completely destroyed while about 500 houses were partially destroyed. A similar disaster was encountered in Sharq Elneel Locality (Marabeea Elshareef and other neighboring towns) in the year 2013.

To contribute to the efforts of building the resilience of the Sudanese nation and communities regarding such recurrent flood disasters, the author investigated the use of low-cost space-related technologies for flood monitoring and mitigation in the area of Sharq Elneel Locality in Khartoum state – Sudan.

The used data was the Shuttle Radar Topography Mission DEM90, multi-temporal MODIS images, Landsat images, IKONOS images downloaded from Google Earth, and point coordinates captured by the GPS at the field. This data was processed using ArcGIS9.3 together with some extensions like ArcHydro, 3D Analyst, Geostatistical Analyst, …..etc.

The obtained results were: terrain classes, contour lines, cross sectional and longitudinal profiles, catchments, drainage lines, drainage points, and the extent of land inundated by flood water during the flood period in the study area.

The output of this study was a dynamic map showing the features necessary for the monitoring and mitigation of the floods, in addition to attribute tables of the features. The result represents an essential input for building a model for flood monitoring. The model shall integrate parameters related to other disciplines such as soil types, vegetation cover, meteorology,….. etc.

The method shown in this paper is recommended to be adopted at many parts of Sudan to get a preliminary idea of the locations vulnerable to floods, particularly because earth observation from space, complemented with other applications, is a cost-effective method for efficient monitoring of floods, environment, and land management, , …etc., and it provides essential data to decision-makers.

The suitability model built by the author was used to demarcate the suitable route for excavating a canal to divert some of the flood water away from Umdawwanban town and towards the Blue Nile.

**2-2-3-2- Volume of water to be harvested using space Technologies, case study: Part of Khartoum State in Sudan:**

(AL-Tayeb, H. Yahya, 2011) stated that unfortunately, there is now water shortage all over the world which is expected - by the concerned parties that monitor the water status - to become severer and more serious in the near future. Moreover, there is a direct relation between security and the warranty of water resources. It is believed that water resources may represent the cause of wars between several countries. It is worth mentioning that, recently, disputes have emerged among the Nile basin countries over the allotment of each country of the Nile water.

In Sudan, the situation is even more critical. There is plenty of water which is lost every year without being exploited for the interest of the Sudanese people, for example, storm and floodwater is lost through the Nile, flowing down-stream to the Nile estuary (the mouth of the River Nile). These quantities of water are not only useessly lost, but also they cause damage to the Sudanese properties and loss of their lives on the way to the estuary.

To solve, or even to mitigate, the impact of the anticipated problem of water shortage, water resources management and development (e.g. rainwater harvesting) in Sudan should be seriously studied, taking into account the social, economic, environmental, and technical dimensions.

Topographic details represent a critical component when performing water harvesting studies because they show the terrain elevations. Thus, this paper highlights the use of space technology data (namely, the Shuttle Radar Topography Mission Global Digital Elevation Model90) to carry out the preliminary topographic studies required for rainwater harvesting in part of Khartoum State in Sudan, as an example.

The SRTMGDEM90 was processed using the ArcHydro Extension and other tools of ArcGIS9.3 to auto generate drainage lines, catchments, terrain classes, contour lines, cross sectional and longitudinal profiles of the study area.

Moreover, the approximate volume of water that can be harvested at a proposed location was determined using the Area and Volume … command of the Surface Analysis of the 3D Analyst Extension of ArcGIS9.3.

The output of this study was a dynamic map showing the features necessary for water harvesting, in addition to attribute tables of the features. The result represents a major step towards building a model for water harvesting. The model shall integrate layers from other disciplines such as rainfall amount, soil types, vegetation cover, ….. etc.

### 2-2-3-3- First Floor Elevation Uncertainty Resulting from LiDAR-Derived Digital Surface Models - Spain:

According to (Bodoque J., *et al.*, 2016) the reliability of flood damage analysis has improved significantly, owing to the increased accuracy of hydrodynamic models. In addition, considerable error reduction has been achieved in the estimation of first floor elevation, which is a critical parameter for determining structural and content damages in buildings. The authors adopted a methodological approach for assessing uncertainty regarding first floor elevation based on implementation of a two-dimensional (2D) hydrodynamic model based on the 500-year flood return period, and LiDAR data with a density of 0.5 points $m^{-2}$, complemented with the river bathymetry obtained from a field survey with a density of 0.3 points $m^{-2}$. Breaklines (also defined as structure lines or skeleton lines) were subsequently added to improve the elevation data. First floor elevation uncertainty (within the 500-year flood zone) was determined by performing Monte Carlo simulations (based on geostatistics and 1997 control elevation points) in order to assess the error. Deviations in first floor elevation (average: 0.56 m and standard deviation: 0.33 m) show that this parameter has to be neatly characterized in order to obtain reliable assessments of flood damage and implement realistic risk management.

The approach adopted here is of paramount importance, particularly with regard to decision-making during the flood risk assessment and management process. This is because it not only enables flood damage to be assessed more reliably but also identifies the parts of the area prone to flooding that require improved topography and aspects assessment that both contribute to a better characterization of hydrodynamic and economic losses.

Comment: the authors of this research paper have used good methods for analysis namely; Break lines and Monte Carlo simulations.

### 2-2-3-4- Assessing flood inundation extent and landscape vulnerability to flood using geospatial technology: A study of Malda district of West Bengal, India

(Sahana M., Ahmed R., Sajjad H., 2015) stated that remote sensing and GIS tools have proved useful for preparing flood inundation, flood risk and flood vulnerability maps. Flood extent was measured by analyzing water versus non-water targets on Landsat 8 images (one acquired before and the other during the flood event). Flood risk zonation map was prepared using equal interval of separation, based on elevation and inundated flooded area.

Flood inundation map and pre monsoon land use land cover map were compared to assess the impact of flood on various land use and land cover classes. Of the total area of the district, 19% area was affected by flood during 2014. The study suggests that efforts should be made to remove the sediments for increasing the depth of river near the affected area of Malda district. Earlier levees were constructed along Farakka covering the parts of Kaliachak, Manikchak and Ratua blocks but these have been eroded. Therefore, the measures such as construction of short spurs and bed bars for diverting flow should be adopted to save agricultural land, property and human lives.

### 2-2-3-5- Flood Progression Modeling and Impact Analysis - USA:

(National Research Council, 2009) report revealed that the Federal Emergency Management Agency's (FEMA's) Flood Insurance Rate Maps (FIRMs, hereafter referred to as flood maps) are used for setting flood insurance rates, regulating floodplain development, and communicating the 1 percent annual chance flood (also known as the 100-year flood) and the 0.2 percent annual chance flood (also known as the 500-year flood).to those who live in floodplains.

FEMA and the National Oceanic and Atmospheric Administration (NOAA) sponsored this study to examine the factors that affect flood map accuracy, assess the benefits and costs of more accurate flood maps, and recommend ways to improve flood mapping, communication, and management of flood-related data. The case studies focused on:

(1) Uncertainties in hydrologic, hydraulic, and topographic data in and near selected streams in Florida and North Carolina.

(2) The economic costs and benefits of creating new digital flood maps in North Carolina. For the economic analysis, two benefits were considered, based - in part - on the availability of geospatial data required to carry out the analysis, namely, avoiding flood losses to new buildings and avoiding repairs to infrastructure through accurate floodplain delineation, and setting flood insurance premiums to better match estimates of actual risk.

# Chapter Three

# Material and Methods

## 3- Material, tools, and Methods:

### 3-1- Material:

The following material were used for conducting this research:

1. Shuttle Radar Topography Mission Global Digital Elevation Model 30 (SRTMGDEM 30, 2020), figure (3-1). Source: www.usgs.gov.

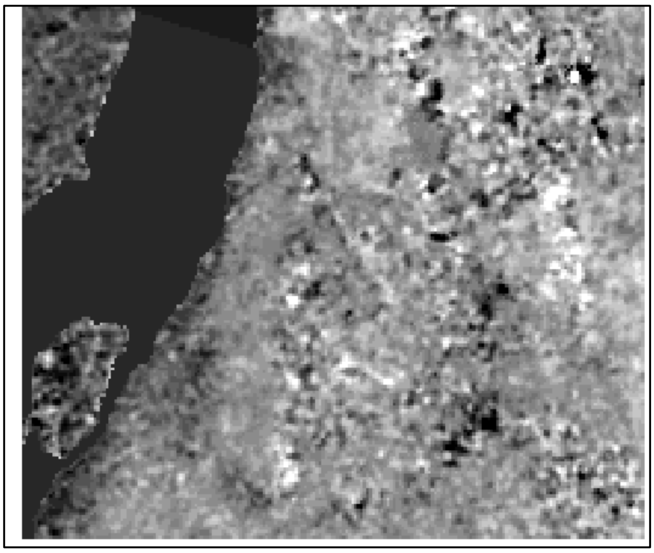

**Figure (3-1): SRTM DEM 30**

2. Light Detection and Ranging Digital Elevation Model (LiDAR DEM 1), figure (3-2). Source: Surveying Department of Khartoum Locality, 2020).

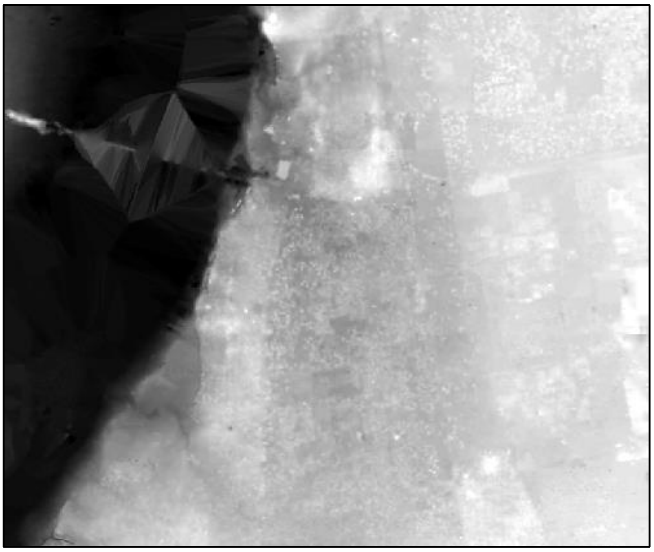

**Figure (3-2): LiDAR DEM 1**

3. An aerial photograph of the study area “Azozab” in the year 2018 (source: Surveying Department of Khartoum Locality), figure (3-3).

**Figure (3-3): Aerial photograph in 2018**

4. Polylines shapefile showing flood extent in 1946, 1988, and the existing protection bank (source: Surveying Department - Khartoum Locality), figure (3-7).
5. A polygons shapefile showing the public administration units (PAUs) of Azozab “source: Surveying Department - Khartoum Locality” but later digitized by the researcher from image 2018), figure (3-8).
6. A table containing the population of the PAUs, obtained from Jabal Awliya locality.

**Table (3-1): Total population of the PAUs in the study area**

| Age & sex / Block | 0-4 M | 0-4 F | 5-14 M | 5-14 F | 15-24 M | 15-24 F | 25-44 M | 25-44 F | 45+ M | 45+ F | Total |
|---|---|---|---|---|---|---|---|---|---|---|---|
| Azozab 2,3 | 396 | 358 | 797 | 718 | 800 | 800 | 1384 | 1342 | 779 | 622 | 7,996 |
| Azozab 1 | 101 | 122 | 220 | 200 | 265 | 270 | 340 | 414 | 238 | 206 | 2,376 |
| Wadajeeb | 184 | 168 | 300 | 304 | 444 | 336 | 567 | 510 | 310 | 245 | 3,368 |
| Dabasin West | 107 | 130 | 239 | 194 | 248 | 215 | 408 | 382 | 219 | 195 | 2,337 |
| Dabasin East | 126 | 141 | 272 | 238 | 353 | 315 | 487 | 489 | 287 | 249 | 2,957 |
| Faroug b 3&10 | 218 | 198 | 369 | 396 | 549 | 467 | 649 | 629 | 377 | 323 | 4,175 |
| Faroug b 1 | 45 | 43 | 91 | 105 | 366 | 88 | 258 | 129 | 80 | 63 | 1,268 |
| Gala b 1 | 151 | 118 | 338 | 303 | 390 | 372 | 450 | 509 | 336 | 298 | 3,265 |
| **Total** | **1,328** | **1,278** | **2,626** | **2,458** | **3,415** | **2,863** | **4,543** | **4,404** | **2,626** | **2,201** | **27,742** |

7. Point coordinates obtained by the researcher through field work carried out using the Global Positioning System (GPS) navigator on (Sept., 2, 2021).

### 3-2- Tools:

1- Laptop Intel(R) Core (TM ) i7-4500U CPU @ 1.80 GHz, 2.40 GHz

2- ArcGIS 10.2 software.

3- GPSMAP60s Navigator.

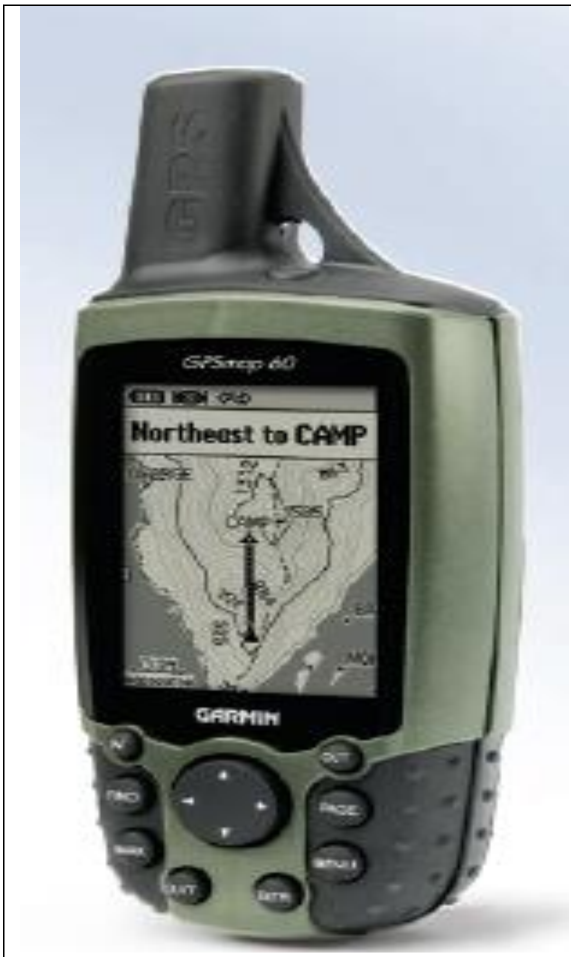


**Figure (3-4): Front face**


**Figure (3-5): Back face**

The general rule of thumb is that **vertical error is three times the horizontal error**. If a decent signal reception is available, a modern GPS receiver should be able to give elevation data accurate to a range of 10 to 20 meters post correction. This represents additional burden on the achievable accuracy. Hence, the calibration of this device is imperative.

### 3-3- Methods:

### 3-3-1- The Study Area:

The study area is Azozab in Khartoum state shown in figure (3-6). The total area is 4,247,568 m² and the Vegetation area is 665,328 $m^2$ (about 166 acre). Azozab is bounded at the north by Alklakla, at the east by Railway, at the west by the White Nile, and at the south by Aldabasin.

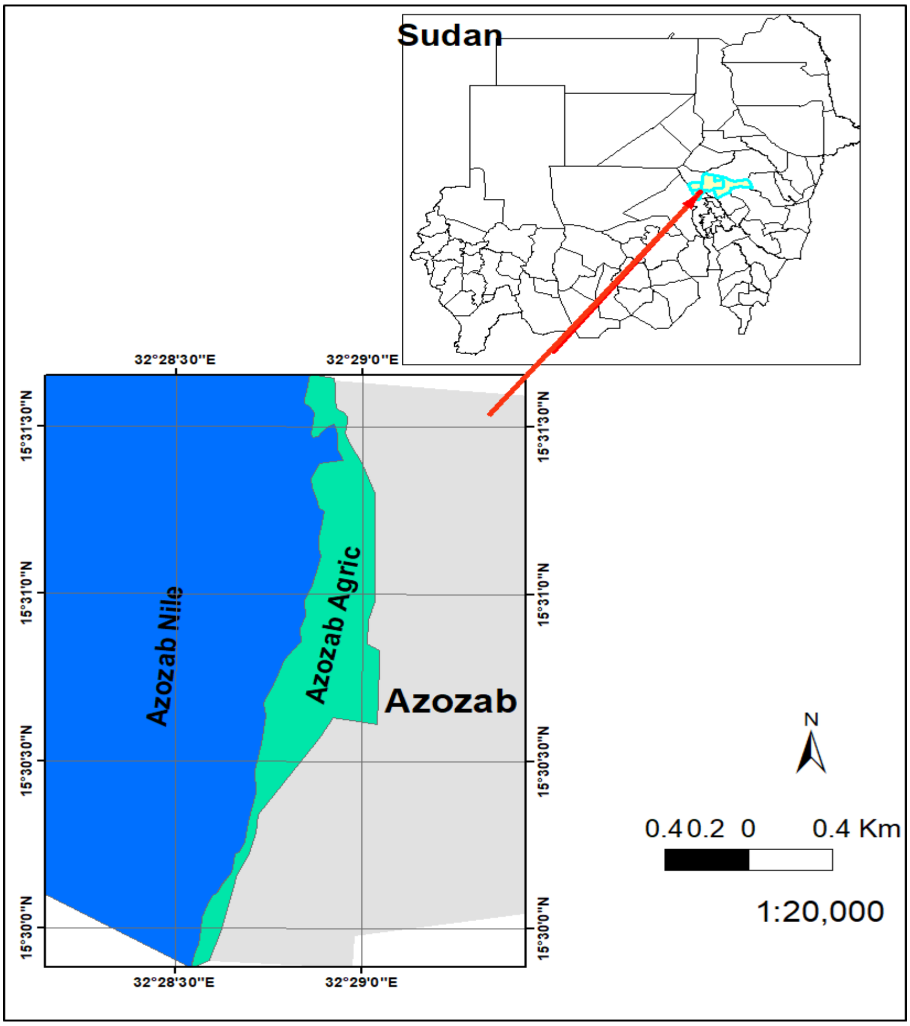


**Figure (3-6): location map of the study area**

### 3-3-2- Research flowchart:

Figure (3-7) reveals the flowchart which was adopted for conducting this research, showing the main steps.

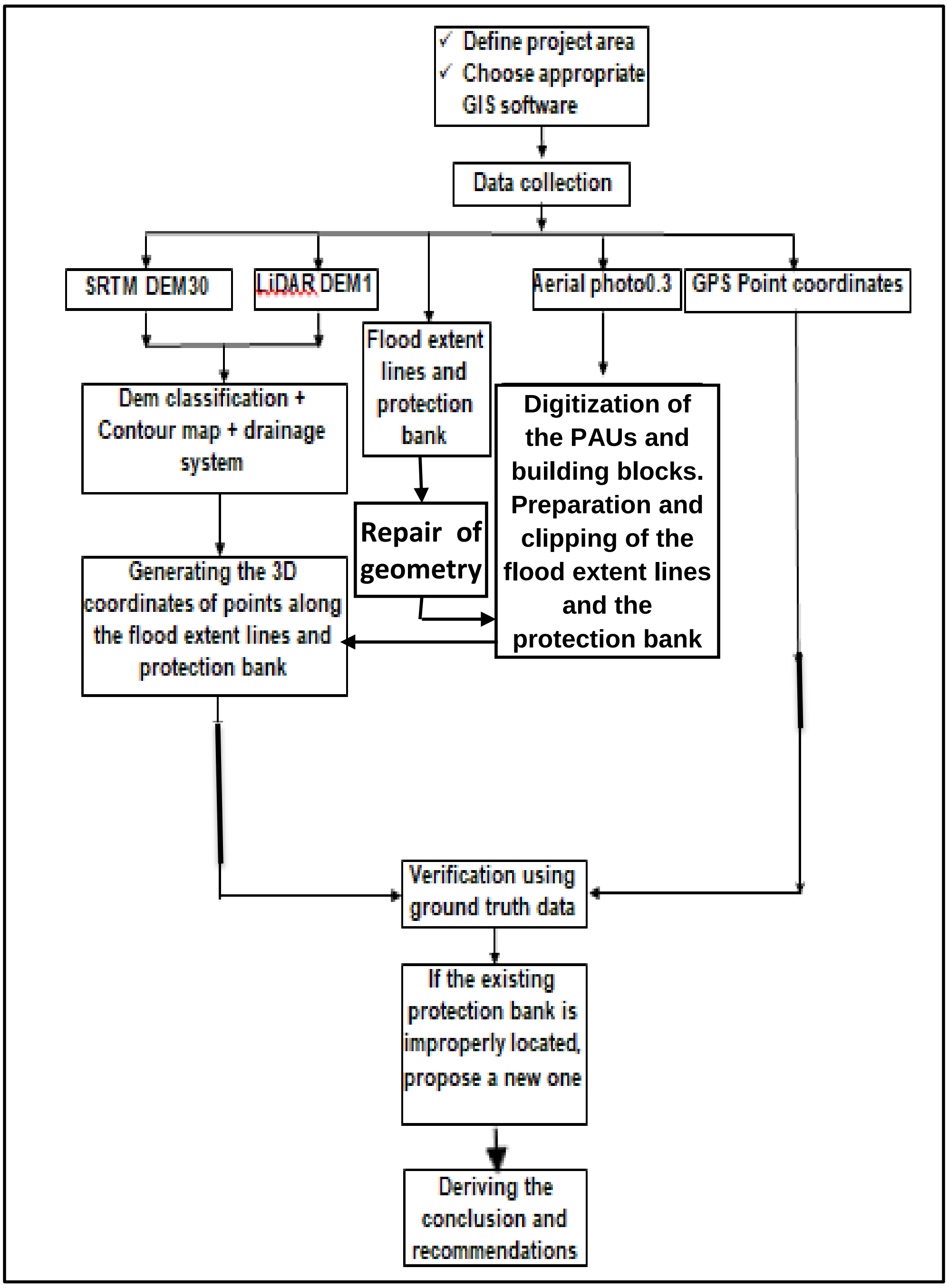


**Figure (3-7): Proposed research flow chart**

### 3-3-3- Research method description:

Following are the details of the method adopted for carrying out the practical part of the research.

#### 3-3-3-1- Classification of LiDAR DEM:

The LiDAR DEM was categorized into 6 classes using the menu item in ArcGIS 10.2 : *Layer properties > Symbology > Classify > then choosing a suitable color ramp*. Result is shown in figure (4-1). The purpose of the DEM classification is to acquire a clear picture of the relief of the study area.

#### 3-3-3-2- Classification of SRTM DEM:

The SRTM DEM was categorized into 6 classes using the menu item in ArcGIS 10.2 : Layer properties > Symbology > Classify > then choosing a suitable color ramp. Result is shown in figure (4-2).

#### 3-3-3-3- Contour from LiDAR DEM:

To acquire an even clearer picture of the relief of the study area, a contour map of the study area was produced from the LiDAR DEM using the tool: *Geostatistical Analyst toolbar*> *Geostatistical Wizard*. Then from the properties of the produced surface, the menu item *Symbology > Classify* was used to fix the contour interval using the equal interval (1 m) method. The interpolation method used for generating the contour map was the *Inverse Distance Weighted (IDW).* Result is shown in figure (4-3).

#### 3-3-3-4- Contour from SRTM DEM:

In the same manner and for the same purpose, a contour map of the study area was produced from the SRTM DEM using the tool: *Geostatistical Analyst toolbar*> *Geostatistical Wizard*. Then from the properties of the produced surface, the menu item *Symbology > Classify* was used to fix the contour interval using the equal interval method. The interpolation method used for generating the contour map was the *Inverse Distance Weighted (IDW).* Result is shown in figure (4-4).

#### 3-3-3-5- Drainage from LiDAR DEM:

Using *ArcHydro tools* to process the LiDAR DEM, the drainage system of the study area was produced. Briefly, the following *ArcHydro menu* items were used in sequence: *1)Fill sinks, 2)Flow direction, 3)Flow accumulation, 4)Stream definition, 5)Stream segmentation, 6)Catchment grid delineation, 7)Catchment polygon processing, 8)Drainage lines, 9)Drainage points, and 10)Adjoint catchment processing*. Figure (4-5).

### 3-3-3-6- Drainage from SRTM DEM:

For comparison of the results obtained from the LiDAR DEM with those obtained from the SRTM DEM. Using the *ArcHydro* tools to process the SRTM DEM, the drainage system of the study area was produced. The *ArcHydro* menu items used in 3-3-3-5 were also used here. Result is shown in figure (4-6).

### 3-3-3-7- Digitized PAUs:

The PAUs of the study area were digitized from the 2018 image which was used as a background for editing using the *Editor toolbar*. The PAUs are shown in figure (4-7).

### 3-3-3-8- Digitized blocks:

The blocks of the study area were digitized using the 2018 image as a background for editing the blocks, using the *Editor* toolbar. The blocks were overlaid on the PAUs and shown in figure (4-8).

### 3-3-3-9- Flood extent lines and protection banks preparation:

The flood extent lines of 1946, 1988, and the existing protection bank shapefile obtained from the Surveying Department of Khartoum Locality were processed as follows:

1) Because the original shapefile obtained from the Surveying Department of Khartoum Locality was topologically incorrect, a separate shapefile was produced for the 1946 flood extent line in the following manner:
    a. A new shapefile was created using *ArcCatalogue*, named 1946 flood line.
    b. The *Start Editing mode* of this new shapefile was enabled.

c. 1946 flood line feature was selected from the original shapefile using the tool: *Select Features* from the *Editor tool bar* .

d. The selected 1946 flood line was copied using the tool: *Edit Tool* from the Editor tool bar.

e. The copied 1946 flood line was pasted in the new shapefile.

f. The 1946 flood line shapefile was saved.

2) The steps from (a) to (f) were repeated to produce the other two lines, namely the 1988 flood extent line and the protection bank. Result is shown in figure (4-9).

### 3-3-3-10- Merging the segments of each line:

Each of the lines prepared in (3-2-3-9), was found containing more than one segment. Thus, each of them was merged using the menu item: *Merge* contained in *the Editor Menu bar.*

### 3-3-3-11- Splitting the merged lines:

Because the From-nodes and To-nodes of the original lines were not properly organized, it was found necessary to create new continuous lines by tracing each of the lines merged as described in (3-2-3-10) using the tool: *Editor* > *Trace.*

It was decided to divide each of the lines into equal segments (intervals) each interval is 60 m long. Unfortunately, it was found that this process could not be completed using the tool: *Split* contained in *the Editor Menu bar* of ArcGIS10.2.

Therefore, the menu item: *Vector* > *Qchainage* or the menu item of the QGIS Desktop 3.4.3.(Madeira) was used to divide each line into 60 m long segments starting from station 0 (t the north) to the end of each line (at the south).

### 3-3-3-12- Converting vertices to points:

The vertices of each of the lines split in (3-2-3-11) were converted into points using the tool: *Arctoolbox> Data Management Tool > Features > Feature Vertices To Points*.

### 3-3-3-13- Clipping the point shapefie:

In order to limit the points to the boundary of the study area, the point shapefile which resulted in (3-3-3-12) was clipped by the study area boundary using the tool: *Analysis Tools* > *Extract* > *Clip*. Result is shown in figure (4-10).

### 3-3-3-14- Calculation of the planimetric coordinates of the points:

The X,Y coordinates of the points of each of the two flood lines and protection bank were calculated using the tool: *ArcToolbox > Data Management Tools> Features> Add XY Coordinates.* Refer to tables (A1, A2, A3, A4, A5, A6, A7, and A8) in the appendices.

### 3-3-3-15- Calculation of the elevations of the points along each of the two flood lines and the protection bank:

**1- Elevations of 1946 flood line points from the LiDAR DEM:**

The elevations (Z) of the points of 1946 flood line were calculated using the tool: *ArcToolbox > 3D Analyst> Functional Surface > Add Surface Information* and the LiDAR DEM as the surface from which the elevation information were acquired. Refer to table (A1) in the appendices.

**2- Elevations of 1988 flood line points from the LiDAR DEM:**

In a similar manner, the elevations (Z) of the points of 1988 flood line were calculated using the LiDAR DEM as the surface from which the elevation information were acquired. Refer to table (A2) in the appendices.

**3- Elevations of the protection bank points from the LiDAR DEM:**

In a similar manner, the elevations (Z) of the protection bank points were calculated using the LiDAR DEM as the surface from which the elevation information were acquired. Refer to table (A3) in the appendices.

Table (A4) in the appendices includes the elevations of the three lines extracted from the LiDAR DEM.

**4- Elevations of 1946 flood line points from SRTM DEM:**

In a similar manner, the elevations (Z) of the points of 1946 flood line were calculated using the SRTM DEM as the surface from which the elevation information were acquired. Refer to table (A5) in the appendices.

**5- Elevations of 1988 flood line points from the SRTM DEM:**

In a similar manner, the elevations (Z) of the points of 1988 flood line were calculated using the SRTM DEM as the surface from which the elevation information were acquired. Refer to table (A6) in the appendices.

**6- Elevations of the protection bank points from the SRTM DEM:**

In a similar manner, the elevations (Z) of the protection bank points were calculated using the SRTM DEM as the surface from which the elevation information were acquired. Refer to table (A7) in the appendices.

Table (A8) in the appendices includes the elevations of the three lines extracted from the SRTM DEM.

### 3-3-3-16- Population Density Calculation:

Table (3-1), which contains the population of the PAUs, obtained from Jabal Awliya locality was used to calculate the population density of each of the PAUs (Persons/Km$^2$) by dividing the population over the area (in Km$^2$). The calculated density is shown in table (4-1) and figure (4-9). The density calculation result of the PAUs was analyzed in conjunction with the 1946 flood extent line.

### 3-3-3-17- QQ plot using ArcGIS10.2:

The General QQ plot was prepared using ArcGIS10.2 tool bar: *Geostatistical Analyst > Explore Data > General QQ plot*. In the dialog box which occurs, each of the two datasets (LiDAR DEM Fishnet and SRTM DEM Fishnet) were added together with the attribute which is to be compared (i.e. the elevation). The result is shown in figure (4-23).

### 3-3-3-18- Overlay the 1946 flood line on the population density map:

For the analysis of the flood impact on the different PAUs, the flood extent line of 1946 was overlaid on the map of the PAUs' population density, and the result was shown in figure (4-7).

### 3-3-3-19- Overlay of the services:

To make sure of the status of the services regarding the flood impact (affected, threatened, or safe), the elevations of the locations of the services should be extracted (calculated) from the LiDAR DEM and compared to the elevations of the corresponding points along the 1946 flood line + 0.30 m (extra height). A problem was faced with ArcGIS 10.2 software when trying to calculate such elevations, hence the Desktop QGIS 3.4.3. tool: *Point Sampling*  was used.

Tables (4-3), (4-4), and (4-5) show the affected services, the threatened ones, and the safe ones in the study area. Figure (4-12) shows the spatial distribution of the same in the study area.

### 3-3-3-20- Preparation of the profiles of each of the lines:

1. The profile of each of the lines (1946, 1988 flood lines and protection bank) were produced from tables A1, A2, and A3 respectively "obtained from the LiDAR DEM" using Excel menu item: *Insert> Line Graph.* Figures (4-13), (4-14), and (4-15).
2. The profile of each of the lines (1946, 1988 flood lines and the protection bank) were produced from the tables A5, A6, and A7 "obtained from the SRTM DEM" using Excel menu item: *Insert> Line Graph.* Figures (4-16), (4-17), and (4-18).
3. For ease of comparison, the profiles of the three lines were produced using the table (4-12) which were based on the LiDAR DEM. Figure (4-19).
4. For ease of comparison, the profiles of the three lines were produced using the tables (4-13) which were based on the SRTM DEM. Figure (4-20), and the statistics
5. Moreover, the profile of the flood line 1946 was prepared from each of the LiDAR DEM and SRTM DEM. Figure (4-21).

6. Also, the profile of the flood line 1988 was prepared from each of the LiDAR DEM and SRTM DEM. Figure (4-22).
7. Likewise, the profile of the protection bank was prepared from each of the LiDAR DEM and SRTM DEM. Figure (4-23).

**3-3-3-21- Calculation and construction of the necessary height increments:**

Since the flood level during 1946 was the highest, it was taken as a reference for calculating the necessary height increments to be added to the level of each station of the existing protection bank.

Table (A9) in the appendices shows the calculated increments. The method of calculation and construction of the increments was as follows:

Level of flood in 1946 at each station **less** level of the existing protection bank at the nearest station **plus** 0.30 m (extra increment to the level of flood in 1946 in order to safeguard against any future flood level which may exceed that of 1946).

For construction purposes, the top surface of the protection bank increments should have the required slope from chainage station to the next, e.g. as shown in the sketch in figure (3-8).

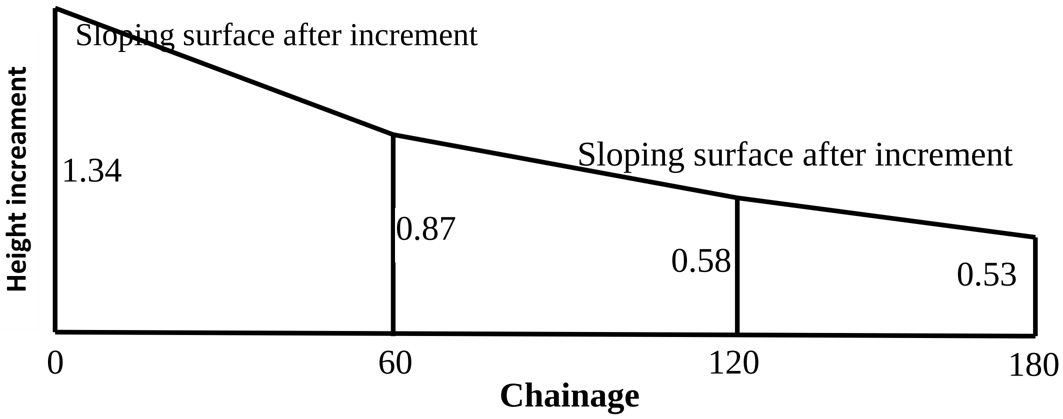


**Figure (3-8): Method of construction of existing protection bank increments**

**Table (3-2): Sample of increments extracted from table (A9)**

| Chainage | Flood 46 level(m) | Protection level(m) | 46 flood – protection(m) | 46-protection + 0.3 m |
|---|---|---|---|---|
| **0** | 383.70 | 382.66 | 1.04 | **1.34** |
| **60** | 383.86 | 383.28 | 0.57 | **0.87** |
| **120** | 384.15 | 383.87 | 0.28 | **0.58** |
| **180** | 384.27 | 384.03 | 0.23 | **0.53** |

**3-3-3-22- LiDAR and SRTM DEMs Accuracy assessment:**

Tables from No. (4-6) up to (4-14) show the statistics of the elevations of points **along** the two flood lines (1946 and 1988), and the protection bank extracted from the LiDAR DEM as well as from the SRTM DEM for the purpose of the assessment of the accuracy of each of the DEMs data. This process yielded fair results and offered a clear picture about how accurate is each dataset compared to the other, but the compared data size is limited to the width of each line.

In order to acquire a clearer picture in this regard, it was decided to use as many data points as may be possible, based on the capacity of the PhD. student's computer processor (i.e. to extend the data points' range so that the data is acquired not from a mere line but from an area). Thus, a fishnet was created from a subset of each dataset (this subset was extracted from both datasets using the same boundary), using the ArcGIS10.2 tool: *Data Management Tools > Feature class > Create Fishnet.* Figure (4-22).

The (X, Y) coordinates of the fishnet points were calculated and the elevations of the same points were extracted once from the LiDAR DEM and then from the SRTM DEM. Table (A10) in the appendices.

**3-3-3-23- Ground truth using Garmin GPSMAP60CSx navigator:**

On Sept. 02, 2021 AD., the PhD. student carried out a field work aiming at collecting points coordinates to be used for ground truthing and to get a general idea about the topography of the study area "Azozab". The collected 3 coordinates of points are shown in table (A11) in the appendices.

To get the altitudes at the ground surface, the measured altitudes were reduced by 0.65 m which the height above the ground surface at which the navigator was held. Both altitude values were plotted and shown in figure (4-23).

# Chapter Four

# Results and Discussions

## 4- Results and Discussions:

### 4-1- Classified LiDAR DEM1m:

In order to get a clear picture of the topography of the study area, the LiDAR digital elevation model was classified and presented in figure (4-1). As expected, the area adjacent to the White Nile is the lowest area (the elevations range from 375.91 m to 382 m above mean sea level). The highest area is located at the south-eastern part and most of the western part of the study area, (the elevations range from 383.25 m to 388.54 m above mean sea level). The elevations of the rest of the study area are medium (elevations range from 382.01 m to 383.24 m above mean sea level). Refer to the legend of the classified LiDAR DEM in figure (4-1).

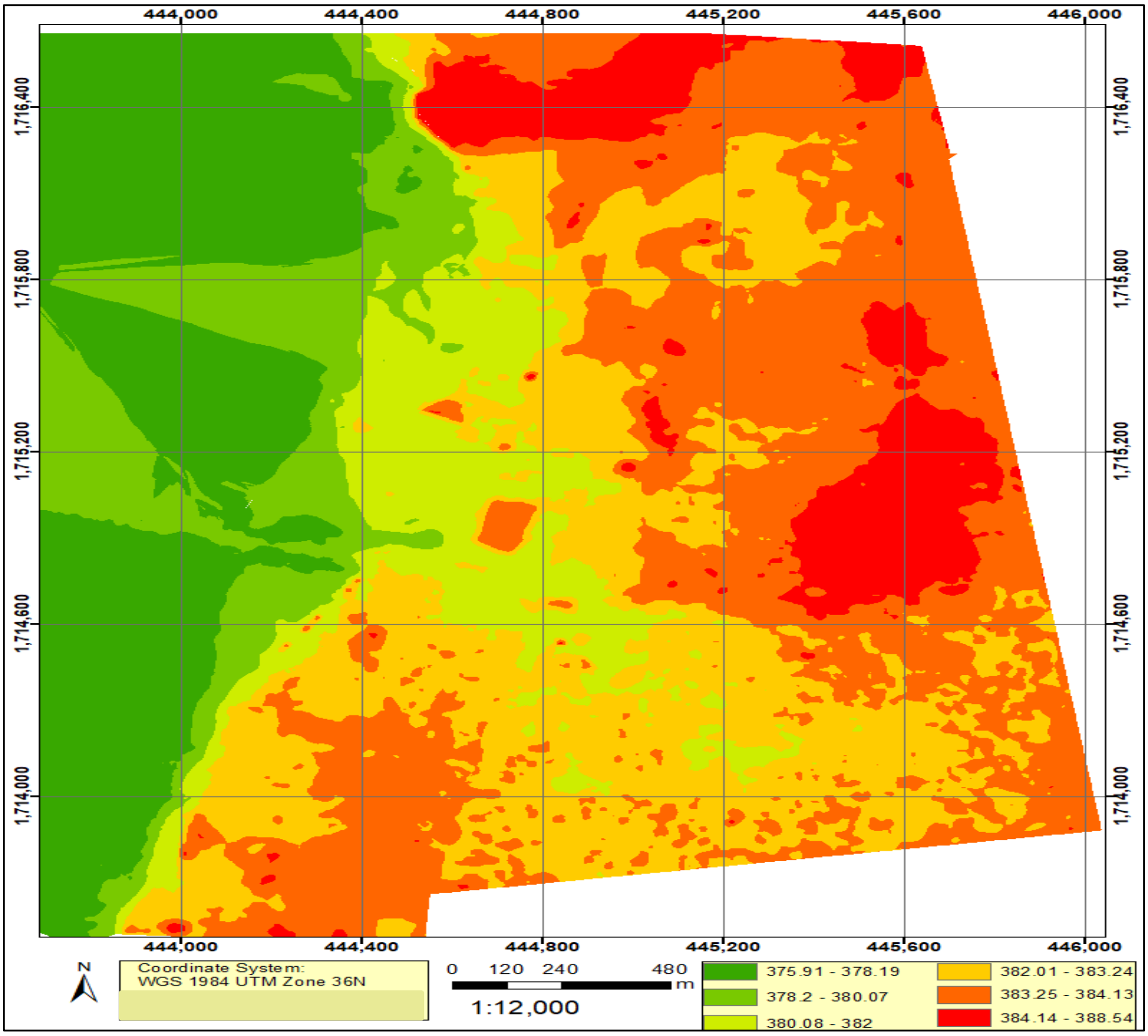


Figure (4-1): classified LiDAR DEM

## 4-2- Classified SRTM DEM30m:

In order to get a clear picture of the topography of the study area, the SRTM digital elevation model was classified and presented in figure (4-2). As expected, the area adjacent to the White Nile is the lowest area (the elevations range from 371 m to 381 m above mean sea level). The rest of the study area varies between low, medium, and high locations (the elevations range from 382 m to 393 m above mean sea level). Refer to the legend of the classified SRTM DEM in figure (4-2).

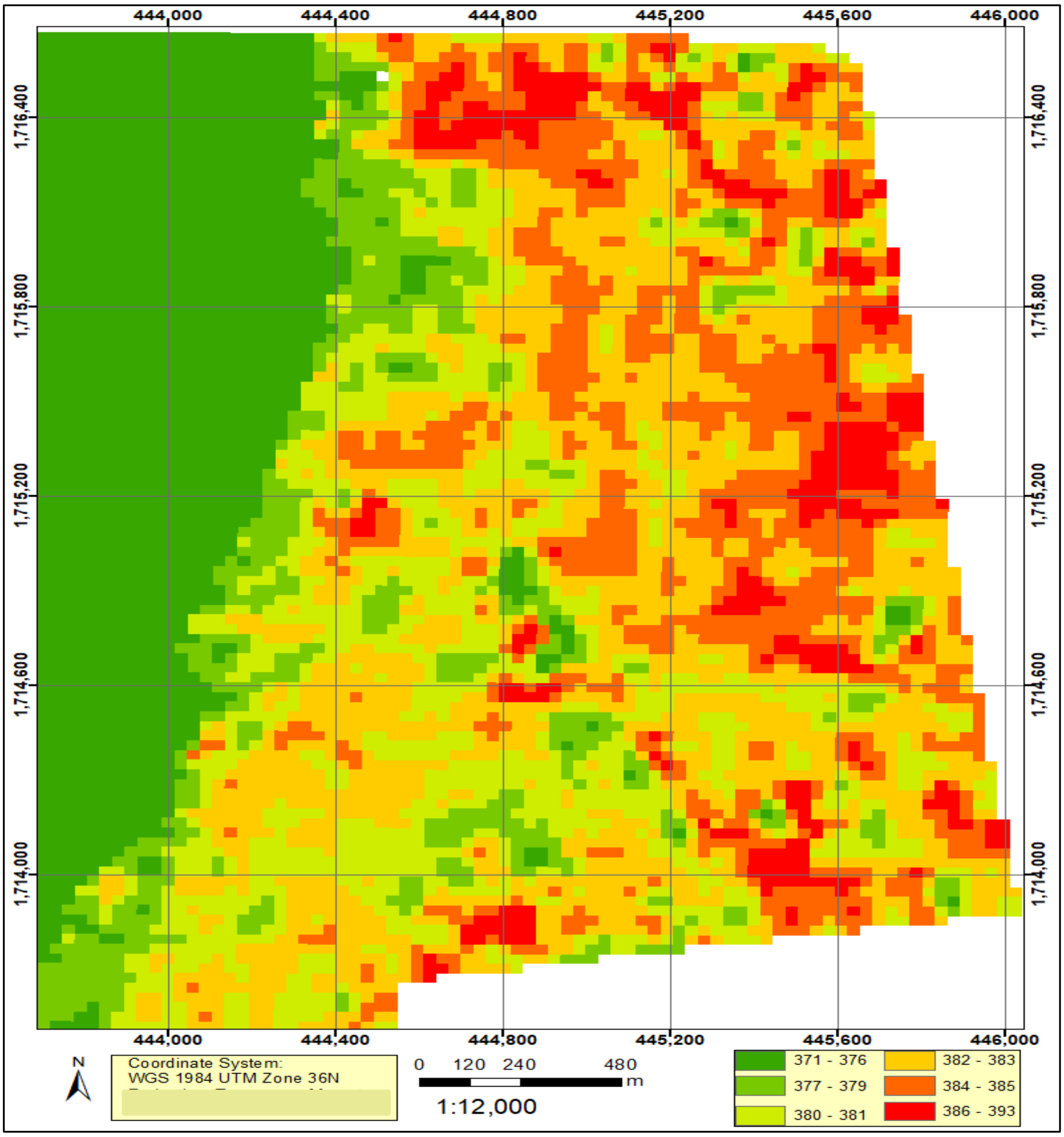


**Figure (4-2): Classified SRTM DEM**

### 4-3- Contour lines from LiDAR DEM:

In order to get a clearer and more detailed picture of the topography of the study area, a contour map which was produced from the LiDAR DEM was shown in figure (4-3). The contour interval (height variation) was 0.5 m.

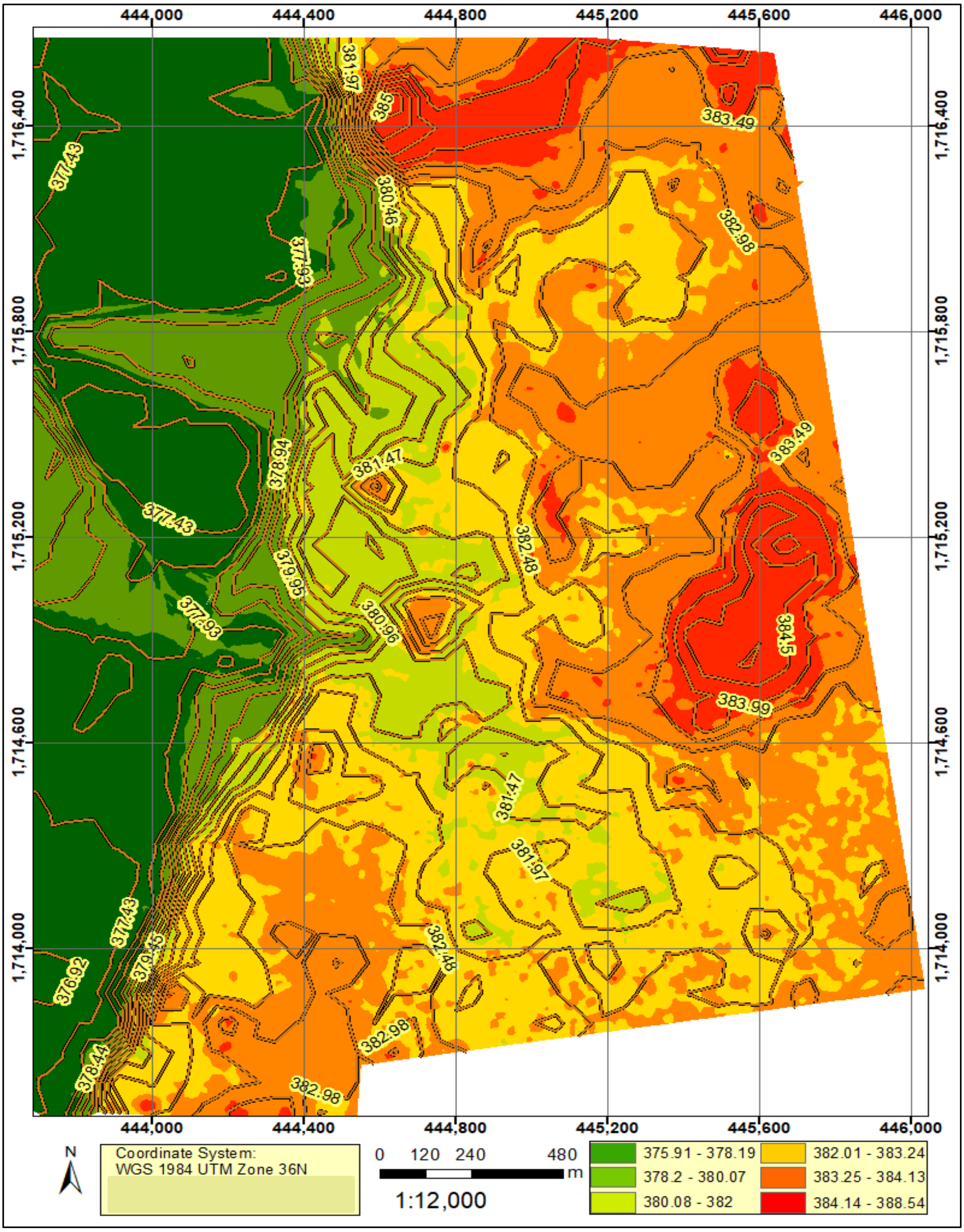


**Figure (4-3): Contour lines from LiDAR DEM**

## 4-4- Contour lines from SRTM DEM:

In order to get a clearer and more detailed picture of the topography of the study area, a contour map which was produced from the SRTM DEM was shown in figure (4-4). The contour interval (height variation) was 1 m.

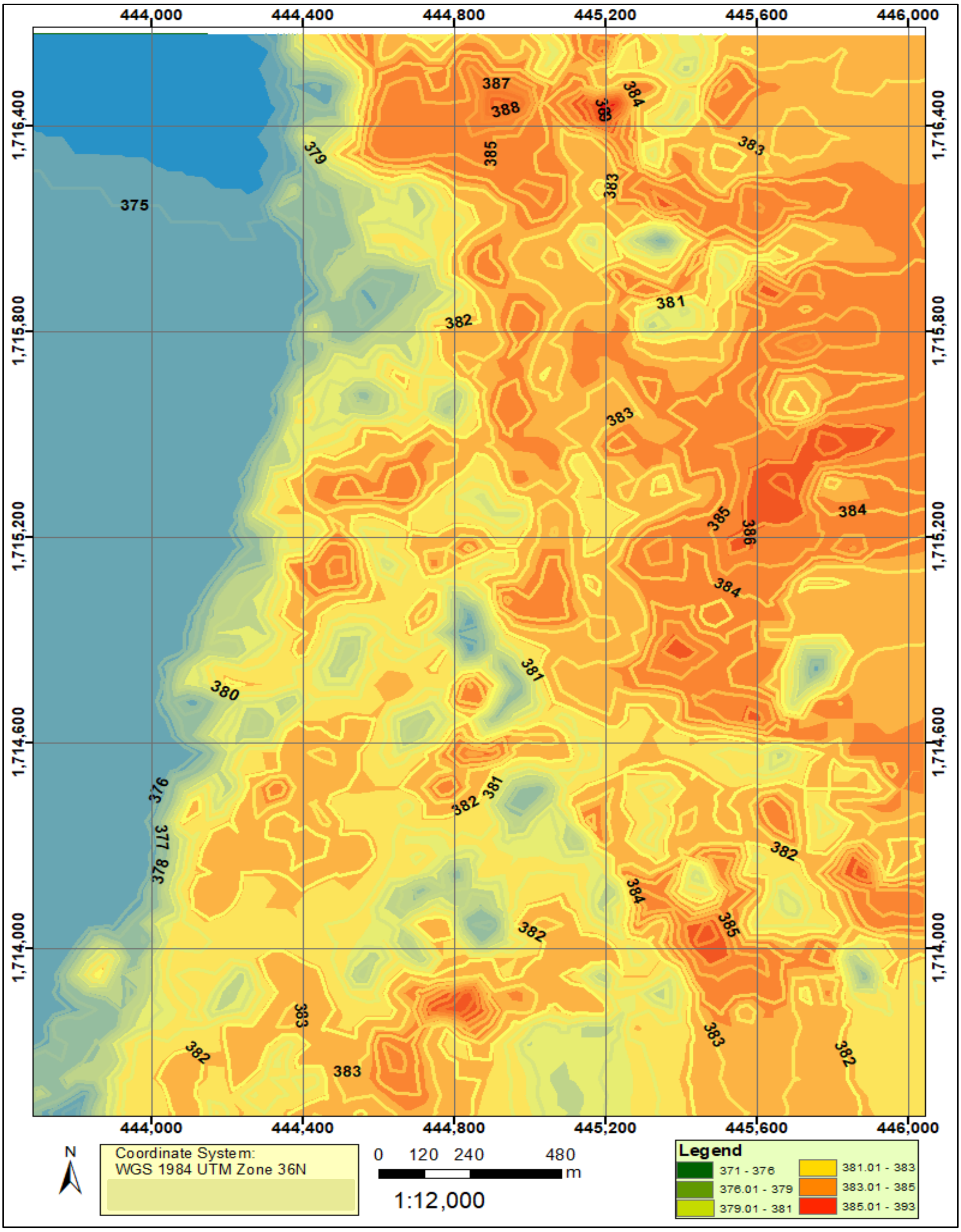


**Figure (4-4): Contour lines from SRTM DEM**

## 4-5- Drainage System from LiDAR DEM:

The drainage system of the study area produced from LiDAR DEM 0.3 is shown figure (4-5).

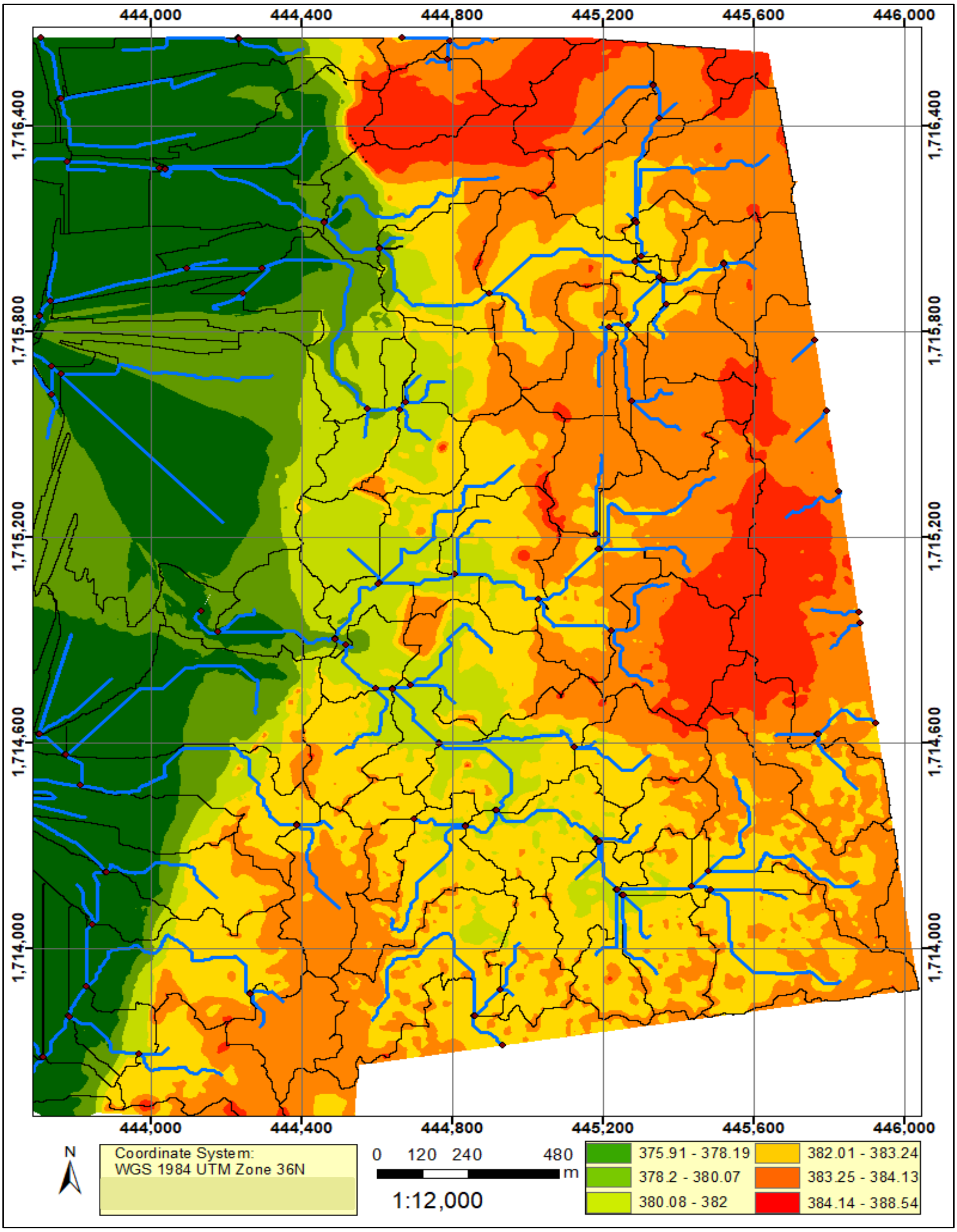


**Figure (4-5): Drainage System from LiDAR DEM**

## 4-6- Drainage System from SRTM DEM 30m:

The drainage system of the study area produced from SRTM DEM 30 is shown figure (4-6).

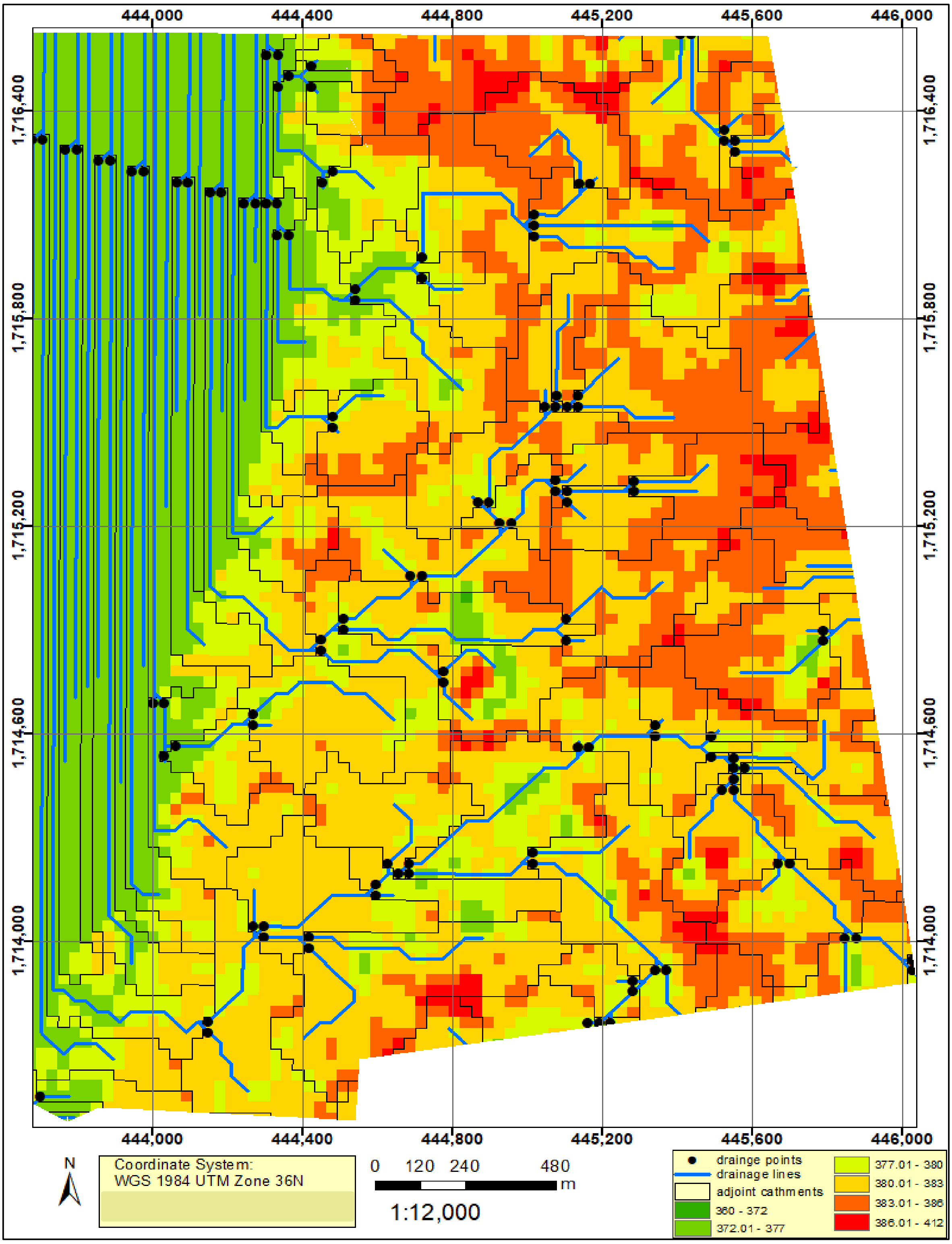


**Figure (4-6): Drainage System from SRTM DEM**

### 4-7- Digitized PAUs:

The PAUs of the study area were digitized from the 2018 image. The populations of the different PAUs (obtained in a table from Jabal Awliya locality) were linked to the digitized PAUs, and the population density of each PAU was calculated and displayed in figure (4-7). This enables the researcher to have a clear picture of the distribution of the population in the study area.

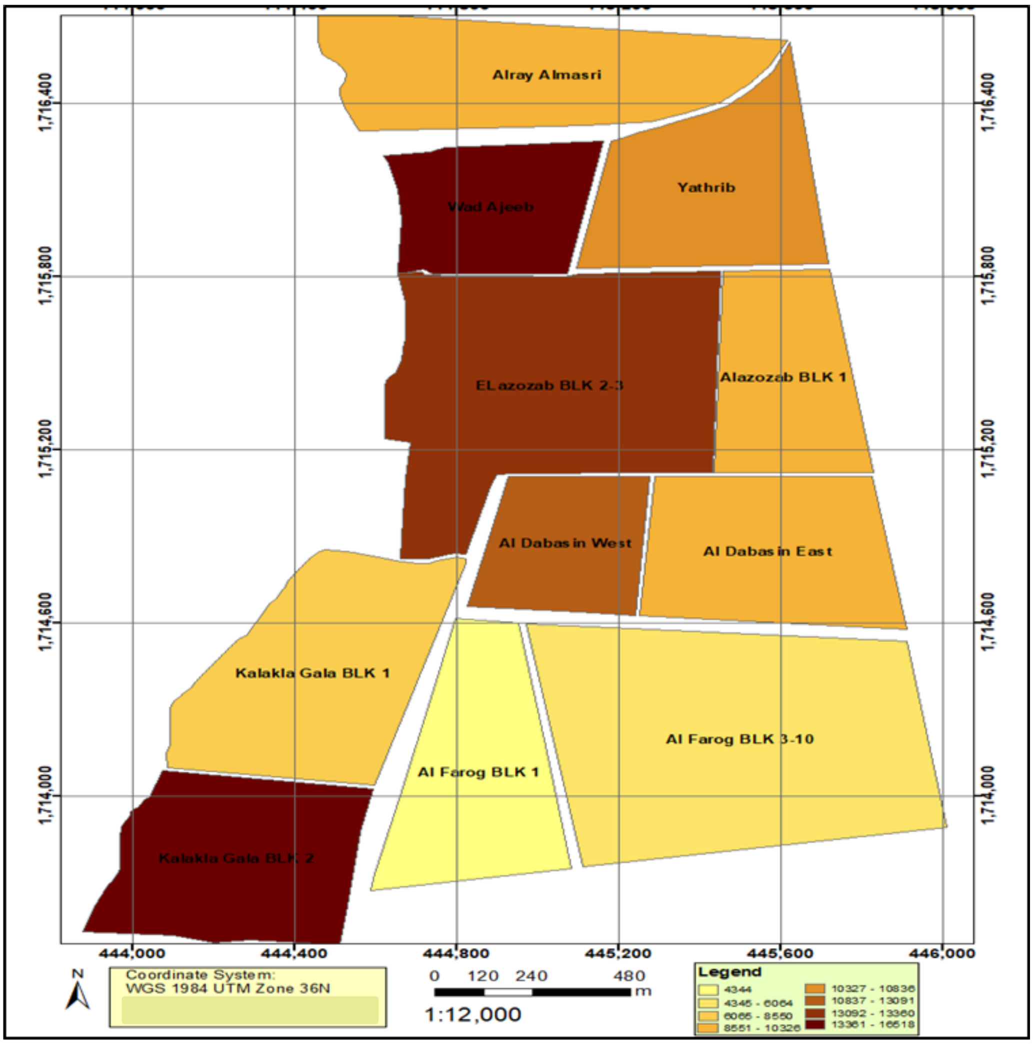


**Figure (4-7): PAUs of the study area**

## 4-8- Digitized blocks:

The blocks of the study area were digitized from the 2018 image. These blocks can be used to get an idea about the population density of each of the PAUs. Figure (4-8).

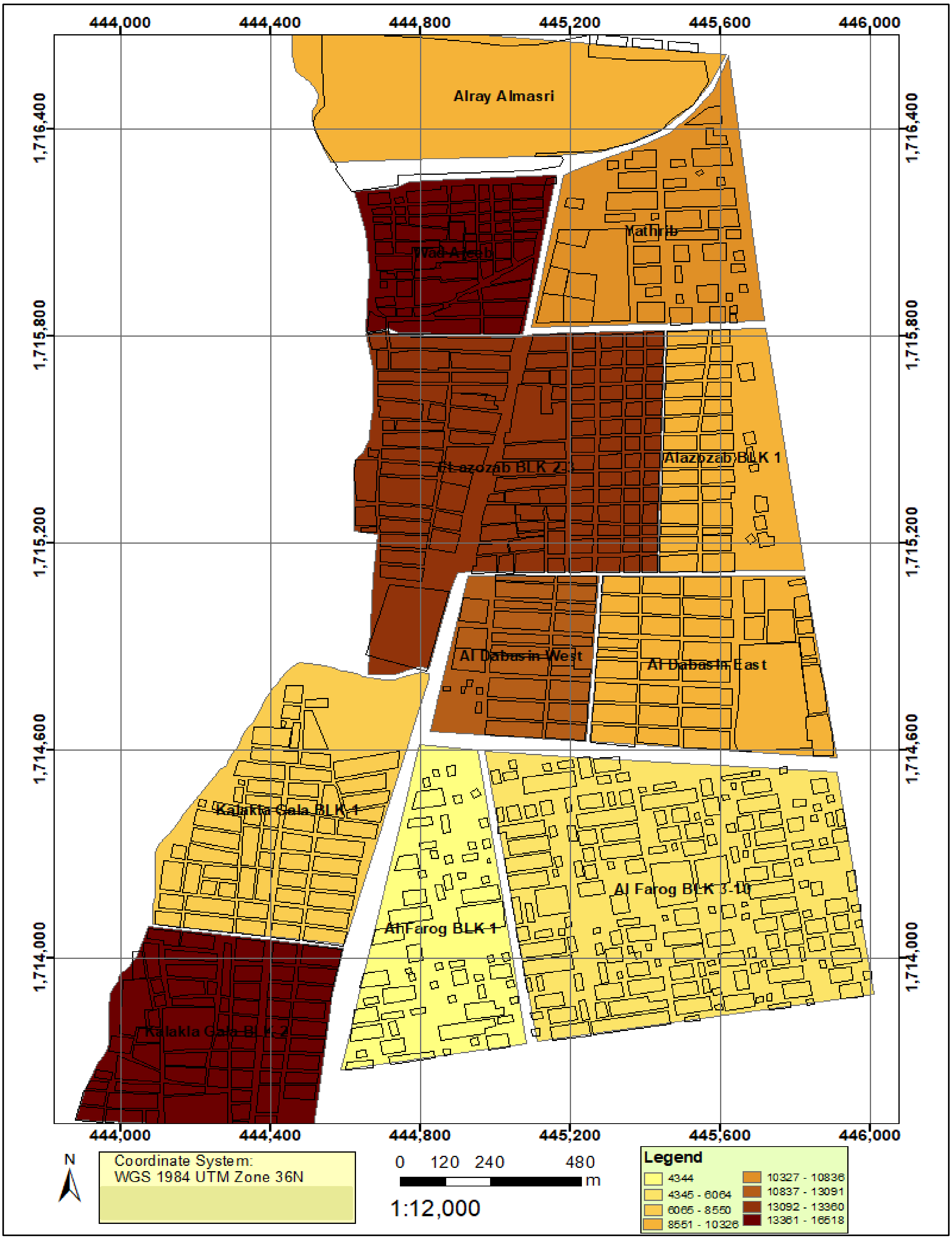


**Figure (4-8): Blocks of the study area**

### 4-9- Flood extent (1946 and 1988) and protection bank:

The polylines shapfiles (showing flood extent in 1946, 1988, and the existing protection bank) after they have been geometrically corrected and before and after clipping them using the study area boundary are shown in figures (4-9) and (4-10) respectively. The planimetric coordinates of the start and end of each of the flood extent lines and the protection bank after being clipped using the boundary of the study area are shown in table (4-1).

**Table (4-1): Coordinates of the start and end points**

| Point No. | Line name | X-start (m) | Y-start (m) | X-end (m) | Y-end (m) |
|---|---|---|---|---|---|
| 1 | Flood extent line 1946 | 445,031.7 | 1,716,654.1 | | |
| 2 | | | | 444,473.5 | 1,713,511.5 |
| 3 | Flood extent line 1988 | 445,022.9 | 1,716,656.2 | | |
| 4 | | | | 444,451.7 | 1,713,499.6 |
| 5 | Protection line | 444,639.2 | 1,716,650.8 | | |
| 6 | | | | 443,865.3 | 1,713,533.3 |

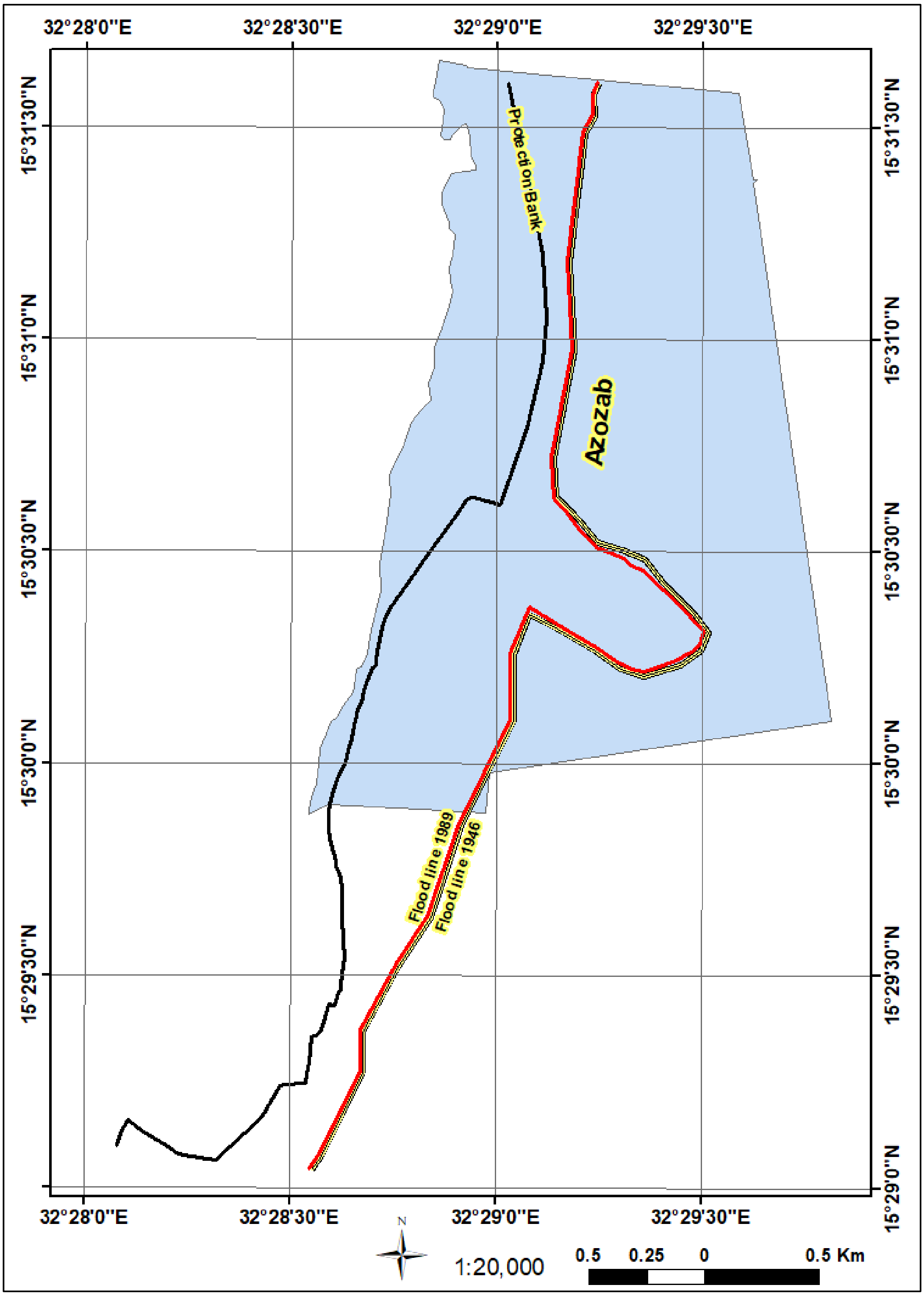


**Figure (4-9): Flood lines and protection bank before clipping using Azozab area**

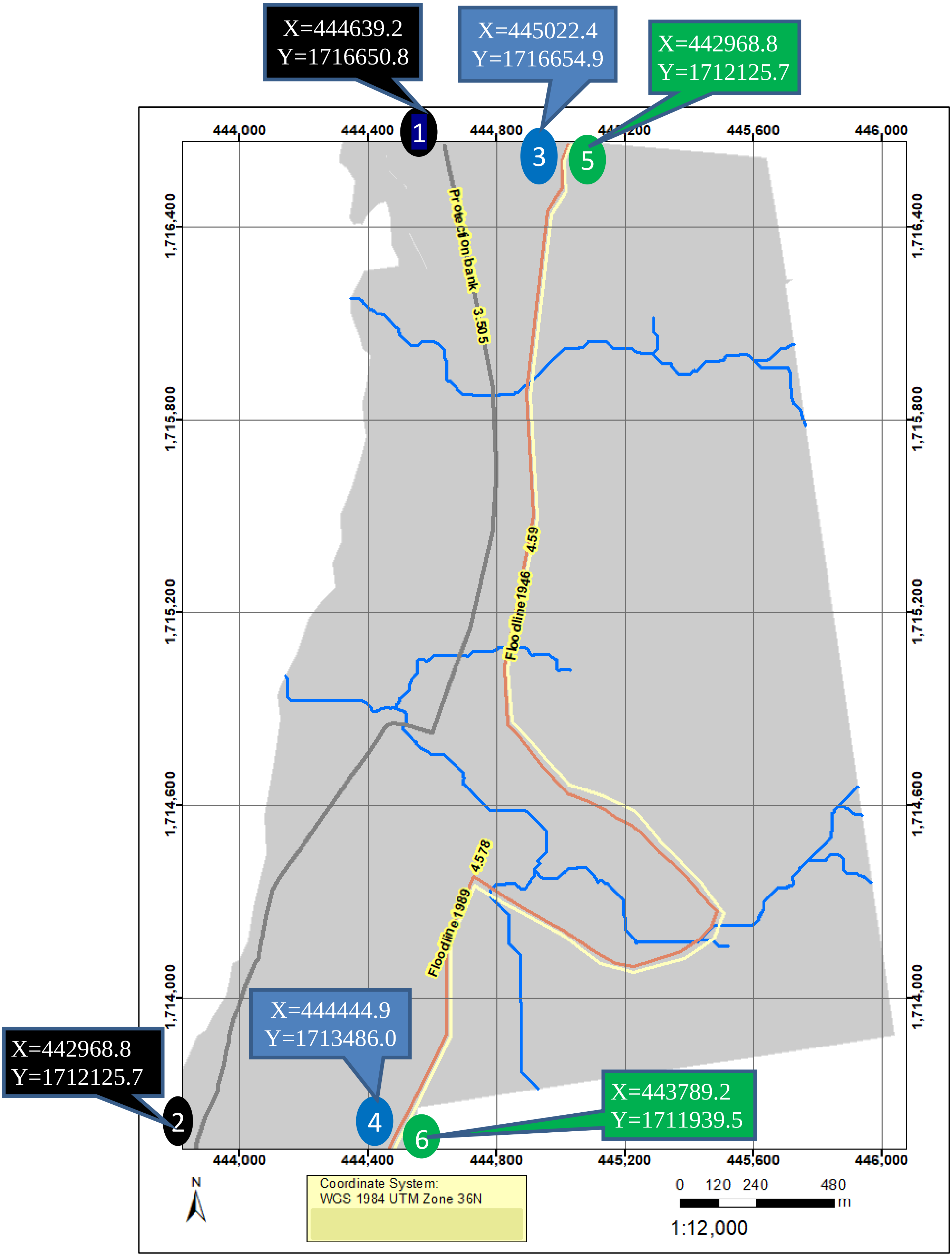


**Figure (4-10): Flood lines and protection bank after clipping using Azozab area**

### 4-10- Population density Analysis:

From table (4-2), which shows the population density in the study area, it is clear that the highest population density is at Wad Ajeeb unit (16,518 persons/Km$^2$) followed by Kalakla Gala Blk 2 (15,488 persons/Km$^2$), then ELazozab BLK 2-3 (13,360 persons/Km$^2$), and Al Dabasin West (13,091 persons/Km$^2$) which are listed at the top of table (4-2) while the lowest density is at Alfarog blk1 (4,344 persons/Km$^2$) which is listed under serial number (11) in the table.

**Table (4-2): Population density in the study area**

| SN | PAU_Name | Population | Area (m$^2$) | Area (Km$^2$) | Density (Population/area) |
|---|---|---|---|---|---|
| *1* | *Wad Ajeeb* | *3,368* | *203,904.8* | *0.2039048* | *16,518* |
| *2* | *Kalakla Gala BLK 2* | *5,066* | *327,082.4* | *0.3270824* | *15,488* |
| *3* | *ELazozab BLK 2-3* | *9,007* | *598,492.8* | *0.5984928* | *13,360* |
| *4* | *Al Dabasin West* | *2,337* | *178,517.3* | *0.1785173* | *13,091* |
| 5 | Yathrib | 3,221 | 297,252.4 | 0.2972524 | 10,836 |
| 6 | Alazozab BLK 1 | 2,376 | 230,104.1 | 0.2301041 | 10,326 |
| 7 | Alray Almasri | 3,604 | 354,040.1 | 0.3540401 | 10,182 |
| 8 | Al Dabasin East | 2,957 | 301,865.3 | 0.3018653 | 9,796 |
| 9 | Kalakla Gala BLK 1 | 3,265 | 381,863.3 | 0.3818633 | 8,550 |
| 10 | Al Farog BLK 3-10 | 4,175 | 688,453.1 | 0.6884531 | 6,064 |
| *11* | *Al Farog BLK 1* | *1,268* | *291,901.5* | *0.2919015* | *4,344* |

Furthermore, from figure (4-11), which shows the highest flood line (46) overlaid on the PAUs' population density map, the four high density population PAUs, which are listed at the top of table (4-2), should be given more attention in order to avoid destructive flood risks.

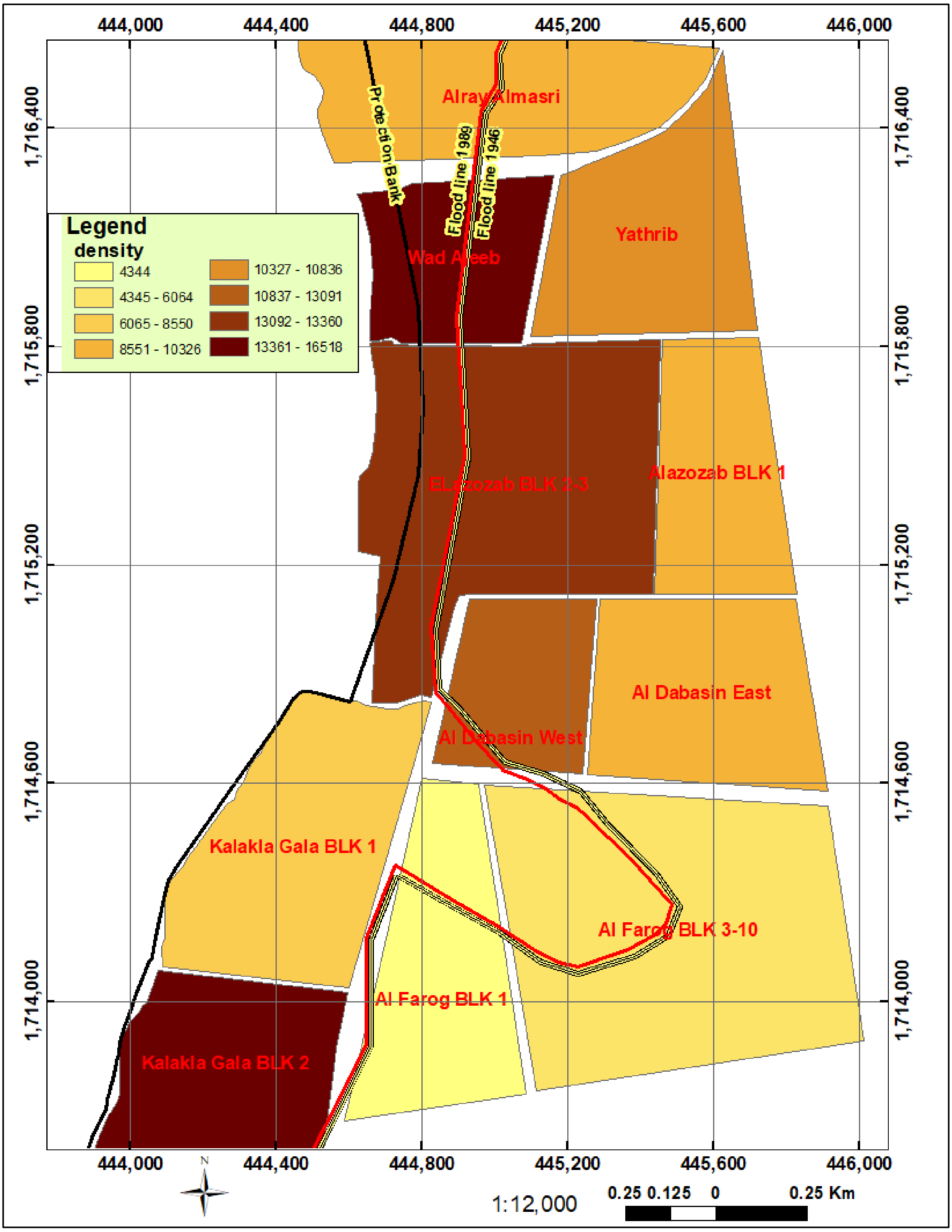


**Figure (4-11):Population Density in the study area**

## 4-11- The situation of services in the study area:

Analysis result of the situation of the services - with respect to the flood impact - existing in the study area is shown in tables (4-3) affected services, (4-4) threatened services, and (4-5) safe services, as well as figure (4-12).

### 1. Affected services:

These are service located inside the flood extent of 1946 and they include 5 mosques + 3 Education + 1 health + 1 WP + 1 PS = 11

**Table (4-3): Affected services**

| SN | Service type | Reduced level (m) | Reduced level rank |
|---|---|---|---|
| 1 | PS | 381.80 | |
| 2 | Mosque | 381.77 | |
| 3 | Education | 381.40 | |
| 4 | Mosque | 382.36 | |
| 5 | Health | 382.45 | |
| 6 | WP | 382.34 | |
| 7 | Education | 382.50 | |
| 8 | Education | 382.56 | |
| 9 | Mosque | 381.77 | |
| ***10*** | ***Mosque*** | ***382.65*** | ***Max.*** |
| ***11*** | ***Mosque*** | ***380.94*** | ***Min.*** |

### 2. Threatened services:

These are the services located at Threatened services are 8 educational ones.

**Table (4-4): Threatened services**

| SN | Services | Reduced Level(m) | Reduced level(m) |
|---|---|---|---|
| 1 | Education | 381.83 | |
| **2** | **Education** | **382.66** | **Max.** |
| 3 | Education | 381.73 | |
| 4 | Education | 381.88 | |

| SN | Services | Reduced Level(m) | Reduced level(m) |
|---|---|---|---|
| ***5*** | ***Education*** | ***381.57*** | ***Min.*** |
| 6 | Education | 381.87 | |
| 7 | Education | 381.94 | |
| 8 | Education | 382.08 | |

**3. Safe services:**

Safe services include 8 mosques + 6 education + 2 health + 1 Market + 1 church + 1 WP.

**Table (4-5) : Safe services**

| SN | Service type | Reduced level (m) | Reduced level rank |
|---|---|---|---|
| 1 | Mosque | 382.54 | |
| 2 | Mosque | 382.64 | |
| ***3*** | ***Education*** | ***385.04*** | ***Max.*** |
| 4 | Mosque | 384.79 | |
| 5 | Mosque | 382.78 | |
| 6 | Mosque | 383.08 | |
| 7 | Church | 383.23 | |
| 8 | Mosque | 382.70 | |
| 9 | Mosque | 382.94 | |
| 10 | Health | 382.38 | |
| 11 | Education | 382.65 | |
| 12 | Education | 382.40 | |
| 13 | WP | 382.88 | |
| 14 | Market | 382.52 | |
| ***15*** | ***Health*** | ***382.28*** | ***Min.*** |
| 16 | Education | 382.66 | |
| 17 | Education | 383.08 | |
| 18 | Mosque | 382.88 | |
| 19 | Education | 382.55 | |

The total number of services in the study area is 38 ones, according the following details: 19 safe services + 8 threatened ones +11 affected ones

Affected services are the ones which are located inside the flood extent of 1946 and shown in the map in a red-coloured symbol and label, threatened ones are those located within 200 meters away from the flood extent line of 1946 and shown in the map in a black-coloured symbol and label, and safe ones are those located at a distance that exceeds 200 meters from the flood extent line of 1946 and shown in the map in a green-coloured symbol and label.

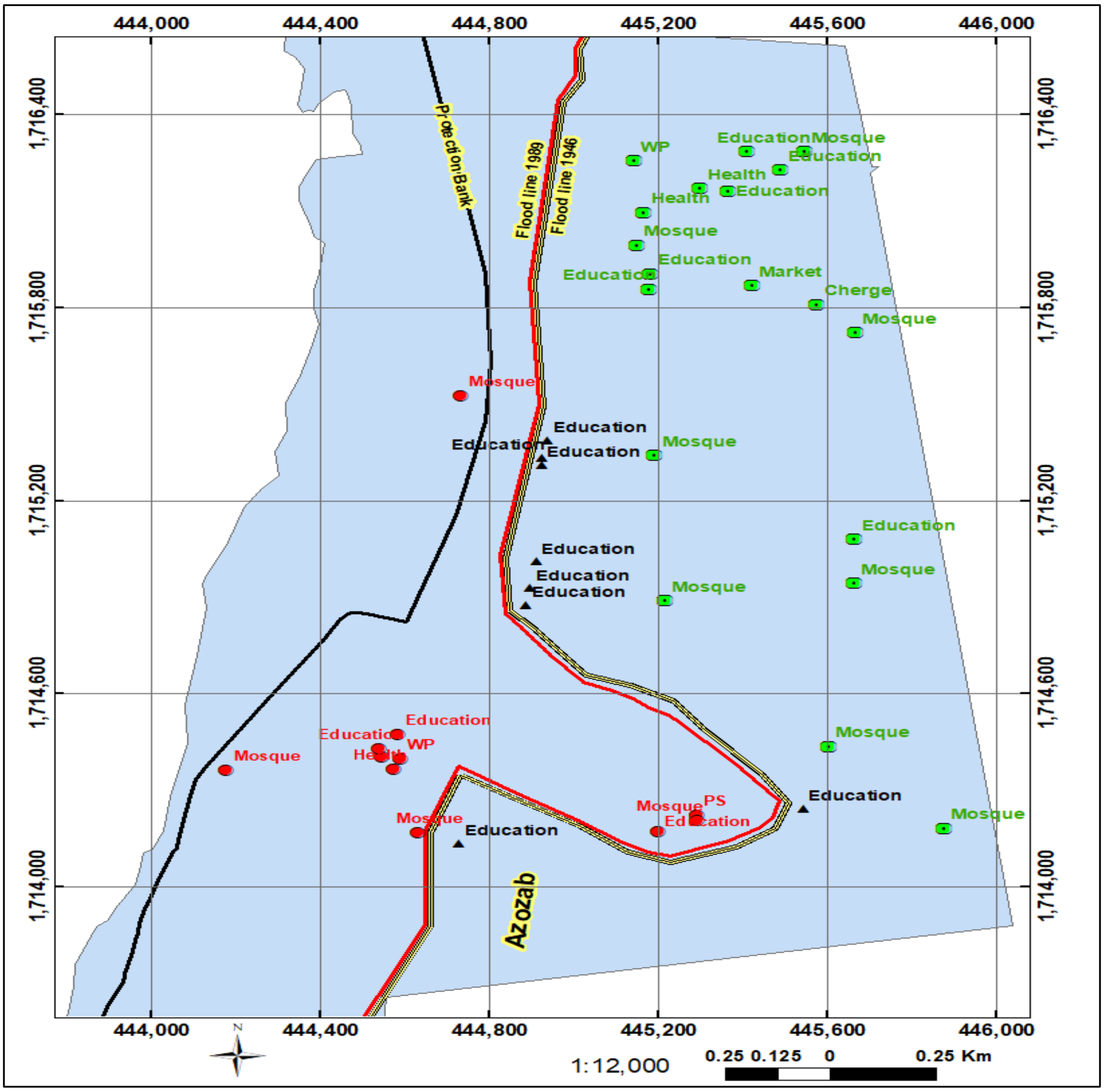


**Figure (4-12): Flood affected services in the study area**

Note: This figure is presented in the appendices in a landscape orientation for clarity.

### 4-12- Three Dimensional Coordinates of 1946 flood extent line (elevations from LiDAR DEM):

Table (A1) in the appendices shows the X,Y coordinates of points (at 60 m planimetric interval) and the elevations (Z) of the same points along the flood extent line of 1946 extracted from the LiDAR DEM.

The statistical analysis of table (A1) reveals the statistics given in table (4-6):

**Table (4-6): The statistics of flood line 46 reduced level (LiDAR DEM)**

| SN | Statistic | Value |
|---|---|---|
| 1- | Count | 77 |
| 2- | Total of reduced level | 29,444.92 |
| 2- | Max. reduced level | 384.27 |
| 4- | Min. reduced level | 380.83 |
| 5- | Variation (Max. – Min.) | 3.44 |
| 6- | Mean reduced level | 382.40 |
| 7- | Sum of diff^2 | 40.43864867 |
| 8- | (Sum of diff^2)/N | 0.525177 |
| 9- | Standard deviation | 0.724691 |

Figure (4-13) shows the profile “the elevations (Z) plots” of the points along the flood extent line of 1946 extracted from the LiDAR DEM. This figure is added to the appendices with a landscape orientation, for clarity.

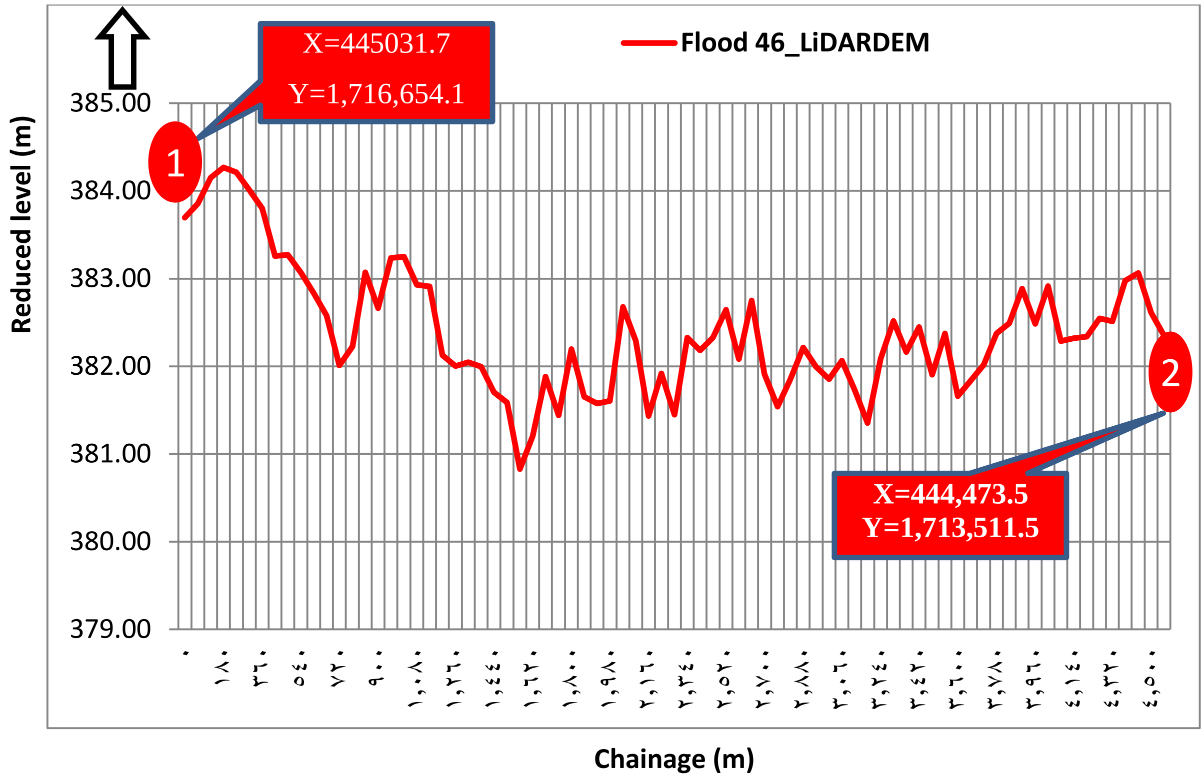


**Figure (4-13): Graph of flood 1946**

### 4-13- Three Dimensional Coordinates of 1988 flood extent line from LiDAR DEM:

Table (A2) in the appendices shows the X,Y coordinates of points (at 60 m planimetric interval) and the elevations (Z) of the same points along the flood extent line of 1988.

The statistical analysis of table (A2) reveals the statistics given in table (4-7):

**Table (4-7): The statistics of flood line 88 reduced level from LiDAR**

| SN | Statistic | Value |
|---|---|---|
| 1- | Count | 77 |
| 2- | Total of reduced level | 29,439.93 |
| 3- | Max. reduced level (m) | 384.20 |
| 4- | Min. reduced level (m) | 380.60 |
| 5- | Variation (Max. – Min.) | 3.60 |
| 6- | Mean reduced level | 382.34 |
| 7- | Sum of diff^2 | 46.1541965 |
| 8- | (Sum of diff^2)/n | 0.59940514 |
| 9- | Standard deviation | 0.774206 |

Figure (4-14) shows the profile "the elevations (Z) plots" of the points along the flood extent line of 1988. This figure is added to the appendices with a landscape orientation, for clarity.

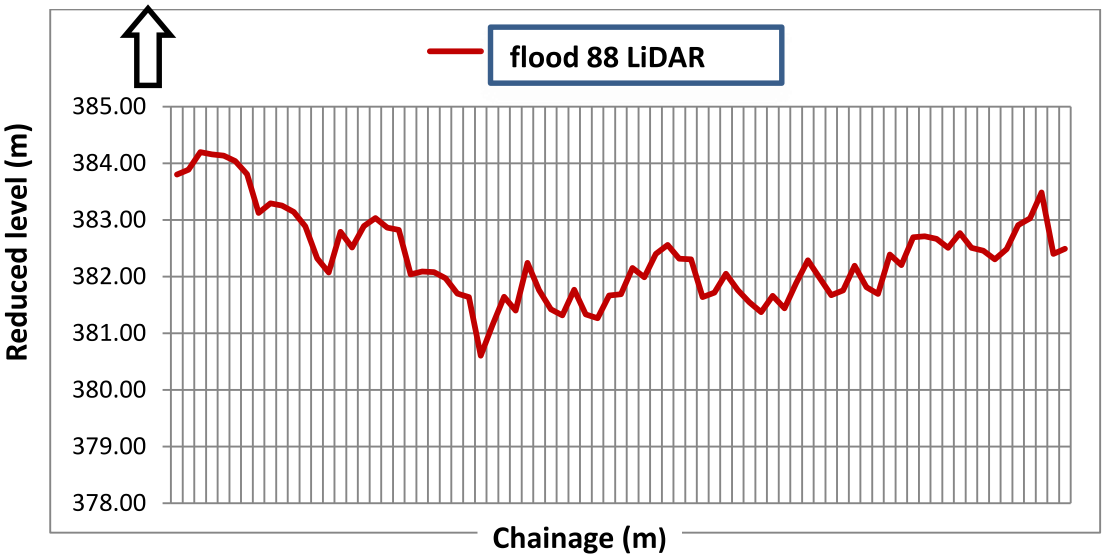


**Figure (4-14): Graph of flood 1988 (LiDAR)**

## 4-14- Three Dimensional Coordinates of the protection bank from LiDAR DEM:

Table (A3) in the appendices shows the X,Y coordinates of points (at 60 m planimetric interval) and the elevations (Z) of the same points along the protection bank.

The statistical analysis of table (A3) reveals the statistics given in table (4-8):

**Table (4-8): The statistics of the protection bank Reduced level from LiDAR**

| SN | Statistic | Value |
|---|---|---|
| 1- | Count | 59 |
| 2- | Total of reduced level | 22,509.81 |
| 3- | Max. reduced level (m) | 384.97 |
| 4- | Min. reduced level (m) | 379.43 |
| 5- | Variation (Max. – Min.) | 5.54 |
| 6- | Mean of reduced level | 381.52 |
| 7- | Sum of diff^2 | 76.17878 |
| 8- | (Sum of diff^2)/n | 1.291131867 |
| 9- | Standard deviation | 1.136279837 |

Figure (4-15) shows the profile "the elevations (Z) plots" of the points along the protection bank captured from the LiDAR DEM. This figure is added to the appendices with a landscape orientation, for clarity.

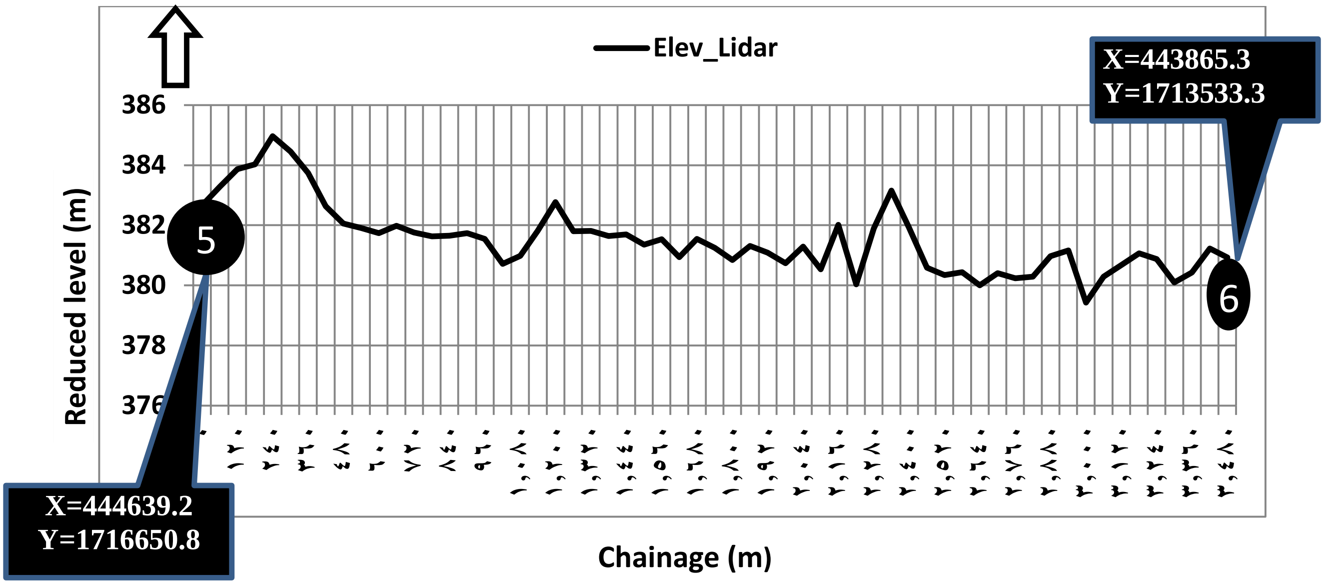


**Figure (4-15): Graph of protection bank (LiDAR)**

**4-15- Three Dimensional Coordinates of 1946 flood extent line from SRTM DEM:**

Table (A5) in the appendices shows the X,Y coordinates of points (at 60 m planimetric interval) and the elevations (Z) of the same points along the flood extent line of 1946 captured from the SRTM DEM.

The statistical analysis of table (A5) reveals the statistics given in table (4-9).

**Table (4-9): The statistics of flood line 46 reduced level from SRTM DEM**

| SN | Item | Value |
|---|---|---|
| 1- | Count | 77 |
| 2- | Total of reduced level | 29,409 |
| 3- | Max. reduced level (m) | 388 |
| 4- | Min. reduced level (m) | 372 |
| 5- | Variation (Max. – Min.) | 16 |

| SN | Item | Value |
|---|---|---|
| 6- | Mean | 382 |
| 7- | Sum of diff^2 | 593 |
| 8- | (Sum of diff^2)/N | 7.6026 |
| 9- | Standard deviation | 2.7573 |

Figure (4-16) shows the profile “the elevations (Z) plots” of the points along the flood extent line of 1946.taken from the SRTM DEM.

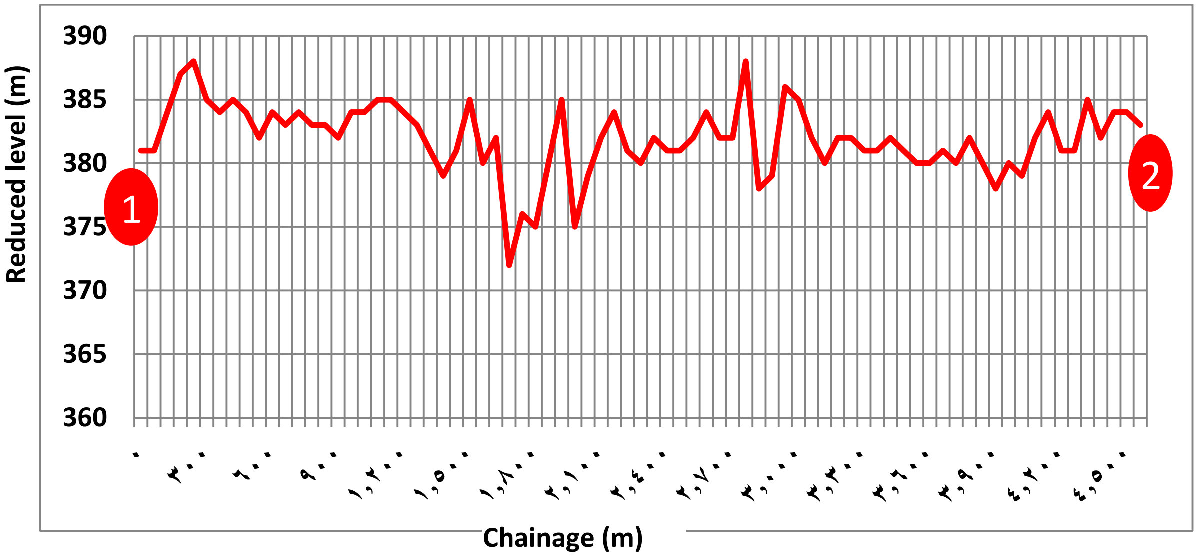


**Figure (4-16): Graph of flood 1946 (SRTM DEM)**

**4-16- Three Dimensional Coordinates of 1988 flood extent line from SRTM DEM:**

Table (A6) in the appendices shows the X,Y coordinates of points (at 60 m planimetric interval) and the elevations (Z) of the same points along the flood extent line of 1988 captured from the SRTM DEM.

The statistical analysis of table (A6) yielded the statistics given in table (4-10).

**Table (4-10): The statistics of flood line 88 elevations from SRTM DEM**

| SN | Item | Value |
|---|---|---|
| 1- | Count | 77 |
| 2- | Total of reduced level | 29,411 |
| 3- | Max. reduced level (m) | 387 |

| SN | Item | Value |
|---|---|---|
| 4- | Min. reduced level (m) | 372 |
| 5- | Variation (Max. – Min.) | 15 |
| 6- | Mean | 381.96 |
| 7- | Sum of diff^2 | 525 |
| 8- | (Sum of diff^2)/N | 6.730769 |
| 9- | Standard deviation | 2.594373 |

Figure (4-17) shows the profile “the elevations (Z) plots” of the points along the flood extent line of 1988 from the SRTM DEM.

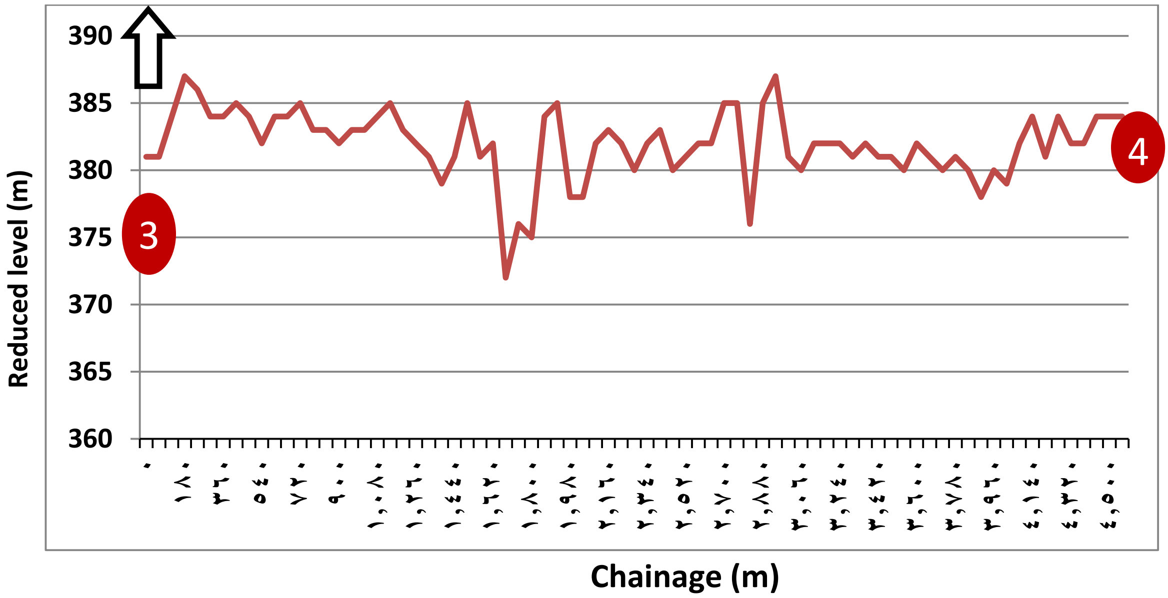


**Figure (4-17): Graph of flood 1988 (SRTM)**

**4-18- Three Dimensional Coordinates of the protection bank from SRTM DEM:**

Table (A7) in the appendices shows the X,Y coordinates of points (at 60 m planimetric interval) and the elevations (Z) of the same points along the protection bank from the SRTM DEM.

The statistical analysis of table (A7) yielded the statistics given in table (4-11).

**Table (4-11): The statistics of the protection bank reduced level from SRTM DEM**

| SN | Item | Value |
|---|---|---|
| 1- | Count | 59 |
| 2- | Total of reduced level | 22,492 |
| 3- | Max. reduced level (m) | 386 |
| 4- | Min. reduced level (m) | 377 |
| 5- | Variation | 9 |
| 6- | Mean | 381.22 |
| 7- | Sum of diff^2 | 223 |
| 8- | (Sum of diff^2)/N | 3.7797 |
| 9- | Standard deviation | 1.9441 |

Figure (4-18) shows the profile "the elevations (Z) plots" of the points along the protection bank.

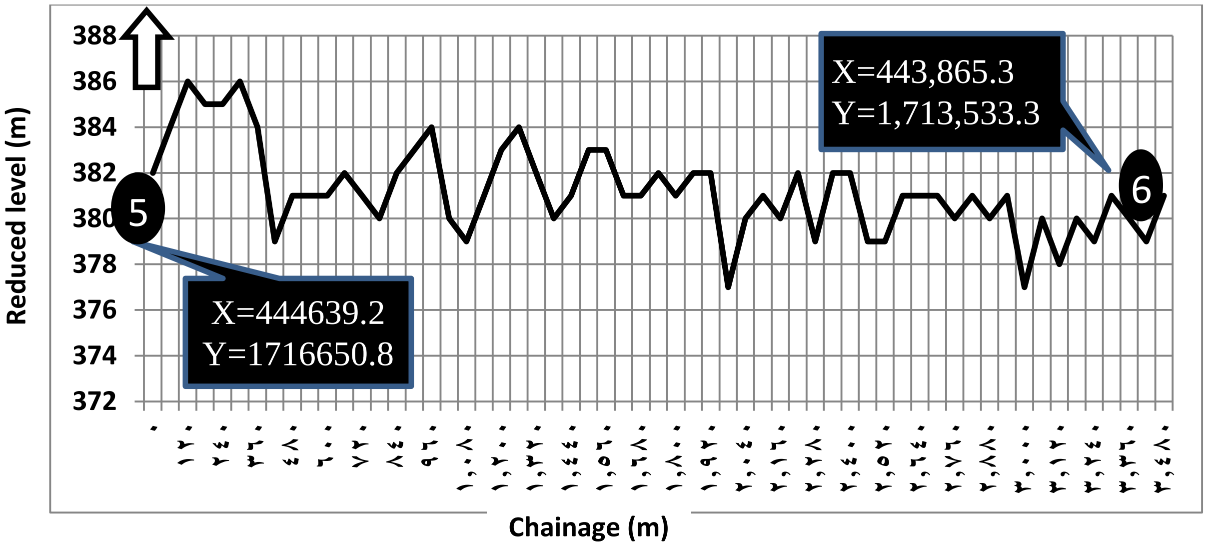


**Figure (4-18): Graph of protection bank (SRTM)**

## 4-19- Three Dimensional Coordinates of the 3 lines reduced level from LiDAR DEM:

Table (A4) in the appendices shows the X,Y coordinates of points (at 60 m planimetric interval) and the elevations (Z) of the same points along each of the flood 46, flood 88, and protection lines extracted from LiDAR DEM.

The statistical analysis of the elevations of the three lines yielded the statistics included in table (4-12).

**Table (4-12): The statistics of the 3 lines' reduced level from LiDAR DEM**

| SN | Statistic | Value | | |
|---|---|---|---|---|
| | | Flood 46 | Flood 88 | Protection |
| 1- | Count | 77 | 77 | 59 |
| 2- | Total of reduced level | 29,444.92 | 29,439.93 | 22,509.81 |
| 3- | Max. reduced level (m) | 384.27 | 384.20 | 384.97 |
| 4- | Min. reduced level (m) | 380.83 | 380.60 | 379.43 |
| 5- | Variation (Max. – Min,) | 3.44 | 3.60 | 5.54 |
| 6- | Mean | 382.40 | 382.34 | 381.52 |
| 7- | Sum of diff^2 | 40.43864867 | 46.1541965 | 76.17878 |
| 8- | (Sum of diff^2)/N | 0.525177 | 0.59940514 | 1.291131867 |
| 9- | Standard deviation | 0.724691 | 0.774206 | 1.136279837 |

Figure (4-19) shows the profile "the elevations (Z) plots" of the points along each of the flood 46, flood 88, and protection line extracted from the LiDAR DEM.. This figure is added to the appendices with a landscape orientation, for clarity.

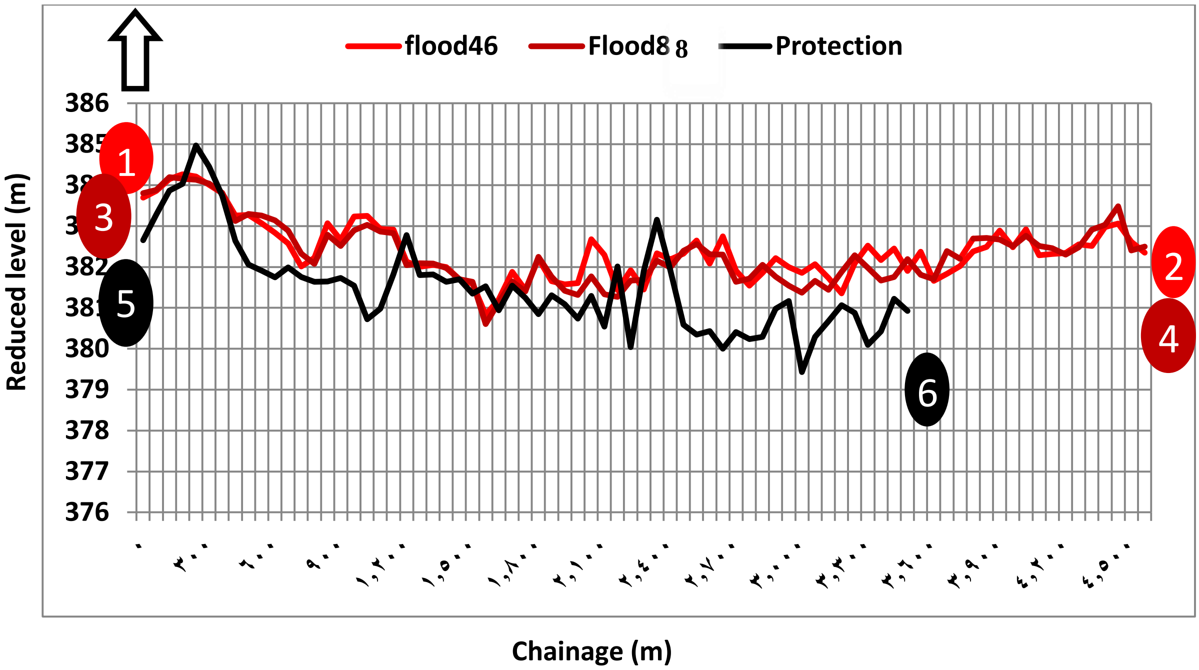


**Figure (4-19): Elevations of points along the 3 lines from LiDAR DEM**

### 4-20- Three Dimensional Coordinates of the three lines from SRTM DEM:

Table (A8) in the appendices shows the X,Y coordinates of points (at 60 m planimetric interval) and the elevations (Z) of the same points along each of the flood 46, flood 88, and protection lines extracted from the SRTM DEM..

The statistical analysis of the elevations included in table (A8) is shown in table No.(4-13).

**Table (4-13): The statistics of the 3 lines' reduced level from the SRTM DEM**

| SN | Statistic | Value | | |
|---|---|---|---|---|
| | | Flood 46 | Flood 88 | Protection |
| 1- | Count | 77 | 77 | 59 |
| 2- | Total of reduced level | 29,409 | 29,411 | 22,492 |
| 3- | Max. reduced level (m) | 388 | 387 | 386 |
| 4- | Min. reduced level (m) | 372 | 372 | 377 |
| 5- | Variation (Max. – Min,) | 16 | 15 | 9 |
| 6- | Mean | 381.93 | 381.96 | 381.22 |

| | | | | |
|---|---|---|---|---|
| 7- | Sum of diff^2 | 593 | 525 | 223 |
| 8- | (Sum of diff^2)/N | 7.6026 | 6.730769 | 3.7797 |
| 9- | Standard deviation | 2.7573 | 2.594373 | 1.9441 |

Figure (4-20) shows the profile “the elevations (Z) plots” of the points along each of the flood 46, flood 88, and protection lines extracted from the SRTM DEM.

**Note:**

For a clearer view, figure (4-19) and (4-20) were also presented in the appendices in a landscape oriented page.

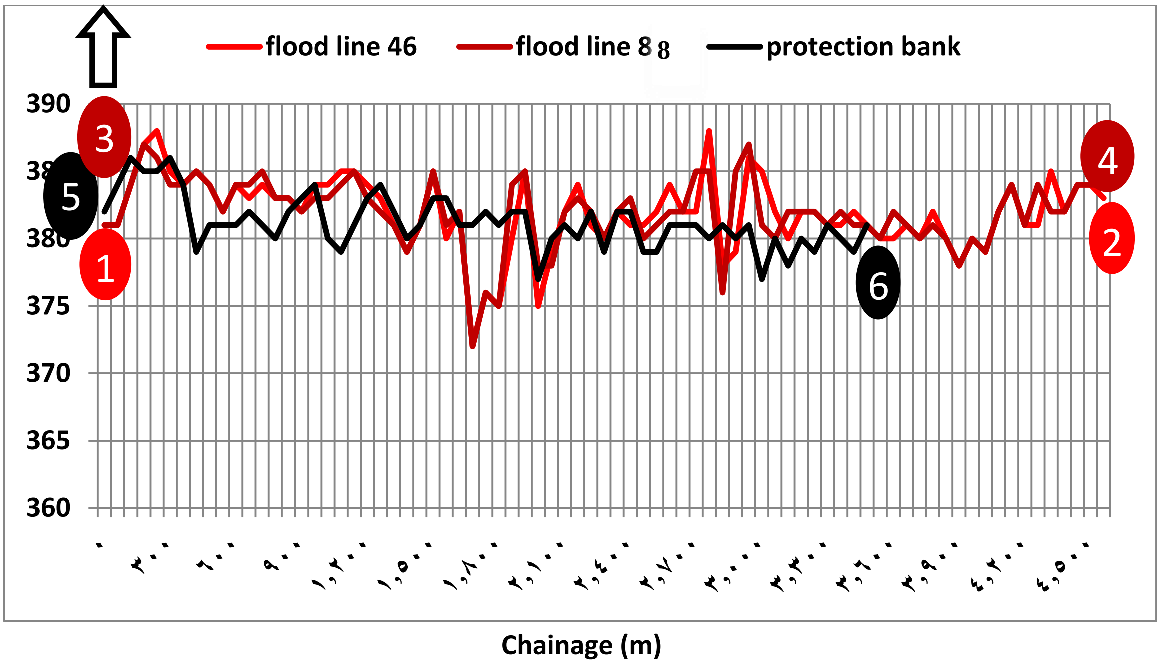


**Figure (4-20): Elevations of points along the 3 lines from SRTM DEM**

**4-21- Comparison of the lines using LiDAR vs. SRTM DEMs:**

**4-21- 1- Flood line 1946 from LiDAR vs. SRTM DEMs:**

Table (A1) in the appendices shows the X,Y coordinates of points (at 60 m planimetric interval) and the elevations (Z) of the same points along the flood extent line of 1946 produced from the LiDAR DEM. Table (A5) in the appendices shows the X,Y coordinates of points (at 60 m planimetric interval) and the elevations (Z) of the same points along the flood extent line of 1946 produced from the SRTM DEM.

Analysis of tables A1 and A5 produced the statistcs included in table (4-14).

**Table (4-14):Statistical Comparison of 46 flood line reduced level from LiDAR and SRTM DEMs**

| SN | Parameter | Value from LiDAR DEM | Value from SRTM DEM |
|---|---|---|---|
| 1- | Count | 77 | 77 |
| 2- | Total of reduced level | 29,444.92 | 29,411 |
| 3- | Max. reduced level (m) | 384.27 | 387 |
| 4- | Min. reduced level (m) | 380.83 | 372 |
| 5- | Variation (max.-min.) | **3.44** | **15** |
| 6- | Mean | 382.40 | 381.96 |
| 7- | Sum of diff^2 | 40.43864867 | 525 |
| 8- | (Sum of diff^2)/N | 0.525177 | 6.730769 |
| 9- | Standard deviation | **0.724691** | **2.594373** |

Table (4-14) confirms that the LiDAR data variation within the 46 flood line equals **3.44** m and the standard deviation equals **0.724691**, while the same parameters produced from the SRTM DEM equal **15** m and **2.594373** respectively. This implies that the LiDAR data is more precise compared to the SRTM data (less variation and smaller standard deviation i.e. smaller distribution around the mean).

Figure (4-21) shows the profile “the elevations (Z) plots” of the points along the flood extent line of 1946 produced from LiDAR data, in addition to the profile of the same points produced from the SRTM DEM. This figure reveals higher variation of the SRTM data (max. – min.) compared to the LiDAR data for the flood line 1946 which is more precise.

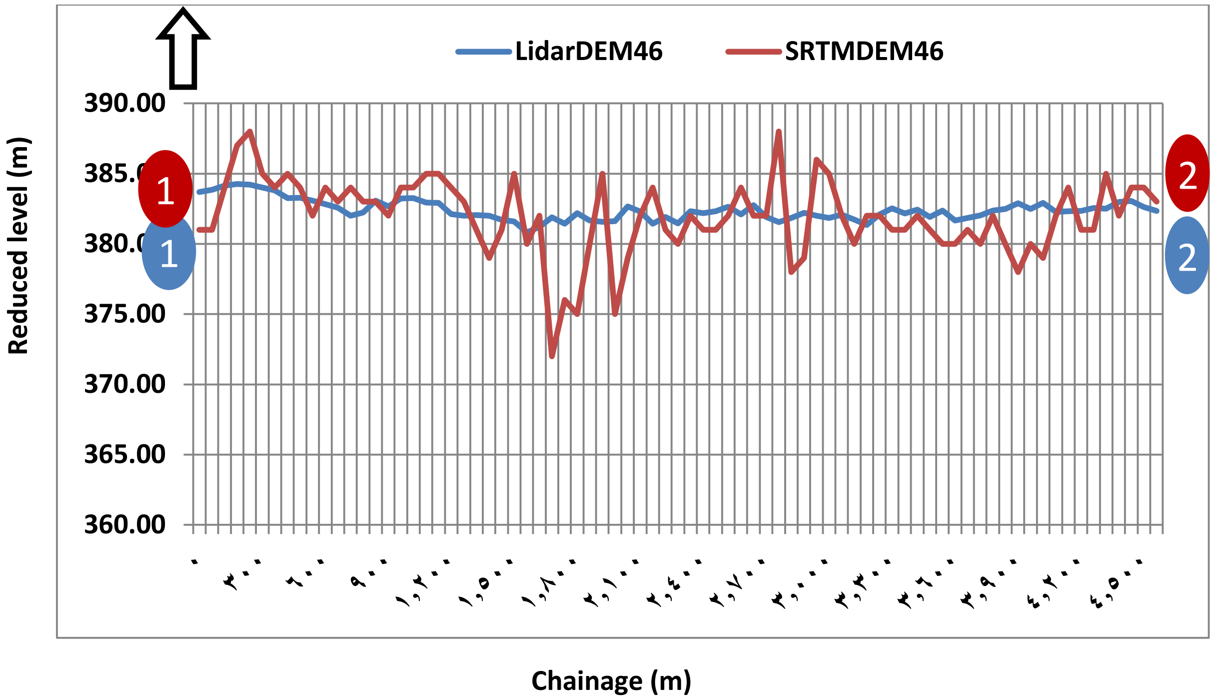


**Figure (4-21): Profiles along the 1946 flood extent line from LiDAR DEM and SRTM DEM**

### 4-21- 2- Flood line 1988 from LiDAR vs. SRTM DEMs:

Table (A2) in the appendices shows the X,Y coordinates of points (at 60 m planimetric interval) and the elevations (Z) of the same points along the flood extent line of 1988 produced from the LiDAR DEM. Table (A6) in the appendices shows the X,Y coordinates of points (at 60 m planimetric interval) and the elevations (Z) of the same points along the flood extent line of 1988 produced from the SRTM DEM.

Analysis of tables (A2) and (A6) produced the statistcs included in table (4-15).

**Table (4-15):Statistical Comparison of 88 flood line's reduced level from LiDAR and SRTM DEM**

| SN | Parameter | Value from LiDAR DEM | Value from SRTM DEM |
|---|---|---|---|
| 1- | Count | 77 | 77 |
| 2- | Total of reduced level | 29,439.93 | 29,411 |
| 3- | Max. reduced level (m) | 384.20 | 387 |
| 4- | Min. reduced level (m) | 380.60 | 372 |
| 5- | Variation (max. – min.) | **3.60** | **15** |

| | | | |
|---|---|---|---|
| 6- | Mean | 382.34 | 381.96 |
| 7- | Sum of diff^2 | 46.1541965 | 525 |
| 8- | (Sum of diff^2)/n | 0.59940514 | 6.730769 |
| 9- | Standard deviation | **0.774206** | **2.594373** |

Table (4-15) shows that the LiDAR data variation within the 1988 flood line equals **3.6** m and the standard deviation equals **0.774206**, while the same parameters produced from the SRTM DEM equal **15** m and **2.594373**. This implies that the LiDAR data is more precise compared to the SRTM data (less variation and smaller standard deviation).

Figure (4-22) shows the profile "the elevations (Z) plots" of the points along the flood extent line of 1988 produced from the LiDAR data, in addition to the profile of the same points produced from the SRTM DEM data. This figure reveals higher variation of the SRTM data (max. – min.) compared to the LiDAR data for the flood line 1988 which is more precise

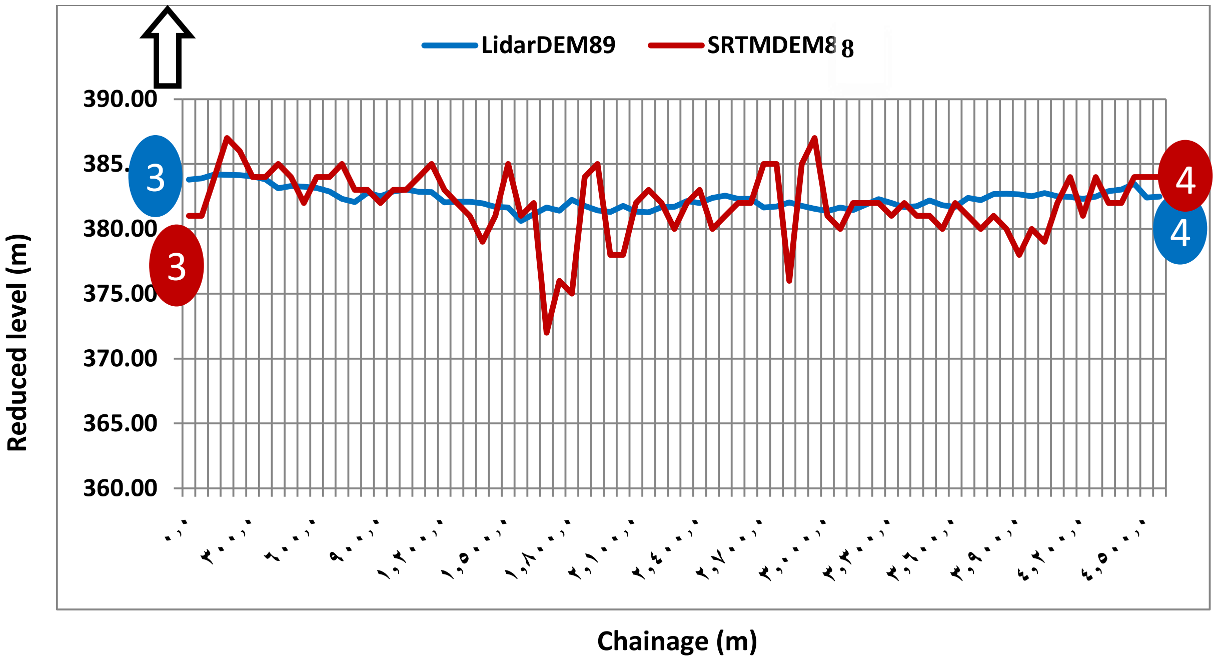


**Figure (4-22): Profiles along the 1988 flood extent line from LiDAR DEM and SRTM DEM**

### 4-21- 3- Protection bank from LiDAR vs. SRTM DEMs:

Table (A3) in the appendices shows the X,Y coordinates of points (at 60 m planimetric interval) and the elevations (Z) of the same points along the protection bank produced from the LiDAR DEM. Table (A7) in the appendices shows the X,Y coordinates of points (at 60 m planimetric interval) and the elevations (Z) of the same points along the protection bank produced from the SRTM DEM.

Analysis of table (A3) and table (A7) yielded the statistics included in table (4-16).

**Table (4-16):Statistical Comparison of protection bank elevations from LiDAR and SRTM DEMs**

| SN | Parameter | Value from LiDAR DEM | Value from SRTM DEM |
|---|---|---:|---:|
| 1- | Count | 59 | 59 |
| 2- | Total of reduced level | 22,509.81 | 22,492 |
| 3- | Max. reduced level (m) | 384.97 | 386 |
| 4- | Min. reduced level (m) | 379.43 | 377 |
| 5- | Variation (max. – min.) | **5.54** | **9** |
| 6- | Mean | 381.52 | 381.22 |
| 7- | Sum of diff^2 | 76.17878 | 223 |
| 8- | (Sum of diff^2)/N | 1.291131867 | 3.7797 |
| 9- | Standard deviation | **1.136279837** | **1.9441** |

Table (4-16) reveals that the LiDAR data variation within the protection bank equals **5.54** m and the standard deviation equals **1.136279837**, while the same parameters produced from the SRTM DEM equal **9** m and **1.9441**. This implies that the LiDAR data is more precise compared to the SRTM data (less variation and smaller standard deviation).

Figure (4-22) shows the profile “the elevations (Z) plots” of the points along the protection bank produced from SRTM DEM, in addition to the profile of the same points produced from the LiDAR data. This figure reveals higher variation of the

SRTM data (max. – min.) compared to the LiDAR data for the protection bank which is more precise

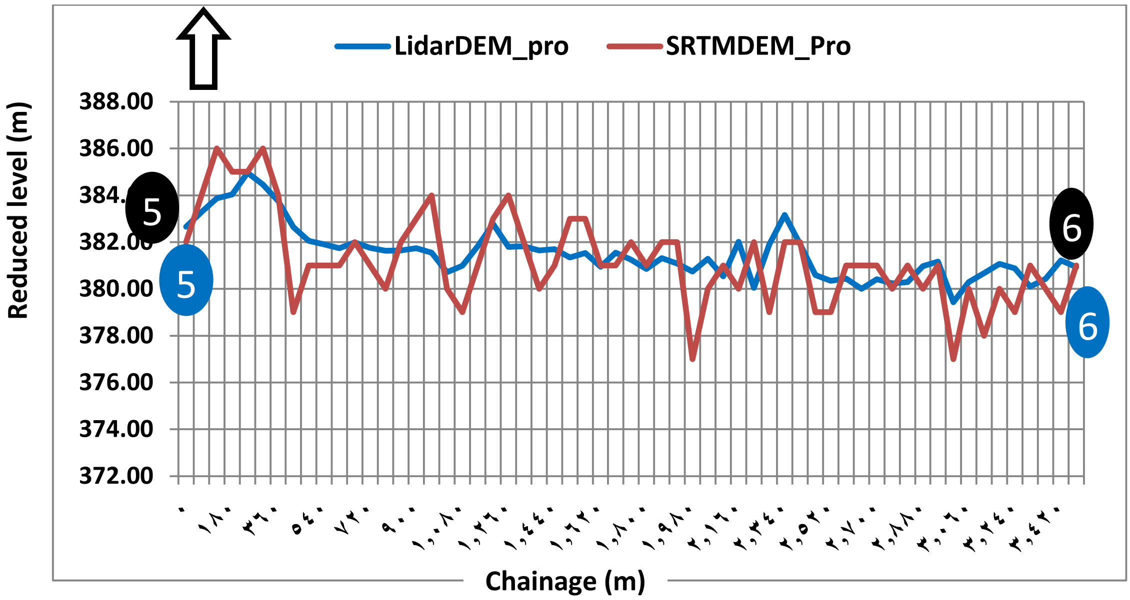


**Figure (4-23): Profiles along the protection bank from LiDAR DEM and SRTM DEM**

**Conclusions:**

Analysis of the graphs in figures (4-21), (4-22), and (4-23) which show comparisons of the profile of each of the three lines produced from the LiDAR DEM (in blue) and SRTM DEM (in brown) confirms that the measurements made by LiDAR DEM are more precise than those made by the SRTM DEM. This is confirmed by the fact that the variations between the elevations of the series of points produced from the LiDAR DEM are minimal compared to those between the elevations of the series of points produced by the SRTM DEM (for the three lines). Hence, LiDAR DEM data can be considered more precise than the SRTM DEM data.

**4-22- Protection bank height increasing:**

Table (A9) in the appendices and figure (4-24) show the incements which are to be added to the protection line heights in order to be equal to the level of the flood line in 1946. In addition to the difference shown in the figure, an extra height of 0.30 m should be added at each station to provide for any future flood level that may exceed the level of 1946 flood.

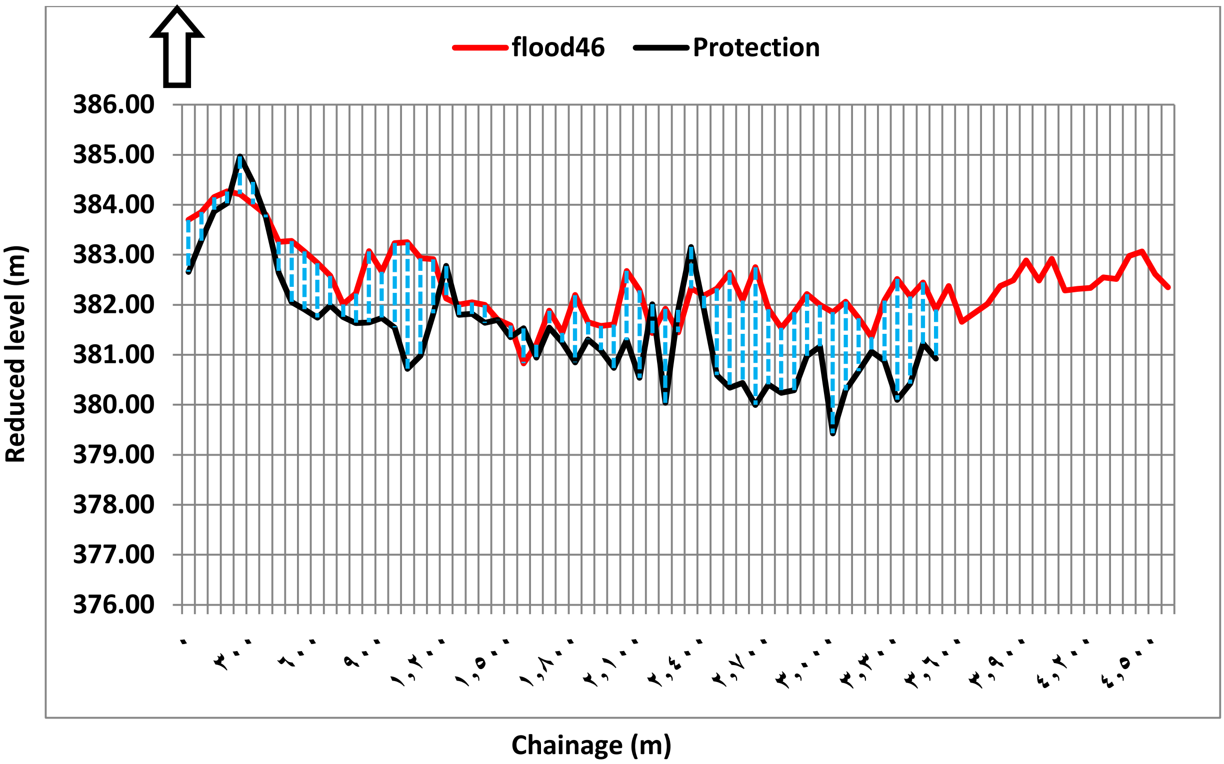


**Figure (4-24): Protection bank height increments (reference is 1946 flood line)**

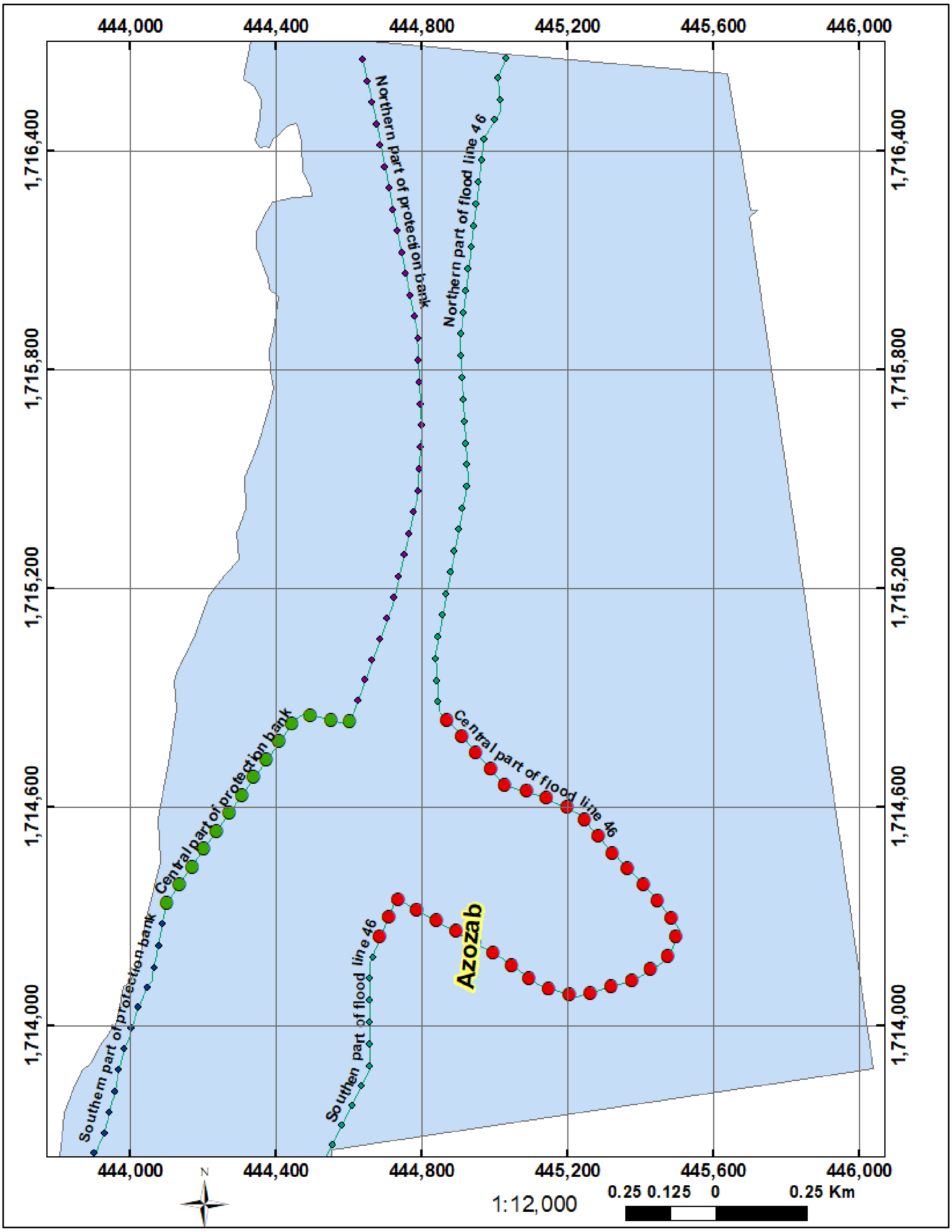


**Figure (4-25): Increasing the protection bank height**

**4-23- Accuracy assessment of the LiDAR DEM and the SRTM DEM:**

Figure (4-23) shows a subset of the SRTM DEM data which was taken (likewise a coincident subset of the LiDAR DEM data was taken) as a sample for the calculation of the statitics necessary for giving a clearer picture of the precision of the LiDAR DEM data compared to the SRTM DEM data.

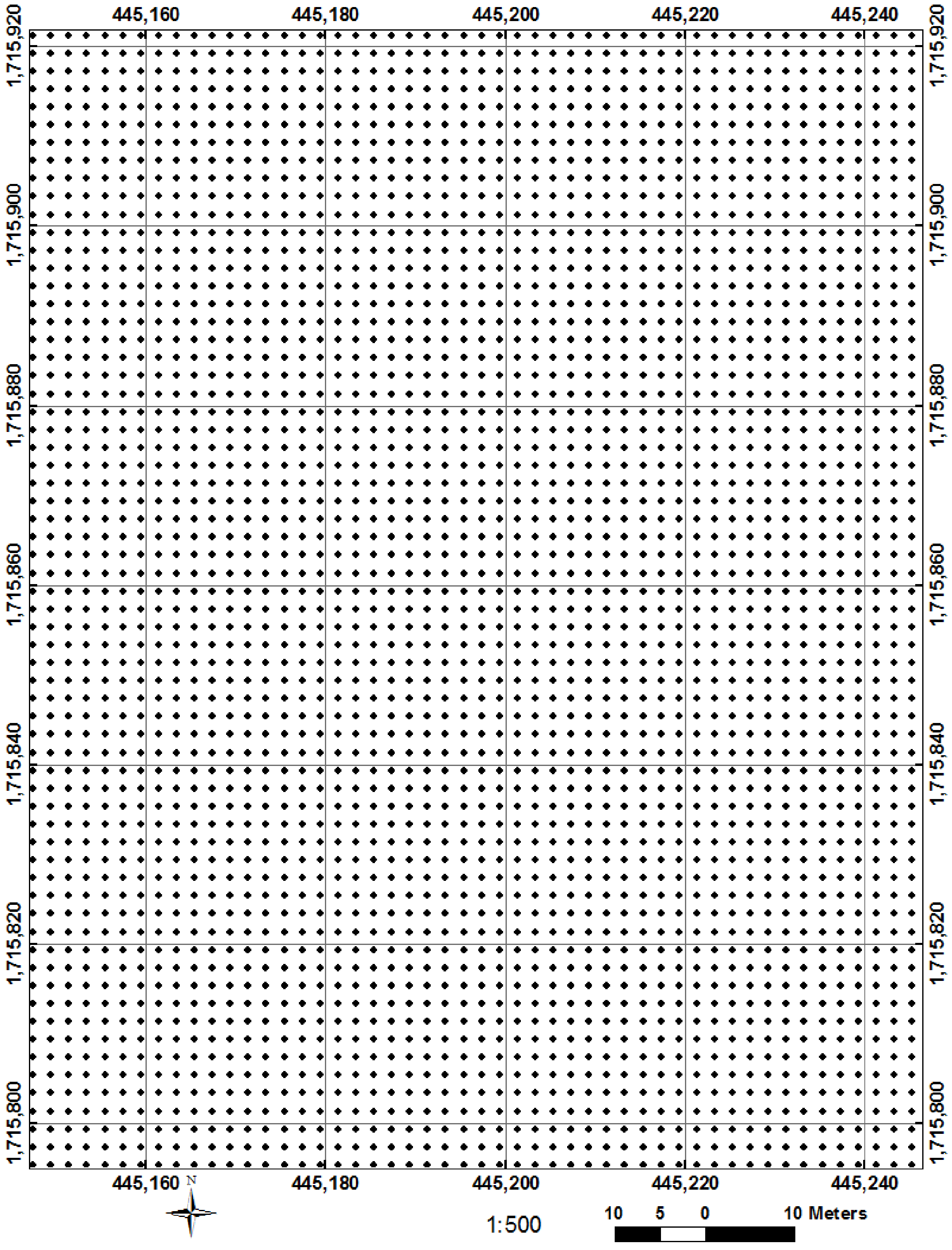


**Figure (4-26): A subset of the SRTM DEM fishnet points**

Table (A10) in the appendices shows the X,Y coordinates of **542,050** points (at 2 m planimetric interval) and the elevations (Z) of the same points within a subset of each of the LiDAR DEM and the SRTM DEM.
The statistical analysis of table (A10) reveals the statistics given in table (4-17):

**Table (4-17): Statistical Comparison of a subset of the LiDAR and SRTM DEMs**

| SN | Parameter \ Data type | SRTM DEM | LiDAR DEM |
|---|---|---|---|
| 1- | Count | 542,050 | 542,050 |
| 2- | Sum | 207,855,164.27 | 207,669,161.46 |
| 3- | Max. (m) | 397.826 | 385.420 |
| 4- | Min. (m) | 372.087 | 380.548 |
| 5- | Variation (Max. – Min.) | 25.74 | 4.87 |
| 6- | Mean | 383.461 | 383.118 |
| 7- | Sum of diff^2 | 2,581,670.290 | 303,701.753 |
| 8- | (Sum of diff^2)/N | 4.7627888 | 0.5602836 |
| 9- | Standard deviation | 2.182 | 0.749 |

Table (4-17) extracted from table A10, reveals that the LiDAR DEM data is more reliable and precise than that of the SRTM DEM data. This is confirmed by the variation (Max. elevation minus Minimum elevation) which is **4.87** m while it is **25.74** m, and the standard deviation which is **0.749** while it is **2.182** for the LiDAR DEM data and the SRTM DEM data respectively. Thus it can be stated that the LiDAR DEM data is about **3 times** more precise that the SRTM DEM data (2.91) i.e. by dividing 2.182 by 0.749.

### 4-24- The QQPlot:

Figure (4-23) shows the QQPlot of the two DEM datasets. Since both datasets are not exactly identical but they are linearly related, the points in the Q–Q plot are approximately lie on a line, but not on the line y = x.

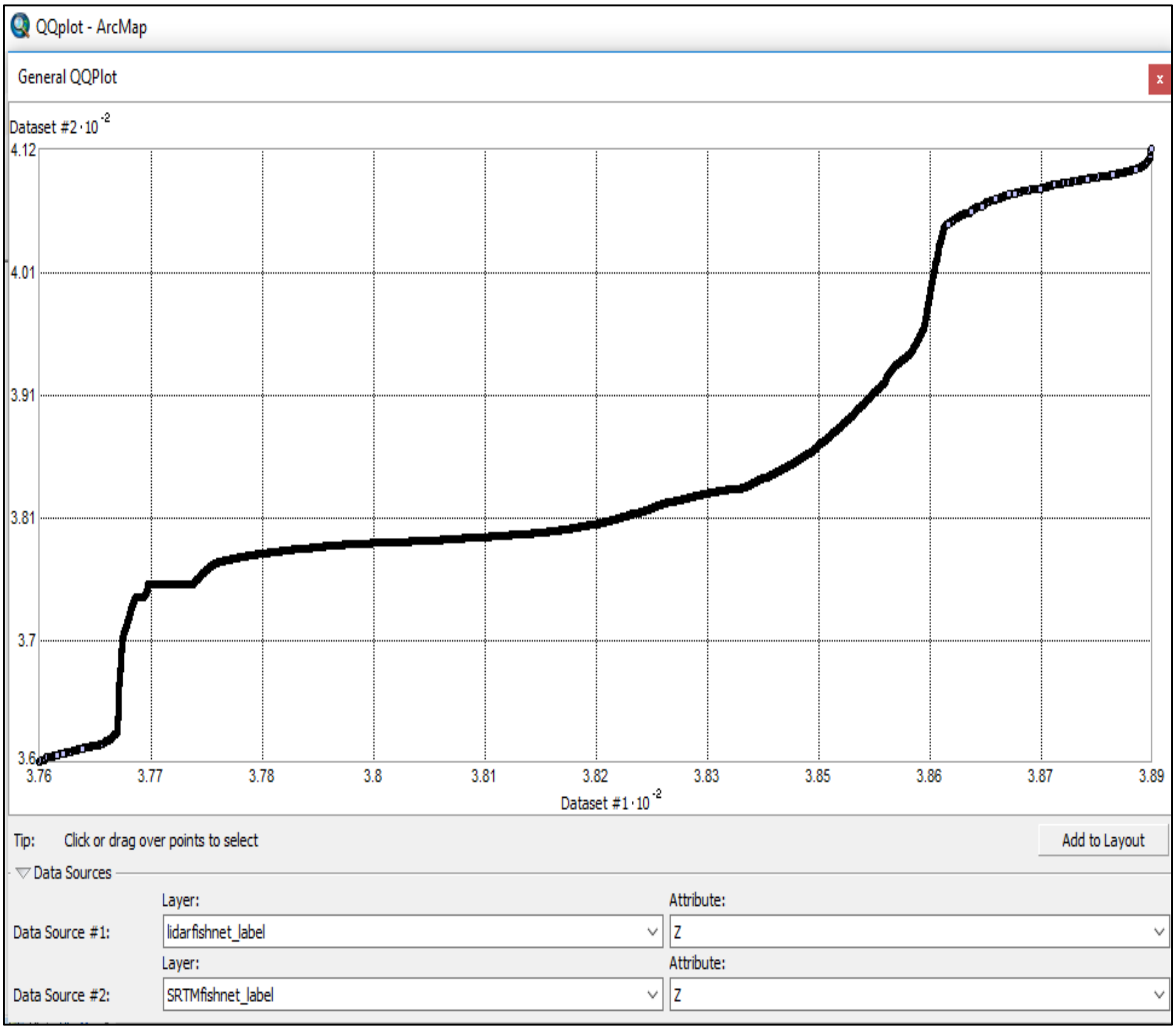


**Figure (4-27): General QQ Plot of the LiDAR DEM and SRTM DEM Elevations**

### 4-25- Ground truth:

The graph in figure (4-23) shows the plotted elevations of the points as measured by the GPS navigator. The height at which the device was held equals 0.65 m approx. The original elevations were plotted in blue, while the corrected (reduced by 0.65 m) elevations were plotted in red. From figure (4-23) it is clear that the terrain of the study area is nearly flat.

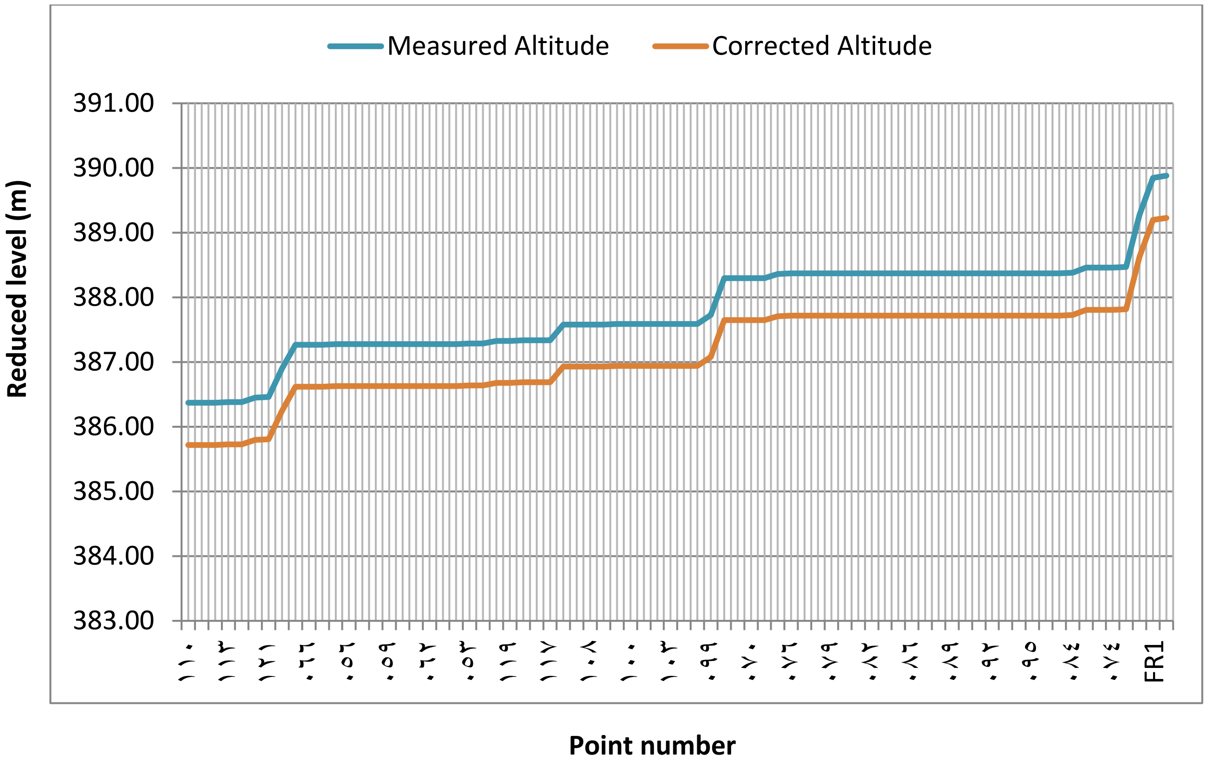


**Figure (4-28): Graph of field-measured points coordinates**

Table (4-18) shows the statistics of the altitudes captured in the field which are presented in Table (A11) in the appendices

**Table (4-18): Statistcis of the altitudes captured in the field**

| SN | Statistic | Value |
|---|---|---|
| 1- | Count | 71 |
| 2- | Sum | 27,482.14 |
| 3- | Max. (m) | 387.82 |
| 4- | Min. (m) | 385.72 |
| 5- | Variation | 2.10 |
| 6- | Mean | 387.07239 |
| 7- | Sum of diff^2 | 32.67631 |
| 8- | (Sum of diff^2)/N | 0.4232013 |
| 9- | Standard deviation | 0.650539 |

From table (4-18), it is found that the standard deviation is 0.650539, value which suggests that the field-collected elevations were precise and fairly clustered around the mean.

**Table (4-19): Statistical Comparison of a subset of the LiDAR and SRTM DEMs and field captured altitudes of points**

| SN | Data type / Parameter | SRTM DEM | LiDAR DEM | Field collected Reduced level |
|---|---|---|---|---|
| 1- | Count | 542,050 | 542,050 | 71 |
| 2- | Sum | 207,855,164.27 | 207,669,161.46 | 27,482.14 |
| 3- | Max. (m) | 397.826 | 385.420 | 387.82 |
| 4- | Min. (m) | 372.087 | 380.548 | 385.72 |
| 5- | Variation (Max. – Min.) | 25.74 | 4.87 | 2.10 |
| 6- | Mean | 383.461 | 383.118 | 387.07239 |
| 7- | Sum of diff^2 | 2,581,670.290 | 303,701.753 | 32.67631 |
| 8- | (Sum of diff^2)/N | 4.7627898 | 0.5602836 | 0.4232013 |
| 9- | Standard deviation | 2.182 | 0.749 | 0.650539 |

From table (4-19), it is found that the variation and standard deviation of the LiDAR data are 4.87 and 0.749 respctively. The variation and standard deviation of the field collected elevations are 0.749 and 0.650539 respectively. These values are highly comparable, but there are notably different from the same parameters for the SRTM data. This implies conformity between the LiDAR Data and GPS data, which is an indication of more precision.

# Chapter Five

# Conclusion and Recommendations

## 5-1- Conclusions:

Flood is the deadliest type of severe weather. The use of remotely sensed data and Geographic Information Systems (GIS) in flood monitoring and management proved to be very helpful. The study area “Azozab”, Khartoum state, Sudan used to be exposed to severe floods frequently, mainly because of the White Nile floods accompanied by storm waters during the rainy season. In view of this fact, the study aims to contribute to the effort for mitigating the adverse impact of floods in the study area, via the analysis of the most severe floods (in 1946 and 1988) as well as the effectiveness of the existing protection bank built along the White Nile’s bank adjacent to the study area.

The 2D (planimetric) coordinates (X, Y) of points along each of the flood extent lines 1946, 1988, and the existing protection bank were obtained from the shapfile of each line, while the elevations (Z-coordinates) of the same points were obtained from the digital elevation model of the study area. Two digital elevation models of the study area (namely, the Suttle Radar Topography Mission 30m and the Light Detection And Ranging 1m) were used, and checked for accuracy. It was found that the LiDAR digital elevation model is more accurate because it yielded a mean of 383.118 and a standard deviation of 0.749 while the Shuttle Radar Topography Mission yielded a mean of 383.461 and a standard deviation of 2.182. (fishnet)

The point coordinates of the mentioned lines (obtained from both digital elevation models) were plotted as graphs. Comparison of the lengths of the 3 lines, it was found that the flood line 1946 is 4.59 km long, flood line 1988 is 4.57 km long, and the protection bank is 3.5 km long, therefore, the protection bank should be extended so that its length becomes equal to the length of 1946 flood line, i.e. to be extended by 1.09 Km, while comparison of the elevations of the points along the 3 lines reveals that Moreover, the elevations of the protection bank were found lower than the elevations of both flood lines for a distance of 3.02 km i.e. a percentage of 86.1% of its total length which represents the length of the protection bank that requires increasing its elevations (i.e.to construct a higher embankment).

## 5-2- Recommendations:

The researcher based on the experience acquired by her through conducting the research, sets forth the following recommendations:

1- The height of the protection bank should be raised by 1.5 m (in average) in order to guard against any future high floods. The height of the highest past flood level (i.e. the flood of 1946) should be taken as a reference, but extra 30 cm should be added to the height of 1946 flood line chainage stations as necessary to safeguard against the flood risk if the height of a future flood exceeds that of 1946.

2- If the digital elevation model (to be used) contains artifacts, they should be removed, and the accuracy of the digital elevation model should be verified.

3- The spatial reference of all of the used datasets should be unified.

4- The use of remotely sensed datasets is recommended for similar studies (particularly, if the study requires repeated data acquisition), because remote sensing facilitates the acquisition of information from a wide area, but the use of such data should be accompanied by field work for the acquisition of ground truth data.

5- Also, the geographic information system techniques should be exploited, since these techniques enables the analysis of spatial data in an efficient manner.

6- If sufficient flood and rainfall monitoring data is available for many years, this will support building a rich and comprehensive database, which, in turns, supports building a reasonable model for predicting flood extent, and consequently support making a suitable decision in this concern.

7- Some other methods for mitigation of the floods impact can be further studied such as the implementation of rainwater harvesting projects at locations across the water courses (valleys) existing within and outside the study area. Cosequently, the quantity of the storm water heading to the White Nile through such valleys is minimized, a situation which leads to the mitigation of the White Nile floods. Likewise, construction of dams at suitable sites across the White Nile can be useful to mitigate the impact of the White Nile floods.

8- The procedure of this research should be replicated at other locations which are subject to similar circumstances.

## Refrences


Adda, P., Mioc, D., Anton F., McGillivray E., Morton A. and Fraser, D. (2013). 3d flood-risk models of government infrastructure, https://isprs.org/proceedings/xxxviii/4-w13/id_39.pdf.

Altayeb H. Yahya, Low-cost space-related technologies for flood mitigation and monitoring, Case study: Sharg Elneel locality, Khartoum State, Sudan. Paper presented at the International University of Africa Disaster Management and refugees Studies Institute (DIMARSI) workshop under the title "Role of the base societies in limiting the disaster risks "Tuti as a sample". In the period 19-20/04/2014.

Altayeb H. Yahya, Volume of water to be harvested using space Technologies Case study: Part of Khartoum State in Sudan presented at ISNET / RJGC Workshop on Applications of Satellite Technology in Water Resources Management,18 - 22 Sep 2011; Amman, Jordan.

Bater, C.W. and Coops, N.C (2009). Evaluating error associated with lidar-derived DEM interpolation. Computers and Geosciences 35: pp. 289-300.

Bodoque, J.M., Guardiola-Albert, C., Aroca-Jiménez, E., Eguibar, M.A. and Martínez-Chenoll, M.L. (2016). Flood Damage Analysis: First Floor Elevation Uncertainty Resulting from LiDAR-Derived Digital Surface Models, https://doi.org/10.3390/rs8070604.

Bodoque, J.M., Guardiola-Albert, C., Aroca-Jimenez, E., Angel Eguibar, M. and Martinez-Chenoll, M.L. (2016). Flood damage analysis: first floor elevation uncertainty resulting from LiDAR-derived digital surface models, Remote Sens 8: pp. 604, https://doi.org/10.3390/rs8070604.

Brzank, A., Heipke, C., Goepfert, J. and Soergel, U. (2008). Aspects of generating precise digital terrain models in Wadde Sea from lidar—water classification and structure line extraction.ISPRS J Photogramm Remote Sens 63: pp. 510–528. https://doi.org/10.1016/j.isprsjprs.2008.02.002.

Darka Mioc, B. Nickerson, A. Ahmad, (2011), Flood Progression Modeling and Impact Analysis, https://doi.org/10.5772/18398.

Diaz-Nieto, J., Blanksby J., Lerner D. and Saul, A.J. (2008). A GIS approach to explore urban flood risk management. https://doi.org/10.1061/(ASCE)HE.1943-5584.0000416

Dowding, S., Kuuskivi, T. and Li, X. (2004). Void fill of SRTM Elevation Data — Principles, Processes and Performance. Proceedings of the Conference "ASPRS Images to Decision: Remote Sensing Foundation for GIS Applications", Kansas City, MO.

Evans, Y. S., Gunn, N. and Williams, D., (2008). Use of GIS in Flood Risk Mapping, CorpusID:14652610,http://idrcgisworkshop.pbworks.com/f/Use+of+GIS+in+flood+risk+Mapping.pdf

Foni, A. and Seal, D. (2004). Shuttle Radar Topography Mission: An Innovative Approach to Shuttle Orbital Control. Acta Astronautica, 54, pp. 565–570.

Gebrehiwot, (2018). Challenges and Opportunities for UAV-Based Digital Elevation Model Generation for Flood-Risk Management: A Case of Princeville. https://doi.org/10.3390/s18113843, Corpus ID: 53306101

Gizachew, K., (2017). LiDAR DEM Data for Flood Mapping and Assessment; Opportunities and Challenges, https://doi.org/10.4172/2469-4134.1000211

Hailea, A.T. and Rientjesb, T.H.M. (2004). Effects of LIDAR DEM resolution in flood modelling: A model sensitivity study for the city of Tegucigalpa, Honduras, https://isprs.org/proceedings/xxxvi/3-w19/papers/168.pdf

Hashemi-Beni, L., Jones, J., Thompson, G., Johnson, C., McDougall K. and Temple-Watts P., (2012). The use of lidar and volunteered geographic information to map flood extents and inundation,Vol. I-4, XXII ISPRS Congress, Melbourne, Australia

Hatzopoulos, J. N. (2002). Geographic Information Systems (GIS) in water management, https://doi.org/10.1007/BF00508896

Hawker, L., Bates, P., Neal, J. and Rougier, J. (2018). Perspectives on Digital Elevation Model (DEM) Simulation for Flood Modeling in the Absence of a High-Accuracy Open Access Global DEM,Vol. 6, Article 233, https://doi.org/10.3389/feart.2018.00233

Hoefle, B., Vetter, M., Pfeifer, N., Mandlburger, G. and Stotter, J. (2009). Water surface mapping from airbone laser scanning using signal intensity and elevation data. Earth Surf Process Landforms 34(12): pp. 1635–1649.

https://www.geodose.com/2019/03/spatial-interpolation-inverse-distance-weighting-idw.html

Islam, M. (2000). Flood damage and management modeling using satellite remote sensing data with GIS: case study of Bangladesh, ISBN: 1901502465, Corpus ID: 127105631 pp. 455-457 ref.2.

J. R. Ternate, M. I. Celeste, E. F. Pineda, F. J. Tan, and F. A. A. Uy**.** (2017). Floodplain Modelling of Malaking-Ilog River in Southern Luzon, Philippines Using

LiDAR Digital Elevation Model for the Design of Water-Related Structures, https://doi.org/10.1088/1757-899X/216/1/012044

Jakovljevic, G. and Govedarica, M. (2018). Water Body Extraction and Flood Risk Assessment Using Lidar and Open Data, https://doi.org/10.1007/978-3-030-03383-5_7

Jarvis, A., Rubiano, J., Nelson, A., Farrow, A. and Mulligan, M. (2004). Practical use of SRTM data in the tropics—comparisons with digital elevation models generated from cartographic data. Working Document, Vol. 198. Centro Internacional de Agricultura Tropical (CIAT), pp. 32.

Kaab, A. (2005). Combination of SRTM3 and repeat ASTER data for deriving alpine glacier flow velocities in the Bhutan Himalaya. Remote Sensing of Environment, 94, pp. 463–474.

Kaplan, G. and Avdan, U. (2017). Object-based water body extraction model using Sentinel-2 satellite imagery. Eur J Remote Sens 50(1): pp. 137–143, https://doi.org/10.1080/22797254.2017.1297540

Kellndorfer, J., Walker, W., Pierce, L., Dobson, C. and Fites, J.A. (2004). Vegetation height estimation from Shuttle Radar Topography Mission and National Elevation Datasets. Remote Sensing of Environment, 93, pp. 339–358, https://doi:10.1016/j.rse.2004.07.017.

Koch, A. and Lohmann, P. (2000). Quality Assessment and Validation of Digital Surface Models derived from the Shuttle Radar Topography Mission (SRTM), IAPRS, Vol. XXXIII, Amsterdam, https://doi.org/10.1109/IGARSS.2001.978187

Mehebub, S., Sajjad, H. and Ahmed, R. (2015). Assessing flood inundation extent and landscape vulnerability to flood using geospatial technology: A study of Malda district of West Bengal, India,Vol. XIV, pp. 156-163, http://dx.doi.org/10.5775/fg.2067-4635.2015.144.d

Miliaresis, G.C. and Paraschou, C.V.E. (2005). Vertical Accuracy of SRTM DTED Level 1 of Crete. International Journal of Applied Earth Observation and Geoinformation, 7, pp. 49-59.

National Research Council of the National Academies (2009) Mapping the zone, improving flood map accuracy. The National Academies Press, Washington, DC., ISBN 978-0-309-13057-8, pp. 7, https://doi.org/10.17226/12573.

Ouma Y., Tateishi R., 2014, Urban Flood Vulnerability and Risk Mapping Using Integrated Multi-Parametric AHP and GIS: Methodological Overview and Case Study Assessment., pp. 1515-1545, https://doi.org/10.3390/w6061515.

Ozah, A.P. and Kufoniyi, O. (2008). Accuracy assessment of Contour Interpolation from 1:50,000 Topographical maps and SRTM data for 1:25,000 Topographical

Mapping. The International Archives of the Photogrammetry, Remote Sensing and Spatial Information Sciences. Vol. XXXVII. Part B7.

Rabus, B., Eineder, M., Roth, A. and Bamler, R. (2003). The Shuttle Radar Topography Mission – a new class of Digital Elevation Models acquired by spaceborne Radar. ISPRS Journal of Photogrammetry and Remote Sensing, 57, pp. 241–262.

Smeeckaert, J., Mallet, C., David, N., Chehata, N. and Ferraz, A. (2013). Large-scale water classification of coastal areas using airborne topographic LiDAR data. In: IEEE International Geoscience and Remote Sensing Symposium, Melbourne, VIC, Australia, https://doi.org/101109./igarss.2013.6721092.

Smith, J. and Rowland, J., (2006). Temporal Analysis of Floodwater Volumes in New Orleans After Hurricane Katrina, https://doi.org/10.3133/cir13063H.

Topaloglu, R. H, Sertel, E. and Musaoglu, N. (2016). Assessment of classification accuracies of Sentinel-2 and Landsat-8 data for land cover/use mapping. In: The International Archives of the Photogrammetry, Remote Sensing and Spatial Information Sciences, Vol XLI-B8, XXIII ISPRS Congress, 12–19 July 2016, Prague, Czech Republic. https://doi.org/10.5194/isprsarchives-xli-b8-1055-2016.

University of Southern Queensland (2015). DEM Generation and Hydrologic Modelling using LiDAR Data, vol. 1, Student number: 0050102572, pp. 26-27.

Van de Sande, B., Lansen, J. and Hoyng, C. (2012). Sensitivity of coastal flood risk assessments to digital elevation models. Water, Vol. 4, pp. 568–579. https://doi.org/10.3390/w4030568.

Van Zyl, J.J. (2001). The Shuttle Radar Topography Mission (SRTM): A breakthrough in remote sensing of topography. Acta Astonautica, 48(5–12), pp. 559–565.

Verpoorter, C., Kutser, T. and Tranvik, L. (2012). Automated mapping of water bodies using Landsat multispectral data. Limnol Oceanogr Methods 10:1037–1050. https://doi.org/10.4319/lom.201210.103

Wedajo, G.K. (2017). LiDAR DEM data for flood mapping and assessment; opportunities and challenges - a review. J Remote Sens GIS 6:4. https://doi.org/10.4172/2469-4134.1000211.

Yang, X., Zhao, S., Qin, X., Thao, N. and Liang, L. (2017). Mapping of urban surface water bodies from Sentinel-2 MSI imagery at 10 m resolution via NDWI-based image sharpening. Remote Sens9(6): pp. 596, https://doi.org/10.3390/rs9060596.

## Appendices:

**Table (A1): X, Y, Z, flood46 from LiDAR DEM**

| SN | Chainage (m) | x-coord. | y-coord. | Reduced level (m) | Direction |
|---|---|---|---|---|---|
| 1 | 0 | 445,031.7 | 1,716,654.1 | 383.70 | |
| 2 | 60 | 445,010.8 | 1,716,600.2 | 383.86 | 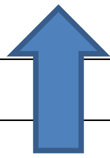 |
| 3 | 120 | 445,014.3 | 1,716,540.3 | 384.15 | |
| 4 | 180 | 445,001.0 | 1,716,484.7 | 384.27 | |
| 5 | 240 | 444,970.9 | 1,716,433.2 | 384.21 | |
| 6 | 300 | 444,963.7 | 1,716,373.6 | 384.01 | |
| 7 | 360 | 444,956.6 | 1,716,314.0 | 383.80 | |
| 8 | 420 | 444,949.4 | 1,716,254.5 | 383.26 | |
| 9 | 480 | 444,942.3 | 1,716,194.9 | 383.27 | |
| 10 | 540 | 444,935.1 | 1,716,135.3 | 383.07 | |
| 11 | 600 | 444,928.0 | 1,716,075.7 | 382.84 | |
| 12 | 660 | 444,920.8 | 1,716,016.2 | 382.58 | |
| 13 | 720 | 444,913.7 | 1,715,956.6 | 382.01 | |
| 14 | 780 | 444,906.5 | 1,715,897.0 | 382.23 | |
| 15 | 840 | 444,906.2 | 1,715,837.2 | 383.07 | |
| 16 | 900 | 444,909.7 | 1,715,777.3 | 382.66 | |
| 17 | 960 | 444,913.3 | 1,715,717.4 | 383.23 | |
| 18 | 1,020 | 444,916.8 | 1,715,657.6 | 383.25 | |
| 19 | 1,080 | 444,920.3 | 1,715,597.7 | 382.93 | |
| 20 | 1,140 | 444,923.8 | 1,715,537.8 | 382.91 | |
| 21 | 1,200 | 444,923.3 | 1,715,478.1 | 382.13 | |
| 22 | 1,260 | 444,912.1 | 1,715,419.2 | 382.00 | |
| 23 | 1,320 | 444,900.9 | 1,715,360.2 | 382.05 | |
| 24 | 1,380 | 444,889.7 | 1,715,301.3 | 382.00 | |
| 25 | 1,440 | 444,878.4 | 1,715,242.4 | 381.70 | |
| 26 | 1,500 | 444,867.2 | 1,715,183.4 | 381.59 | |

| SN | Chainage (m) | x-coord. | y-coord. | Reduced level (m) | Direction |
|---|---|---|---|---|---|
| 27 | 1,560 | 444,855.9 | 1,715,124.5 | 380.83 | |
| 28 | 1,620 | 444,844.7 | 1,715,065.6 | 381.20 | |
| 29 | 1,680 | 444,837.6 | 1,715,006.4 | 381.88 | 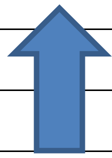 |
| 30 | 1,740 | 444,841.3 | 1,714,946.5 | 381.44 | |
| 31 | 1,800 | 444,845.0 | 1,714,886.6 | 382.20 | |
| 32 | 1,860 | 444,869.7 | 1,714,836.4 | 381.65 | |
| 33 | 1,920 | 444,911.7 | 1,714,793.6 | 381.58 | |
| 34 | 1,980 | 444,950.3 | 1,714,747.7 | 381.61 | |
| 35 | 2,040 | 444,989.3 | 1,714,702.1 | 382.68 | |
| 36 | 2,100 | 445,029.8 | 1,714,658.9 | 382.29 | |
| 37 | 2,160 | 445,087.3 | 1,714,641.7 | 381.43 | |
| 38 | 2,220 | 445,144.1 | 1,714,622.6 | 381.92 | |
| 39 | 2,280 | 445,198.4 | 1,714,597.2 | 381.45 | |
| 40 | 2,340 | 445,246.9 | 1,714,564.1 | 382.33 | |
| 41 | 2,400 | 445,285.0 | 1,714,517.8 | 382.18 | |
| 42 | 2,460 | 445,324.6 | 1,714,472.8 | 382.33 | |
| 43 | 2,520 | 445,366.3 | 1,714,429.7 | 382.64 | |
| 44 | 2,580 | 445,408.0 | 1,714,386.5 | 382.08 | |
| 45 | 2,640 | 445,448.7 | 1,714,342.5 | 382.75 | |
| 46 | 2,700 | 445,484.6 | 1,714,294.4 | 381.91 | |
| 47 | 2,760 | 445,499.7 | 1,714,243.6 | 381.54 | |
| 48 | 2,820 | 445,477.4 | 1,714,187.9 | 381.85 | |
| 49 | 2,880 | 445,429.1 | 1,714,153.4 | 382.21 | |
| 50 | 2,940 | 445,378.2 | 1,714,122.1 | 382.00 | |
| 51 | 3,000 | 445,320.7 | 1,714,105.2 | 381.85 | |
| 52 | 3,060 | 445,263.1 | 1,714,088.4 | 382.06 | |
| 53 | 3,120 | 445,205.5 | 1,714,084.0 | 381.73 | |
| 54 | 3,180 | 445,148.0 | 1,714,101.1 | 381.35 | |

| SN | Chainage (m) | x-coord. | y-coord. | Reduced level (m) | Direction |
|---|---|---|---|---|---|
| 55 | 3,240 | 445,095.9 | 1,714,129.1 | 382.09 | |
| 56 | 3,300 | 445,047.4 | 1,714,164.4 | 382.52 | |
| 57 | 3,360 | 444,997.8 | 1,714,198.0 | 382.16 | |
| 58 | 3,420 | 444,945.6 | 1,714,227.6 | 382.45 | |
| 59 | 3,480 | 444,893.4 | 1,714,257.2 | 381.90 | |
| 60 | 3,540 | 444,841.1 | 1,714,286.7 | 382.37 | |
| 61 | 3,600 | 444,788.4 | 1,714,315.4 | 381.66 | |
| 62 | 3,660 | 444,735.8 | 1,714,344.1 | 381.84 | |
| 63 | 3,720 | 444,709.5 | 1,714,298.4 | 382.02 | |
| 64 | 3,780 | 444,686.8 | 1,714,242.9 | 382.38 | |
| 65 | 3,840 | 444,665.8 | 1,714,186.6 | 382.49 | |
| 66 | 3,900 | 444,656.8 | 1,714,128.2 | 382.88 | |
| 67 | 3,960 | 444,656.8 | 1,714,068.2 | 382.48 | |
| 68 | 4,020 | 444,656.8 | 1,714,008.2 | 382.92 | |
| 69 | 4,080 | 444,656.8 | 1,713,948.2 | 382.29 | |
| 70 | 4,140 | 444,656.8 | 1,713,888.2 | 382.32 | |
| 71 | 4,200 | 444,634.6 | 1,713,833.5 | 382.34 | |
| 72 | 4,260 | 444,607.8 | 1,713,779.8 | 382.55 | |
| 73 | 4,320 | 444,580.9 | 1,713,726.2 | 382.51 | |
| 74 | 4,380 | 444,554.0 | 1,713,672.5 | 382.98 | |
| 75 | 4,440 | 444,527.2 | 1,713,618.8 | 383.06 | |
| 76 | 4,500 | 444,500.3 | 1,713,565.2 | 382.61 | |
| 77 | 4,560 | 444,473.5 | 1,713,511.5 | 382.35 | |

**Table (A2): X, Y, Z, flood88 from LiDAR DEM**

| SN | chainage (m) | x-coord. (m) | y-coord. (m) | Reduced level(m) | Direction |
|---|---|---|---|---|---|
| 1 | 0 | 445,022.9 | 1,716,656.2 | 383.80 | |
| 2 | 60 | 445,008.4 | 1,716,597.9 | 383.88 | |
| 3 | 120 | 445,002.4 | 1,716,538.7 | 384.20 | |
| 4 | 180 | 444,981.6 | 1,716,484.1 | 384.16 | 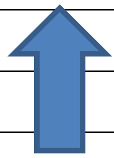 |
| 5 | 240 | 444,957.4 | 1,716,430.1 | 384.13 | |
| 6 | 300 | 444,950.3 | 1,716,370.5 | 384.04 | |
| 7 | 360 | 444,943.1 | 1,716,311.0 | 383.81 | |
| 8 | 420 | 444,936.0 | 1,716,251.4 | 383.12 | |
| 9 | 480 | 444,928.8 | 1,716,191.8 | 383.29 | |
| 10 | 540 | 444,921.7 | 1,716,132.2 | 383.25 | |
| 11 | 600 | 444,914.5 | 1,716,072.7 | 383.14 | |
| 12 | 660 | 444,907.3 | 1,716,013.1 | 382.89 | |
| 13 | 720 | 444,900.2 | 1,715,953.5 | 382.32 | |
| 14 | 780 | 444,893.0 | 1,715,893.9 | 382.07 | |
| 15 | 840 | 444,894.6 | 1,715,834.1 | 382.79 | |
| 16 | 900 | 444,898.1 | 1,715,774.2 | 382.51 | |
| 17 | 960 | 444,901.6 | 1,715,714.3 | 382.89 | |
| 18 | 1,020 | 444,905.2 | 1,715,654.4 | 383.03 | |
| 19 | 1,080 | 444,908.7 | 1,715,594.5 | 382.86 | |
| 20 | 1,140 | 444,912.2 | 1,715,534.6 | 382.83 | |
| 21 | 1,200 | 444,909.2 | 1,715,475.2 | 382.04 | |
| 22 | 1,260 | 444,898.0 | 1,715,416.2 | 382.09 | |
| 23 | 1,320 | 444,886.8 | 1,715,357.3 | 382.08 | |
| 24 | 1,380 | 444,875.5 | 1,715,298.3 | 381.97 | |
| 25 | 1,440 | 444,864.3 | 1,715,239.4 | 381.70 | |
| 26 | 1,500 | 444,853.0 | 1,715,180.5 | 381.64 | |
| 27 | 1,560 | 444,841.8 | 1,715,121.5 | 380.60 | |
| 28 | 1,620 | 444,830.6 | 1,715,062.6 | 381.14 | |

| SN | chainage (m) | x-coord. (m) | y-coord. (m) | Reduced level(m) | Direction |
|---|---|---|---|---|---|
| 29 | 1,680 | 444,826.0 | 1,715,003.2 | 381.64 | |
| 30 | 1,740 | 444,829.7 | 1,714,943.3 | 381.40 | |
| 31 | 1,800 | 444,833.5 | 1,714,883.5 | 382.24 | 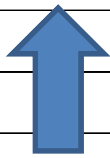 |
| 32 | 1,860 | 444,853.0 | 1,714,830.0 | 381.76 | |
| 33 | 1,920 | 444,891.5 | 1,714,784.1 | 381.42 | |
| 34 | 1,980 | 444,929.2 | 1,714,737.3 | 381.31 | |
| 35 | 2,040 | 444,968.8 | 1,714,692.3 | 381.77 | |
| 36 | 2,100 | 445,009.2 | 1,714,648.0 | 381.33 | |
| 37 | 2,160 | 445,061.5 | 1,714,621.2 | 381.27 | |
| 38 | 2,220 | 445,116.6 | 1,714,597.4 | 381.67 | |
| 39 | 2,280 | 445,165.8 | 1,714,564.0 | 381.69 | |
| 40 | 2,340 | 445,218.5 | 1,714,535.8 | 382.15 | |
| 41 | 2,400 | 445,264.8 | 1,714,497.9 | 381.98 | |
| 42 | 2,460 | 445,306.4 | 1,714,454.7 | 382.40 | |
| 43 | 2,520 | 445,351.0 | 1,714,414.6 | 382.56 | |
| 44 | 2,580 | 445,392.9 | 1,714,371.7 | 382.31 | |
| 45 | 2,640 | 445,433.1 | 1,714,327.2 | 382.30 | |
| 46 | 2,700 | 445,473.3 | 1,714,282.6 | 381.63 | |
| 47 | 2,760 | 445,471.6 | 1,714,229.2 | 381.72 | |
| 48 | 2,820 | 445,434.7 | 1,714,183.6 | 382.05 | |
| 49 | 2,880 | 445,382.8 | 1,714,153.5 | 381.76 | |
| 50 | 2,940 | 445,327.8 | 1,714,130.3 | 381.55 | |
| 51 | 3,000 | 445,270.9 | 1,714,111.2 | 381.37 | |
| 52 | 3,060 | 445,213.3 | 1,714,099.9 | 381.66 | |
| 53 | 3,120 | 445,156.2 | 1,714,116.5 | 381.44 | |
| 54 | 3,180 | 445,103.5 | 1,714,145.1 | 381.88 | |
| 55 | 3,240 | 445,053.4 | 1,714,178.2 | 382.29 | |
| 56 | 3,300 | 445,003.2 | 1,714,210.9 | 381.98 | |
| 57 | 3,360 | 444,951.1 | 1,714,240.9 | 381.67 | |

| SN | chainage (m) | x-coord. (m) | y-coord. (m) | Reduced level(m) | Direction |
|---|---|---|---|---|---|
| 58 | 3,420 | 444,899.1 | 1,714,270.8 | 381.75 | |
| 59 | 3,480 | 444,847.6 | 1,714,301.5 | 382.19 | |
| 60 | 3,540 | 444,796.4 | 1,714,332.7 | 381.81 | |
| 61 | 3,600 | 444,745.1 | 1,714,363.9 | 381.70 | |
| 62 | 3,660 | 444,711.8 | 1,714,340.8 | 382.39 | |
| 63 | 3,720 | 444,689.0 | 1,714,285.3 | 382.20 | |
| 64 | 3,780 | 444,666.3 | 1,714,229.8 | 382.69 | |
| 65 | 3,840 | 444,644.6 | 1,714,174.0 | 382.71 | |
| 66 | 3,900 | 444,644.6 | 1,714,114.0 | 382.67 | |
| 67 | 3,960 | 444,644.6 | 1,714,054.0 | 382.51 | |
| 68 | 4,020 | 444,644.6 | 1,713,994.0 | 382.76 | |
| 69 | 4,080 | 444,644.6 | 1,713,934.0 | 382.51 | |
| 70 | 4,140 | 444,639.7 | 1,713,875.2 | 382.46 | |
| 71 | 4,200 | 444,612.8 | 1,713,821.5 | 382.30 | |
| 72 | 4,260 | 444,586.0 | 1,713,767.9 | 382.48 | |
| 73 | 4,320 | 444,559.1 | 1,713,714.2 | 382.91 | |
| 74 | 4,380 | 444,532.3 | 1,713,660.6 | 383.03 | |
| 75 | 4,440 | 444,505.4 | 1,713,606.9 | 383.48 | |
| 76 | 4,500 | 444,478.6 | 1,713,553.3 | 382.40 | |
| 77 | 4,560 | 444,451.7 | 1,713,499.6 | 382.49 | |

Table (A3): X, Y, Z, protection bank from LiDAR DEM

| SN | Chainage (m) | x-coord. (m) | y-coord. (m) | Reduced level (m) | Direction |
|---|---|---|---|---|---|
| 1 | 0 | 444,639.2 | 1,716,650.8 | 382.66 | |
| 2 | 60 | 444,650.9 | 1,716,592.0 | 383.28 | |
| 3 | 120 | 444,662.6 | 1,716,533.2 | 383.87 | 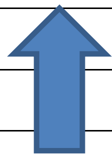 |
| 4 | 180 | 444,674.3 | 1,716,474.3 | 384.03 | |
| 5 | 240 | 444,686.1 | 1,716,415.5 | 384.97 | |
| 6 | 300 | 444,697.8 | 1,716,356.6 | 384.45 | |
| 7 | 360 | 444,709.5 | 1,716,297.8 | 383.74 | |
| 8 | 420 | 444,721.2 | 1,716,238.9 | 382.64 | |
| 9 | 480 | 444,732.9 | 1,716,180.1 | 382.06 | |
| 10 | 540 | 444,744.7 | 1,716,121.3 | 381.91 | |
| 11 | 600 | 444,756.4 | 1,716,062.4 | 381.74 | |
| 12 | 660 | 444,768.1 | 1,716,003.6 | 381.99 | |
| 13 | 720 | 444,779.8 | 1,715,944.7 | 381.76 | |
| 14 | 780 | 444,788.7 | 1,715,885.5 | 381.63 | |
| 15 | 840 | 444,791.4 | 1,715,825.6 | 381.65 | |
| 16 | 900 | 444,794.1 | 1,715,765.7 | 381.73 | |
| 17 | 960 | 444,796.8 | 1,715,705.7 | 381.55 | |
| 18 | 1,020 | 444,799.5 | 1,715,645.8 | 380.72 | |
| 19 | 1,080 | 444,796.9 | 1,715,585.9 | 380.98 | |
| 20 | 1,140 | 444,792.8 | 1,715,526.0 | 381.83 | |
| 21 | 1,200 | 444,788.8 | 1,715,466.2 | 382.78 | |
| 22 | 1,260 | 444,778.1 | 1,715,407.3 | 381.80 | |
| 23 | 1,320 | 444,764.4 | 1,715,348.9 | 381.82 | |
| 24 | 1,380 | 444,750.8 | 1,715,290.4 | 381.64 | |
| 25 | 1,440 | 444,737.3 | 1,715,232.0 | 381.70 | |
| 26 | 1,500 | 444,723.6 | 1,715,173.6 | 381.35 | |
| 27 | 1,560 | 444,705.4 | 1,715,116.5 | 381.53 | |

| SN | Chainage (m) | x-coord. (m) | y-coord. (m) | Reduced level (m) | Direction |
|---|---|---|---|---|---|
| 28 | 1,620 | 444,684.9 | 1,715,060.1 | 380.94 | |
| 29 | 1,680 | 444,664.5 | 1,715,003.7 | 381.54 | |
| 30 | 1,740 | 444,644.1 | 1,714,947.3 | 381.25 | |
| 31 | 1,800 | 444,623.6 | 1,714,890.9 | 380.85 | ↑ |
| 32 | 1,860 | 444,603.2 | 1,714,834.4 | 381.31 | |
| 33 | 1,920 | 444,552.2 | 1,714,837.3 | 381.09 | |
| 34 | 1,980 | 444,494.0 | 1,714,851.2 | 380.74 | |
| 35 | 2,040 | 444,443.3 | 1,714,827.7 | 381.29 | |
| 36 | 2,100 | 444,409.1 | 1,714,778.4 | 380.54 | |
| 37 | 2,160 | 444,374.8 | 1,714,729.2 | 382.01 | |
| 38 | 2,220 | 444,340.5 | 1,714,679.9 | 380.04 | |
| 39 | 2,280 | 444,306.3 | 1,714,630.7 | 381.90 | |
| 40 | 2,340 | 444,272.0 | 1,714,581.4 | 383.16 | |
| 41 | 2,400 | 444,237.8 | 1,714,532.2 | 381.92 | |
| 42 | 2,460 | 444,203.5 | 1,714,482.9 | 380.59 | |
| 43 | 2,520 | 444,169.2 | 1,714,433.7 | 380.34 | |
| 44 | 2,580 | 444,134.9 | 1,714,384.4 | 380.43 | |
| 45 | 2,640 | 444,100.9 | 1,714,335.1 | 380.00 | |
| 46 | 2,700 | 444,089.1 | 1,714,276.2 | 380.41 | |
| 47 | 2,760 | 444,077.3 | 1,714,217.4 | 380.24 | |
| 48 | 2,820 | 444,065.5 | 1,714,158.6 | 380.29 | |
| 49 | 2,880 | 444,046.6 | 1,714,102.4 | 380.98 | |
| 50 | 2,940 | 444,021.6 | 1,714,047.9 | 381.17 | |
| 51 | 3,000 | 444,003.3 | 1,713,990.9 | 379.43 | |
| 52 | 3,060 | 443,982.7 | 1,713,934.7 | 380.29 | |
| 53 | 3,120 | 443,968.5 | 1,713,876.4 | 380.67 | |
| 54 | 3,180 | 443,956.6 | 1,713,817.7 | 381.07 | |
| 55 | 3,240 | 443,941.9 | 1,713,759.6 | 380.88 | |
| 56 | 3,300 | 443,927.7 | 1,713,701.5 | 380.10 | |

| SN | Chainage (m) | x-coord. (m) | y-coord. (m) | Reduced level (m) | Direction |
|---|---|---|---|---|---|
| 57 | 3,360 | 443,902.0 | 1,713,647.3 | 380.42 | |
| 58 | 3,420 | 443,881.4 | 1,713,591.1 | 381.22 | |
| 59 | 3,480 | 443,865.3 | 1,713,533.3 | 380.93 | |

,

**Table (A4): Chainage and Reduced level of 46 and 88 flood lines and protection bank**

| SN | Chainage (m) | 46 R.L.(m) | 88 R.L.(m) | protection R.L. (m) | |
|---|---|---|---|---|---|
| 1 | 0 | 383.70 | 383.80 | 382.66 | |
| 2 | 60 | 383.86 | 383.88 | 383.28 | |
| 3 | 120 | 384.15 | 384.20 | 383.87 | |
| 4 | 180 | 384.27 | 384.16 | 384.03 | |
| 5 | 240 | 384.21 | 384.13 | 384.97 | |
| 6 | 300 | 384.01 | 384.04 | 384.45 | |
| 7 | 360 | 383.80 | 383.81 | 383.74 | |
| 8 | 420 | 383.26 | 383.12 | 382.64 | |
| 9 | 480 | 383.27 | 383.29 | 382.06 | |
| 10 | 540 | 383.07 | 383.25 | 381.91 | |
| 11 | 600 | 382.84 | 383.14 | 381.74 | |
| 12 | 660 | 382.58 | 382.89 | 381.99 | |
| 13 | 720 | 382.01 | 382.32 | 381.76 | |
| 14 | 780 | 382.23 | 382.07 | 381.63 | |
| 15 | 840 | 383.07 | 382.79 | 381.65 | |
| 16 | 900 | 382.66 | 382.51 | 381.73 | |
| 17 | 960 | 383.23 | 382.89 | 381.55 | |
| 18 | 1,020 | 383.25 | 383.03 | 380.72 | |
| 19 | 1,080 | 382.93 | 382.86 | 380.98 | |
| 20 | 1,140 | 382.91 | 382.83 | 381.83 | |
| 21 | 1,200 | 382.13 | 382.04 | 382.78 | |
| 22 | 1,260 | 382.00 | 382.09 | 381.80 | |
| 23 | 1,320 | 382.05 | 382.08 | 381.82 | |
| 24 | 1,380 | 382.00 | 381.97 | 381.64 | |
| 25 | 1,440 | 381.70 | 381.70 | 381.70 | |
| 26 | 1,500 | 381.59 | 381.64 | 381.35 | |

| SN | Chainage (m) | 46 R.L.(m) | 88 R.L.(m) | protection R.L. (m) | |
|---|---|---|---|---|---|
| 27 | 1,560 | 380.83 | 380.60 | 381.53 | |
| 28 | 1,620 | 381.20 | 381.14 | 380.94 | |
| 29 | 1,680 | 381.88 | 381.64 | 381.54 | |
| 30 | 1,740 | 381.44 | 381.40 | 381.25 | |
| 31 | 1,800 | 382.20 | 382.24 | 380.85 | |
| 32 | 1,860 | 381.65 | 381.76 | 381.31 | |
| 33 | 1,920 | 381.58 | 381.42 | 381.09 | |
| 34 | 1,980 | 381.61 | 381.31 | 380.74 | |
| 35 | 2,040 | 382.68 | 381.77 | 381.29 | |
| 36 | 2,100 | 382.29 | 381.33 | 380.54 | |
| 37 | 2,160 | 381.43 | 381.27 | 382.01 | |
| 38 | 2,220 | 381.92 | 381.67 | 380.04 | |
| 39 | 2,280 | 381.45 | 381.69 | 381.90 | |
| 40 | 2,340 | 382.33 | 382.15 | 383.16 | |
| 41 | 2,400 | 382.18 | 381.98 | 381.92 | |
| 42 | 2,460 | 382.33 | 382.40 | 380.59 | |
| 43 | 2,520 | 382.64 | 382.56 | 380.34 | |
| 44 | 2,580 | 382.08 | 382.31 | 380.43 | |
| 45 | 2,640 | 382.75 | 382.30 | 380.00 | |
| 46 | 2,700 | 381.91 | 381.63 | 380.41 | |
| 47 | 2,760 | 381.54 | 381.72 | 380.24 | |
| 48 | 2,820 | 381.85 | 382.05 | 380.29 | |
| 49 | 2,880 | 382.21 | 381.76 | 380.98 | |
| 50 | 2,940 | 382.00 | 381.55 | 381.17 | |
| 51 | 3,000 | 381.85 | 381.37 | 379.43 | |
| 52 | 3,060 | 382.06 | 381.66 | 380.29 | |
| 53 | 3,120 | 381.73 | 381.44 | 380.67 | |

| SN | Chainage (m) | 46 R.L.(m) | 88 R.L.(m) | protection R.L. (m) | |
|---|---|---|---|---|---|
| 54 | 3,180 | 381.35 | 381.88 | 381.07 | |
| 55 | 3,240 | 382.09 | 382.29 | 380.88 | |
| 56 | 3,300 | 382.52 | 381.98 | 380.10 | |
| 57 | 3,360 | 382.16 | 381.67 | 380.42 | |
| 58 | 3,420 | 382.45 | 381.75 | 381.22 | |
| 59 | 3,480 | 381.90 | 382.19 | 380.93 | |
| 60 | 3,540 | 382.37 | 381.81 | | |
| 61 | 3,600 | 381.66 | 381.70 | | |
| 62 | 3,660 | 381.84 | 382.39 | | |
| 63 | 3,720 | 382.02 | 382.20 | | |
| 64 | 3,780 | 382.38 | 382.69 | | |
| 65 | 3,840 | 382.49 | 382.71 | | |
| 66 | 3,900 | 382.88 | 382.67 | | |
| 67 | 3,960 | 382.48 | 382.51 | | |
| 68 | 4,020 | 382.92 | 382.76 | | |
| 69 | 4,080 | 382.29 | 382.51 | | |
| 70 | 4,140 | 382.32 | 382.46 | | |
| 71 | 4,200 | 382.34 | 382.30 | | |
| 72 | 4,260 | 382.55 | 382.48 | | |
| 73 | 4,320 | 382.51 | 382.91 | | |
| 74 | 4,380 | 382.98 | 383.03 | | |
| 75 | 4,440 | 383.06 | 383.48 | | |
| 76 | 4,500 | 382.61 | 382.40 | | |
| 77 | 4,560 | 382.35 | 382.49 | | |

**Table (A5): X, Y, Z, 1946 flood extent line from SRTM DEM**

| SN | Chainage (m) | x – coord. (m) | y-coord. (m) | Reduced level (m) | Direction |
|---|---|---|---|---|---|
| 1 | 0 | 445,031.7 | 1,716,654.1 | 381 | |
| 2 | 60 | 445,010.8 | 1,716,600.2 | 381 | |
| 3 | 120 | 445,014.3 | 1,716,540.3 | 384 | |
| 4 | 180 | 445,001.0 | 1,716,484.7 | 387 | 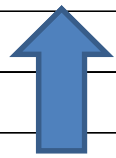 |
| 5 | 240 | 444,970.9 | 1,716,433.2 | 388 | |
| 6 | 300 | 444,963.7 | 1,716,373.6 | 385 | |
| 7 | 360 | 444,956.6 | 1,716,314.0 | 384 | |
| 8 | 420 | 444,949.4 | 1,716,254.5 | 385 | |
| 9 | 480 | 444,942.3 | 1,716,194.9 | 384 | |
| 10 | 540 | 444,935.1 | 1,716,135.3 | 382 | |
| 11 | 600 | 444,928.0 | 1,716,075.7 | 384 | |
| 12 | 660 | 444,920.8 | 1,716,016.2 | 383 | |
| 13 | 720 | 444,913.7 | 1,715,956.6 | 384 | |
| 14 | 780 | 444,906.5 | 1,715,897.0 | 383 | |
| 15 | 840 | 444,906.2 | 1,715,837.2 | 383 | |
| 16 | 900 | 444,909.7 | 1,715,777.3 | 382 | |
| 17 | 960 | 444,913.3 | 1,715,717.4 | 384 | |
| 18 | 1,020 | 444,916.8 | 1,715,657.6 | 384 | |
| 19 | 1,080 | 444,920.3 | 1,715,597.7 | 385 | |
| 20 | 1,140 | 444,923.8 | 1,715,537.8 | 385 | |
| 21 | 1,200 | 444,923.3 | 1,715,478.1 | 384 | |
| 22 | 1,260 | 444,912.1 | 1,715,419.2 | 383 | |
| 23 | 1,320 | 444,900.9 | 1,715,360.2 | 381 | |
| 24 | 1,380 | 444,889.7 | 1,715,301.3 | 379 | |
| 25 | 1,440 | 444,878.4 | 1,715,242.4 | 381 | |
| 26 | 1,500 | 444,867.2 | 1,715,183.4 | 385 | |
| 27 | 1,560 | 444,855.9 | 1,715,124.5 | 380 | |

| SN | Chainage (m) | x – coord. (m) | y-coord. (m) | Reduced level (m) | Direction |
|---|---|---|---|---|---|
| 28 | 1,620 | 444,844.7 | 1,715,065.6 | 382 | |
| 29 | 1,680 | 444,837.6 | 1,715,006.4 | 372 | |
| 30 | 1,740 | 444,841.3 | 1,714,946.5 | 376 | |
| 31 | 1,800 | 444,845.0 | 1,714,886.6 | 375 | |
| 32 | 1,860 | 444,869.7 | 1,714,836.4 | 380 | |
| 33 | 1,920 | 444,911.7 | 1,714,793.6 | 385 | |
| 34 | 1,980 | 444,950.3 | 1,714,747.7 | 375 | |
| 35 | 2,040 | 444,989.3 | 1,714,702.1 | 379 | |
| 36 | 2,100 | 445,029.8 | 1,714,658.9 | 382 | |
| 37 | 2,160 | 445,087.3 | 1,714,641.7 | 384 | |
| 38 | 2,220 | 445,144.1 | 1,714,622.6 | 381 | |
| 39 | 2,280 | 445,198.4 | 1,714,597.2 | 380 | |
| 40 | 2,340 | 445,246.9 | 1,714,564.1 | 382 | |
| 41 | 2,400 | 445,285.0 | 1,714,517.8 | 381 | |
| 42 | 2,460 | 445,324.6 | 1,714,472.8 | 381 | |
| 43 | 2,520 | 445,366.3 | 1,714,429.7 | 382 | |
| 44 | 2,580 | 445,408.0 | 1,714,386.5 | 384 | |
| 45 | 2,640 | 445,448.7 | 1,714,342.5 | 382 | |
| 46 | 2,700 | 445,484.6 | 1,714,294.4 | 382 | |
| 47 | 2,760 | 445,499.7 | 1,714,243.6 | 388 | |
| 48 | 2,820 | 445,477.4 | 1,714,187.9 | 378 | |
| 49 | 2,880 | 445,429.1 | 1,714,153.4 | 379 | |
| 50 | 2,940 | 445,378.2 | 1,714,122.1 | 386 | |
| 51 | 3,000 | 445,320.7 | 1,714,105.2 | 385 | |
| 52 | 3,060 | 445,263.1 | 1,714,088.4 | 382 | |
| 53 | 3,120 | 445,205.5 | 1,714,084.0 | 380 | |
| 54 | 3,180 | 445,148.0 | 1,714,101.1 | 382 | |
| 55 | 3,240 | 445,095.9 | 1,714,129.1 | 382 | |
| 56 | 3,300 | 445,047.4 | 1,714,164.4 | 381 | |

| SN | Chainage (m) | x – coord. (m) | y-coord. (m) | Reduced level (m) | Direction |
|---|---|---|---|---|---|
| 57 | 3,360 | 444,997.8 | 1,714,198.0 | 381 | |
| 58 | 3,420 | 444,945.6 | 1,714,227.6 | 382 | |
| 59 | 3,480 | 444,893.4 | 1,714,257.2 | 381 | |
| 60 | 3,540 | 444,841.1 | 1,714,286.7 | 380 | |
| 61 | 3,600 | 444,788.4 | 1,714,315.4 | 380 | 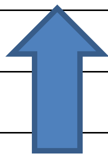 |
| 62 | 3,660 | 444,735.8 | 1,714,344.1 | 381 | |
| 63 | 3,720 | 444,709.5 | 1,714,298.4 | 380 | |
| 64 | 3,780 | 444,686.8 | 1,714,242.9 | 382 | |
| 65 | 3,840 | 444,665.8 | 1,714,186.6 | 380 | |
| 66 | 3,900 | 444,656.8 | 1,714,128.2 | 378 | |
| 67 | 3,960 | 444,656.8 | 1,714,068.2 | 380 | |
| 68 | 4,020 | 444,656.8 | 1,714,008.2 | 379 | |
| 69 | 4,080 | 444,656.8 | 1,713,948.2 | 382 | |
| 70 | 4,140 | 444,656.8 | 1,713,888.2 | 384 | |
| 71 | 4,200 | 444,634.6 | 1,713,833.5 | 381 | |
| 72 | 4,260 | 444,607.8 | 1,713,779.8 | 381 | |
| 73 | 4,320 | 444,580.9 | 1,713,726.2 | 385 | |
| 74 | 4,380 | 444,554.0 | 1,713,672.5 | 382 | |
| 75 | 4,440 | 444,527.2 | 1,713,618.8 | 384 | |
| 76 | 4,500 | 444,500.3 | 1,713,565.2 | 384 | |
| 77 | 4,560 | 444,473.5 | 1,713,511.5 | 383 | |

**Table (A6): X, Y, Z, 1988 flood extent line from SRTM DEM**

| SN | Chainage (m) | x-coord. (m) | y-coord. (m) | Reduced level (m) | Direction |
|---|---|---|---|---|---|
| 1 | 0 | 445,022.9 | 1,716,656.2 | 381 | |
| 2 | 60 | 445,008.4 | 1,716,597.9 | 381 | |
| 3 | 120 | 445,002.4 | 1,716,538.7 | 384 | 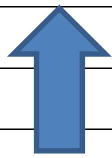 |
| 4 | 180 | 444,981.6 | 1,716,484.1 | 387 | |
| 5 | 240 | 444,957.4 | 1,716,430.1 | 386 | |
| 6 | 300 | 444,950.3 | 1,716,370.5 | 384 | |
| 7 | 360 | 444,943.1 | 1,716,311.0 | 384 | |
| 8 | 420 | 444,936.0 | 1,716,251.4 | 385 | |
| 9 | 480 | 444,928.8 | 1,716,191.8 | 384 | |
| 10 | 540 | 444,921.7 | 1,716,132.2 | 382 | |
| 11 | 600 | 444,914.5 | 1,716,072.7 | 384 | |
| 12 | 660 | 444,907.3 | 1,716,013.1 | 384 | |
| 13 | 720 | 444,900.2 | 1,715,953.5 | 385 | |
| 14 | 780 | 444,893.0 | 1,715,893.9 | 383 | |
| 15 | 840 | 444,894.6 | 1,715,834.1 | 383 | |
| 16 | 900 | 444,898.1 | 1,715,774.2 | 382 | |
| 17 | 960 | 444,901.6 | 1,715,714.3 | 383 | |
| 18 | 1,020 | 444,905.2 | 1,715,654.4 | 383 | |
| 19 | 1,080 | 444,908.7 | 1,715,594.5 | 384 | |
| 20 | 1,140 | 444,912.2 | 1,715,534.6 | 385 | |
| 21 | 1,200 | 444,909.2 | 1,715,475.2 | 383 | |
| 22 | 1,260 | 444,898.0 | 1,715,416.2 | 382 | |
| 23 | 1,320 | 444,886.8 | 1,715,357.3 | 381 | |
| 24 | 1,380 | 444,875.5 | 1,715,298.3 | 379 | |
| 25 | 1,440 | 444,864.3 | 1,715,239.4 | 381 | |
| 26 | 1,500 | 444,853.0 | 1,715,180.5 | 385 | |
| 27 | 1,560 | 444,841.8 | 1,715,121.5 | 381 | |
| 28 | 1,620 | 444,830.6 | 1,715,062.6 | 382 | |

| SN | Chainage (m) | x-coord. (m) | y-coord. (m) | Reduced level (m) | Direction |
|---|---|---|---|---|---|
| 29 | 1,680 | 444,826.0 | 1,715,003.2 | 372 | |
| 30 | 1,740 | 444,829.7 | 1,714,943.3 | 376 | |
| 31 | 1,800 | 444,833.5 | 1,714,883.5 | 375 | |
| 32 | 1,860 | 444,853.0 | 1,714,830.0 | 384 | ↑ |
| 33 | 1,920 | 444,891.5 | 1,714,784.1 | 385 | |
| 34 | 1,980 | 444,929.2 | 1,714,737.3 | 378 | |
| 35 | 2,040 | 444,968.8 | 1,714,692.3 | 378 | |
| 36 | 2,100 | 445,009.2 | 1,714,648.0 | 382 | |
| 37 | 2,160 | 445,061.5 | 1,714,621.2 | 383 | |
| 38 | 2,220 | 445,116.6 | 1,714,597.4 | 382 | |
| 39 | 2,280 | 445,165.8 | 1,714,564.0 | 380 | |
| 40 | 2,340 | 445,218.5 | 1,714,535.8 | 382 | |
| 41 | 2,400 | 445,264.8 | 1,714,497.9 | 383 | |
| 42 | 2,460 | 445,306.4 | 1,714,454.7 | 380 | |
| 43 | 2,520 | 445,351.0 | 1,714,414.6 | 381 | |
| 44 | 2,580 | 445,392.9 | 1,714,371.7 | 382 | |
| 45 | 2,640 | 445,433.1 | 1,714,327.2 | 382 | |
| 46 | 2,700 | 445,473.3 | 1,714,282.6 | 385 | |
| 47 | 2,760 | 445,471.6 | 1,714,229.2 | 385 | |
| 48 | 2,820 | 445,434.7 | 1,714,183.6 | 376 | |
| 49 | 2,880 | 445,382.8 | 1,714,153.5 | 385 | |
| 50 | 2,940 | 445,327.8 | 1,714,130.3 | 387 | |
| 51 | 3,000 | 445,270.9 | 1,714,111.2 | 381 | |
| 52 | 3,060 | 445,213.3 | 1,714,099.9 | 380 | |
| 53 | 3,120 | 445,156.2 | 1,714,116.5 | 382 | |
| 54 | 3,180 | 445,103.5 | 1,714,145.1 | 382 | |
| 55 | 3,240 | 445,053.4 | 1,714,178.2 | 382 | |
| 56 | 3,300 | 445,003.2 | 1,714,210.9 | 381 | |
| 57 | 3,360 | 444,951.1 | 1,714,240.9 | 382 | |

| SN | Chainage (m) | x-coord. (m) | y-coord. (m) | Reduced level (m) | Direction |
|---|---|---|---|---|---|
| 58 | 3,420 | 444,899.1 | 1,714,270.8 | 381 | |
| 59 | 3,480 | 444,847.6 | 1,714,301.5 | 381 | |
| 60 | 3,540 | 444,796.4 | 1,714,332.7 | 380 | 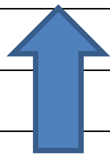 |
| 61 | 3,600 | 444,745.1 | 1,714,363.9 | 382 | |
| 62 | 3,660 | 444,711.8 | 1,714,340.8 | 381 | |
| 63 | 3,720 | 444,689.0 | 1,714,285.3 | 380 | |
| 64 | 3,780 | 444,666.3 | 1,714,229.8 | 381 | |
| 65 | 3,840 | 444,644.6 | 1,714,174.0 | 380 | |
| 66 | 3,900 | 444,644.6 | 1,714,114.0 | 378 | |
| 67 | 3,960 | 444,644.6 | 1,714,054.0 | 380 | |
| 68 | 4,020 | 444,644.6 | 1,713,994.0 | 379 | |
| 69 | 4,080 | 444,644.6 | 1,713,934.0 | 382 | |
| 70 | 4,140 | 444,639.7 | 1,713,875.2 | 384 | |
| 71 | 4,200 | 444,612.8 | 1,713,821.5 | 381 | |
| 72 | 4,260 | 444,586.0 | 1,713,767.9 | 384 | |
| 73 | 4,320 | 444,559.1 | 1,713,714.2 | 382 | |
| 74 | 4,380 | 444,532.3 | 1,713,660.6 | 382 | |
| 75 | 4,440 | 444,505.4 | 1,713,606.9 | 384 | |
| 76 | 4,500 | 444,478.6 | 1,713,553.3 | 384 | |
| 77 | 4,560 | 444,451.7 | 1,713,499.6 | 384 | |

Table (A7): X, Y, Z, protection bank from SRTM DEM

| SN | Chainage (m) | x-coord. (m) | y-coord. (m) | Reduced level (m) | Direction |
|---|---|---|---|---|---|
| 1 | 0 | 444,639.2 | 1,716,650.8 | 382 | |
| 2 | 60 | 444,650.9 | 1,716,592.0 | 384 | |
| 3 | 120 | 444,662.6 | 1,716,533.2 | 386 | 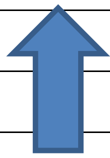 |
| 4 | 180 | 444,674.3 | 1,716,474.3 | 385 | |
| 5 | 240 | 444,686.1 | 1,716,415.5 | 385 | |
| 6 | 300 | 444,697.8 | 1,716,356.6 | 386 | |
| 7 | 360 | 444,709.5 | 1,716,297.8 | 384 | |
| 8 | 420 | 444,721.2 | 1,716,238.9 | 379 | |
| 9 | 480 | 444,732.9 | 1,716,180.1 | 381 | |
| 10 | 540 | 444,744.7 | 1,716,121.3 | 381 | |
| 11 | 600 | 444,756.4 | 1,716,062.4 | 381 | |
| 12 | 660 | 444,768.1 | 1,716,003.6 | 382 | |
| 13 | 720 | 444,779.8 | 1,715,944.7 | 381 | |
| 14 | 780 | 444,788.7 | 1,715,885.5 | 380 | |
| 15 | 840 | 444,791.4 | 1,715,825.6 | 382 | |
| 16 | 900 | 444,794.1 | 1,715,765.7 | 383 | |
| 17 | 960 | 444,796.8 | 1,715,705.7 | 384 | |
| 18 | 1,020 | 444,799.5 | 1,715,645.8 | 380 | |
| 19 | 1,080 | 444,796.9 | 1,715,585.9 | 379 | |
| 20 | 1,140 | 444,792.8 | 1,715,526.0 | 381 | |
| 21 | 1,200 | 444,788.8 | 1,715,466.2 | 383 | |
| 22 | 1,260 | 444,778.1 | 1,715,407.3 | 384 | |
| 23 | 1,320 | 444,764.4 | 1,715,348.9 | 382 | |
| 24 | 1,380 | 444,750.8 | 1,715,290.4 | 380 | |
| 25 | 1,440 | 444,737.3 | 1,715,232.0 | 381 | |
| 26 | 1,500 | 444,723.6 | 1,715,173.6 | 383 | |
| 27 | 1,560 | 444,705.4 | 1,715,116.5 | 383 | |
| 28 | 1,620 | 444,684.9 | 1,715,060.1 | 381 | |

| SN | Chainage (m) | x-coord. (m) | y-coord. (m) | Reduced level (m) | Direction |
|---|---|---|---|---|---|
| 29 | 1,680 | 444,664.5 | 1,715,003.7 | 381 | |
| 30 | 1,740 | 444,644.1 | 1,714,947.3 | 382 | |
| 31 | 1,800 | 444,623.6 | 1,714,890.9 | 381 | |
| 32 | 1,860 | 444,603.2 | 1,714,834.4 | 382 | |
| 33 | 1,920 | 444,552.2 | 1,714,837.3 | 382 | |
| 34 | 1,980 | 444,494.0 | 1,714,851.2 | 377 | |
| 35 | 2,040 | 444,443.3 | 1,714,827.7 | 380 | |
| 36 | 2,100 | 444,409.1 | 1,714,778.4 | 381 | |
| 37 | 2,160 | 444,374.8 | 1,714,729.2 | 380 | |
| 38 | 2,220 | 444,340.5 | 1,714,679.9 | 382 | |
| 39 | 2,280 | 444,306.3 | 1,714,630.7 | 379 | |
| 40 | 2,340 | 444,272.0 | 1,714,581.4 | 382 | |
| 41 | 2,400 | 444,237.8 | 1,714,532.2 | 382 | |
| 42 | 2,460 | 444,203.5 | 1,714,482.9 | 379 | |
| 43 | 2,520 | 444,169.2 | 1,714,433.7 | 379 | |
| 44 | 2,580 | 444,134.9 | 1,714,384.4 | 381 | |
| 45 | 2,640 | 444,100.9 | 1,714,335.1 | 381 | |
| 46 | 2,700 | 444,089.1 | 1,714,276.2 | 381 | |
| 47 | 2,760 | 444,077.3 | 1,714,217.4 | 380 | |
| 48 | 2,820 | 444,065.5 | 1,714,158.6 | 381 | |
| 49 | 2,880 | 444,046.6 | 1,714,102.4 | 380 | |
| 50 | 2,940 | 444,021.6 | 1,714,047.9 | 381 | |
| 51 | 3,000 | 444,003.3 | 1,713,990.9 | 377 | |
| 52 | 3,060 | 443,982.7 | 1,713,934.7 | 380 | |
| 53 | 3,120 | 443,968.5 | 1,713,876.4 | 378 | |
| 54 | 3,180 | 443,956.6 | 1,713,817.7 | 380 | |
| 55 | 3,240 | 443,941.9 | 1,713,759.6 | 379 | |
| 56 | 3,300 | 443,927.7 | 1,713,701.5 | 381 | |
| 57 | 3,360 | 443,902.0 | 1,713,647.3 | 380 | |

| SN | Chainage (m) | x-coord. (m) | y-coord. (m) | Reduced level (m) | Direction |
|---|---|---|---|---|---|
| 58 | 3,420 | 443,881.4 | 1,713,591.1 | 379 | |
| 59 | 3,480 | 443,865.3 | 1,713,533.3 | 381 | |

**Table (A8): Chainage and Reduced level of 46and 88 flood lines and protection bank from SRTM DEM**

| SN | Chainage (m) | R.L. 46 (m) | R.L. 89 (m) | Protection R.L. (m) | Direction |
|---|---|---|---|---|---|
| 1 | 0 | 381 | 381 | 382 | |
| 2 | 60 | 381 | 381 | 384 | |
| 3 | 120 | 384 | 384 | 386 | 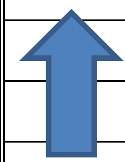 |
| 4 | 180 | 387 | 387 | 385 | |
| 5 | 240 | 388 | 386 | 385 | |
| 6 | 300 | 385 | 384 | 386 | |
| 7 | 360 | 384 | 384 | 384 | |
| 8 | 420 | 385 | 385 | 379 | |
| 9 | 480 | 384 | 384 | 381 | |
| 10 | 540 | 382 | 382 | 381 | |
| 11 | 600 | 384 | 384 | 381 | |
| 12 | 660 | 383 | 384 | 382 | |
| 13 | 720 | 384 | 385 | 381 | |
| 14 | 780 | 383 | 383 | 380 | |
| 15 | 840 | 383 | 383 | 382 | |
| 16 | 900 | 382 | 382 | 383 | |
| 17 | 960 | 384 | 383 | 384 | |
| 18 | 1,020 | 384 | 383 | 380 | |
| 19 | 1,080 | 385 | 384 | 379 | |
| 20 | 1,140 | 385 | 385 | 381 | |
| 21 | 1,200 | 384 | 383 | 383 | |

| SN | Chainage (m) | R.L. 46 (m) | R.L. 89 (m) | Protection R.L. (m) | Direction |
|---|---|---|---|---|---|
| 22 | 1,260 | 383 | 382 | 384 | |
| 23 | 1,320 | 381 | 381 | 382 | |
| 24 | 1,380 | 379 | 379 | 380 | |
| 25 | 1,440 | 381 | 381 | 381 | 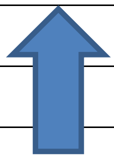 |
| 26 | 1500 | 385 | 385 | 383 | |
| 27 | 1,560 | 380 | 381 | 383 | |
| 28 | 1,620 | 382 | 382 | 381 | |
| 29 | 1,680 | 372 | 372 | 381 | |
| 30 | 1,740 | 376 | 376 | 382 | |
| 31 | 1,800 | 375 | 375 | 381 | |
| 32 | 1,860 | 380 | 384 | 382 | |
| 33 | 1,920 | 385 | 385 | 382 | |
| 34 | 1,980 | 375 | 378 | 377 | |
| 35 | 2,040 | 379 | 378 | 380 | |
| 36 | 2,100 | 382 | 382 | 381 | |
| 37 | 2,160 | 384 | 383 | 380 | |
| 38 | 2,220 | 381 | 382 | 382 | |
| 39 | 2,280 | 380 | 380 | 379 | |
| 40 | 2,340 | 382 | 382 | 382 | |
| 41 | 2,400 | 381 | 383 | 382 | |
| 42 | 2,460 | 381 | 380 | 379 | |
| 43 | 2,520 | 382 | 381 | 379 | |
| 44 | 2,580 | 384 | 382 | 381 | |
| 45 | 2,640 | 382 | 382 | 381 | |
| 46 | 2,700 | 382 | 385 | 381 | |
| 47 | 2,760 | 388 | 385 | 380 | |
| 48 | 2,820 | 378 | 376 | 381 | |
| 49 | 2,880 | 379 | 385 | 380 | |
| 50 | 2,940 | 386 | 387 | 381 | |

| SN | Chainage (m) | R.L. 46 (m) | R.L. 89 (m) | Protection R.L. (m) | Direction |
|---|---|---|---|---|---|
| 51 | 3,000 | 385 | 381 | 377 | |
| 52 | 3,060 | 382 | 380 | 380 | |
| 53 | 3,120 | 380 | 382 | 378 | |
| 54 | 3,180 | 382 | 382 | 380 | |
| 55 | 3,240 | 382 | 382 | 379 | |
| 56 | 3,300 | 381 | 381 | 381 | |
| 57 | 3,360 | 381 | 382 | 380 | |
| 58 | 3,420 | 382 | 381 | 379 | |
| 59 | 3,480 | 381 | 381 | 381 | |
| 60 | 3,540 | 380 | 380 | | |
| 61 | 3,600 | 380 | 382 | | |
| 62 | 3,660 | 381 | 381 | | |
| 63 | 3,720 | 380 | 380 | | |
| 64 | 3,780 | 382 | 381 | | |
| 65 | 3,840 | 380 | 380 | | |
| 66 | 3,900 | 378 | 378 | | |
| 67 | 3,960 | 380 | 380 | | |
| 68 | 4,020 | 379 | 379 | | |
| 69 | 4,080 | 382 | 382 | | |
| 70 | 4,140 | 384 | 384 | | |
| 71 | 4,200 | 381 | 381 | | |
| 72 | 4,260 | 381 | 384 | | |
| 73 | 4,320 | 385 | 382 | | |
| 74 | 4,380 | 382 | 382 | | |
| 75 | 4,440 | 384 | 384 | | |
| 76 | 4,500 | 384 | 384 | | |
| 77 | 4,560 | 383 | 384 | | |

**Table (A9): Calculation of the necessary height increments**

| SN | Chainage (m) | 46Lidar (m) | Protection LiDAR (m) | Flood 46-protection (m) | Flood 46-protection +0.30 (m) | Direction |
|---|---|---|---|---|---|---|
| 1 | 0 | 383.70 | 382.66 | 1.04 | 1.34 | |
| 2 | 60 | 383.86 | 383.28 | 0.57 | 0.87 | |
| 3 | 120 | 384.15 | 383.87 | 0.28 | 0.58 | |
| 4 | 180 | 384.27 | 384.03 | 0.23 | 0.53 | |
| 5 | 240 | 384.21 | 384.97 | **-0.76** | **0** | |
| 6 | 300 | 384.01 | 384.45 | **-0.44** | **0** | |
| 7 | 360 | 383.80 | 383.74 | 0.06 | 0.36 | |
| 8 | 420 | 383.26 | 382.64 | 0.62 | 0.92 | |
| 9 | 480 | 383.27 | 382.06 | 1.22 | 1.52 | |
| 10 | 540 | 383.07 | 381.91 | 1.16 | 1.46 | |
| 11 | 600 | 382.84 | 381.74 | 1.09 | 1.39 | |
| 12 | 660 | 382.58 | 381.99 | 0.59 | 0.89 | |
| 13 | 720 | 382.01 | 381.76 | 0.25 | 0.55 | |
| 14 | 780 | 382.23 | 381.63 | 0.59 | 0.89 | |
| 15 | 840 | 383.07 | 381.65 | 1.42 | 1.72 | |
| 16 | 900 | 382.66 | 381.73 | 0.93 | 1.23 | |
| 17 | 960 | 383.23 | 381.55 | 1.69 | 1.99 | |
| 18 | 1,020 | 383.25 | 380.72 | 2.53 | 2.83 | |
| 19 | 1,080 | 382.93 | 380.98 | 1.95 | 2.25 | |
| 20 | 1,140 | 382.91 | 381.83 | 1.08 | 1.38 | |
| 21 | 1,200 | 382.13 | 382.78 | **-0.65** | **0** | |
| 22 | 1,260 | 382.00 | 381.80 | 0.21 | 0.51 | |
| 23 | 1,320 | 382.05 | 381.82 | 0.23 | 0.53 | |
| 24 | 1,380 | 382.00 | 381.64 | 0.36 | 0.66 | |
| 25 | 1,440 | 381.70 | 381.70 | 0.01 | 0.31 | |

| SN | Chainage (m) | 46Lidar (m) | Protection LiDAR (m) | Flood 46-protection (m) | Flood 46-protection +0.30 (m) | Direction |
|---|---|---|---|---|---|---|
| 26 | 1,500 | 381.59 | 381.35 | 0.24 | 0.54 | |
| 27 | 1,560 | 380.83 | 381.53 | **-0.70** | 0 | |
| 28 | 1,620 | 381.20 | 380.94 | 0.26 | 0.56 | |
| 29 | 1,680 | 381.88 | 381.54 | 0.34 | 0.64 | |
| 30 | 1,740 | 381.44 | 381.25 | 0.19 | 0.49 | |
| 31 | 1,800 | 382.20 | 380.85 | 1.35 | 1.65 | ↑ |
| 32 | 1,860 | 381.65 | 381.31 | 0.34 | 0.64 | |
| 33 | 1,920 | 381.58 | 381.09 | 0.49 | 0.79 | |
| 34 | 1,980 | 381.61 | 380.74 | 0.87 | 1.17 | |
| 35 | 2,040 | 382.68 | 381.29 | 1.38 | 1.68 | |
| 36 | 2,100 | 382.29 | 380.54 | 1.75 | 2.05 | |
| 37 | 2,160 | 381.43 | 382.01 | **-0.58** | **0** | |
| 38 | 2,220 | 381.92 | 380.04 | 1.88 | 2.18 | |
| 39 | 2,280 | 381.45 | 381.90 | **-0.44934** | **0** | |
| 40 | 2,340 | 382.33 | 383.16 | **-0.82825** | **0** | |
| 41 | 2,400 | 382.18 | 381.92 | 0.26 | 0.56 | |
| 42 | 2,460 | 382.33 | 380.59 | 1.73 | 2.03 | |
| 43 | 2,520 | 382.64 | 380.34 | 2.30 | 2.60 | |
| 44 | 2,580 | 382.08 | 380.43 | 1.65 | 1.95 | |
| 45 | 2,640 | 382.75 | 380.00 | 2.75 | 3.05 | |
| 46 | 2,700 | 381.91 | 380.41 | 1.51 | 1.81 | |
| 47 | 2,760 | 381.54 | 380.24 | 1.30 | 1.60 | |
| 48 | 2,820 | 381.85 | 380.29 | 1.56 | 1.86 | |
| 49 | 2,880 | 382.21 | 380.98 | 1.24 | 1.54 | |
| 50 | 2,940 | 382.00 | 381.17 | 0.83 | 1.13 | |
| 51 | 3,000 | 381.85 | 379.43 | 2.42 | 2.72 | |
| 52 | 3,060 | 382.06 | 380.29 | 1.78 | 2.08 | |
| 53 | 3,120 | 381.73 | 380.67 | 1.06 | 1.36 | |

| SN | Chainage (m) | 46Lidar (m) | Protection LiDAR (m) | Flood 46-protection (m) | Flood 46-protection +0.30 (m) | Direction |
|---|---|---|---|---|---|---|
| 54 | 3,180 | 381.35 | 381.07 | 0.29 | 0.59 | |
| 55 | 3,240 | 382.09 | 380.88 | 1.21 | 1.51 | |
| 56 | 3,300 | 382.52 | 380.10 | 2.42 | 2.72 | |
| 57 | 3,360 | 382.16 | 380.42 | 1.74 | 2.04 | |
| 58 | 3,420 | 382.45 | 381.22 | 1.23 | 1.53 | |
| 59 | 3,480 | 381.90 | 380.93 | 0.98 | 1.28 | |
| 60 | 3,540 | 382.37 | | **51.06** | **71.07** | |
| 61 | 3,600 | 381.66 | | | | |
| 62 | 3,660 | 381.84 | | | | |
| 63 | 3,720 | 382.02 | | | | |
| 64 | 3,780 | 382.38 | | | | |
| 65 | 3,840 | 382.49 | | | | |
| 66 | 3,900 | 382.88 | | | | |
| 67 | 3,960 | 382.48 | | | | |
| 68 | 4,020 | 382.92 | | | | |
| 69 | 4,080 | 382.29 | | | | |
| 70 | 4,140 | 382.32 | | | | |
| 71 | 4,200 | 382.34 | | | | |
| 72 | 4,260 | 382.55 | | | | |
| 73 | 4,320 | 382.51 | | | | |
| 74 | 4,380 | 382.98 | | | | |
| 75 | 4,440 | 383.06 | | | | |
| 76 | 4,500 | 382.61 | | | | |
| 77 | 4,560 | 382.35 | | | | |

Table (A10): Accuracy assessment parameters of the Digital Elevation Models

| SRTM DEM fishnetsub | | | | | | LiDAR DEM fishnetsub | | | | |
|---|---|---|---|---|---|---|---|---|---|---|
| X-coord (m) | Y-coord (m) | Elevation (m) | diff | diff^2 | | X-coord (m) | Y-coord (m) | Elevation (m) | diff | diff^2 |
| 444789.4 | 1714707 | 381.5376 | -1.92362 | 3.700315 | | 444788 | 1714706 | 381.1046 | -2.01345 | 4.053967 |
| 444791.4 | 1714707 | 381.7202 | -1.74101 | 3.031126 | | 444790 | 1714706 | 381.0988 | -2.01928 | 4.077504 |
| 444793.4 | 1714707 | 381.9029 | -1.55838 | 2.428563 | | 444792 | 1714706 | 381.0957 | -2.02242 | 4.090178 |
| 444795.4 | 1714707 | 382.0855 | -1.37574 | 1.892648 | | 444794 | 1714706 | 381.0911 | -2.02695 | 4.108529 |
| 444797.4 | 1714707 | 382.2682 | -1.19307 | 1.423405 | | 444796 | 1714706 | 381.0855 | -2.03254 | 4.131231 |
| 444799.4 | 1714707 | 382.4509 | -1.01037 | 1.020856 | | 444798 | 1714706 | 381.097 | -2.02108 | 4.084779 |
| 444801.4 | 1714707 | 382.6336 | -0.82766 | 0.685025 | | 444800 | 1714706 | 381.157 | -1.96105 | 3.845709 |
| 444803.4 | 1714707 | 382.8163 | -0.64493 | 0.415933 | | 444802 | 1714706 | 381.2209 | -1.89717 | 3.599272 |
| 444805.4 | 1714707 | 382.9991 | -0.46217 | 0.213606 | | 444804 | 1714706 | 381.243 | -1.87511 | 3.516039 |
| 444807.4 | 1714707 | 383.1854 | -0.2758 | 0.076065 | | 444806 | 1714706 | 381.2397 | -1.87841 | 3.528439 |
| 444809.4 | 1714707 | 383.3873 | -0.07394 | 0.005467 | | 444808 | 1714706 | 381.2329 | -1.88523 | 3.55411 |
| 444811.4 | 1714707 | 383.5892 | 0.127924 | 0.016365 | | 444810 | 1714706 | 381.22 | -1.89811 | 3.602833 |
| 444813.4 | 1714707 | 383.791 | 0.329786 | 0.108759 | | 444812 | 1714706 | 381.2029 | -1.91514 | 3.667768 |
| 444815.4 | 1714707 | 383.9929 | 0.531647 | 0.282649 | | 444814 | 1714706 | 381.1843 | -1.93378 | 3.739507 |
| 444817.4 | 1714707 | 384.1947 | 0.733509 | 0.538035 | | 444816 | 1714706 | 381.1648 | -1.95327 | 3.815248 |
| 444819.4 | 1714707 | 384.3966 | 0.93537 | 0.874917 | | 444818 | 1714706 | 381.1439 | -1.97415 | 3.897259 |
| 444821.4 | 1714707 | 384.5985 | 1.137232 | 1.293296 | | 444820 | 1714706 | 381.116 | -2.00212 | 4.008472 |
| 444823.4 | 1714707 | 384.8003 | 1.339093 | 1.79317 | | 444822 | 1714706 | 381.0756 | -2.04248 | 4.17171 |
| 444825.4 | 1714707 | 385.0022 | 1.540954 | 2.374541 | | 444824 | 1714706 | 381.0233 | -2.09478 | 4.388086 |
| 444827.4 | 1714707 | 385.2041 | 1.742816 | 3.037407 | | 444826 | 1714706 | 380.9676 | -2.15045 | 4.624425 |
| 444829.4 | 1714707 | 385.4059 | 1.944677 | 3.781769 | | 444828 | 1714706 | 380.9158 | -2.2023 | 4.850112 |
| 444831.4 | 1714707 | 385.6078 | 2.146539 | 4.607628 | | 444830 | 1714706 | 380.8731 | -2.24499 | 5.039985 |
| 444833.4 | 1714707 | 385.8096 | 2.3484 | 5.514982 | | 444832 | 1714706 | 380.8427 | -2.27542 | 5.177523 |
| 444835.4 | 1714707 | 386.0115 | 2.550261 | 6.503832 | | 444834 | 1714706 | 380.8315 | -2.28656 | 5.228374 |

| SRTM DEM fishnetsub | | | | | | LiDAR DEM fishnetsub | | | | |
|---|---|---|---|---|---|---|---|---|---|---|
| X-coord (m) | Y-coord (m) | Elevation (m) | diff | diff^2 | | X-coord (m) | Y-coord (m) | Elevation (m) | diff | diff^2 |
| 444837.4 | 1714707 | 386.1041 | 2.642886 | 6.984849 | | 444836 | 1714706 | 380.8423 | -2.27579 | 5.179225 |
| 444839.4 | 1714707 | 385.9325 | 2.471279 | 6.107221 | | 444838 | 1714706 | 380.8709 | -2.24716 | 5.049718 |
| 444841.4 | 1714707 | 385.761 | 2.299714 | 5.288685 | | 444840 | 1714706 | 380.9097 | -2.20843 | 4.877168 |
| 444843.4 | 1714707 | 385.5894 | 2.128191 | 4.529197 | | 444842 | 1714706 | 380.9511 | -2.16698 | 4.695805 |
| 444845.4 | 1714707 | 385.4179 | 1.95671 | 3.828712 | | 444844 | 1714706 | 380.9898 | -2.12829 | 4.529626 |
| 444847.4 | 1714707 | 385.2465 | 1.78527 | 3.18719 | | 444846 | 1714706 | 381.0246 | -2.09353 | 4.382878 |
| 444849.4 | 1714707 | 385.0751 | 1.613873 | 2.604585 | | 444848 | 1714706 | 381.0561 | -2.06202 | 4.251939 |
| 444851.4 | 1714707 | 384.9038 | 1.442517 | 2.080856 | | 444850 | 1714706 | 381.0841 | -2.03404 | 4.137312 |
| 444853.4 | 1714707 | 384.7324 | 1.271204 | 1.615959 | | 444852 | 1714706 | 381.1078 | -2.01033 | 4.041442 |
| 444855.4 | 1714707 | 384.5612 | 1.099932 | 1.20985 | | 444854 | 1714706 | 381.127 | -1.99112 | 3.96454 |
| 444857.4 | 1714707 | 384.3899 | 0.928702 | 0.862488 | | 444856 | 1714706 | 381.1416 | -1.97647 | 3.906422 |
| 444859.4 | 1714707 | 384.2188 | 0.757514 | 0.573828 | | 444858 | 1714706 | 381.1525 | -1.96564 | 3.863744 |
| 444861.4 | 1714707 | 384.0476 | 0.586368 | 0.343828 | | 444860 | 1714706 | 381.1608 | -1.95726 | 3.830881 |
| 444863.4 | 1714707 | 383.8765 | 0.415264 | 0.172445 | | 444862 | 1714706 | 381.1645 | -1.95356 | 3.81641 |
| 444865.4 | 1714707 | 383.7054 | 0.244202 | 0.059635 | | 444864 | 1714706 | 381.1619 | -1.95621 | 3.826761 |
| 444867.4 | 1714707 | 383.4503 | -0.0109 | 0.000119 | | 444866 | 1714706 | 381.1578 | -1.96029 | 3.842717 |
| 444869.4 | 1714707 | 383.0671 | -0.39416 | 0.155361 | | 444868 | 1714706 | 381.1515 | -1.96663 | 3.867614 |
| 444871.4 | 1714707 | 382.6838 | -0.77744 | 0.604406 | | 444870 | 1714706 | 381.1443 | -1.97383 | 3.896024 |
| 444873.4 | 1714707 | 382.3005 | -1.16073 | 1.347301 | | 444872 | 1714706 | 381.1371 | -1.98096 | 3.924205 |
| 444875.4 | 1714707 | 381.9172 | -1.54405 | 2.384095 | | 444874 | 1714706 | 381.1319 | -1.98615 | 3.944786 |
| 444877.4 | 1714707 | 381.5338 | -1.92739 | 3.714837 | | 444876 | 1714706 | 381.1274 | -1.99065 | 3.962687 |
| 444879.4 | 1714707 | 381.1505 | -2.31075 | 5.339574 | | 444878 | 1714706 | 381.1245 | -1.99359 | 3.97439 |
| 444881.4 | 1714707 | 380.7671 | -2.69413 | 7.258356 | | 444880 | 1714706 | 381.1213 | -1.99682 | 3.987299 |
| 444883.4 | 1714707 | 380.3837 | -3.07754 | 9.471229 | | 444882 | 1714706 | 381.1078 | -2.01027 | 4.041166 |
| 444885.4 | 1714707 | 380.0003 | -3.46096 | 11.97824 | | 444884 | 1714706 | 381.0922 | -2.02592 | 4.104355 |

| SRTM DEM fishnetsub | | | | | | LiDAR DEM fishnetsub | | | | |
|---|---|---|---|---|---|---|---|---|---|---|
| X-coord (m) | Y-coord (m) | Elevation (m) | diff | diff^2 | | X-coord (m) | Y-coord (m) | Elevation (m) | diff | diff^2 |
| 444887.4 | 1714707 | 379.6168 | -3.8444 | 14.77945 | | 444886 | 1714706 | 381.085 | -2.03305 | 4.133309 |
| 444889.4 | 1714707 | 379.2334 | -4.22787 | 17.87488 | | 444888 | 1714706 | 381.084 | -2.03409 | 4.137529 |
| 444891.4 | 1714707 | 378.8499 | -4.61136 | 21.26461 | | 444890 | 1714706 | 381.0815 | -2.03659 | 4.147685 |
| 444893.4 | 1714707 | 378.4664 | -4.99486 | 24.94867 | | 444892 | 1714706 | 381.0749 | -2.04315 | 4.174453 |
| 444895.4 | 1714707 | 378.0828 | -5.37839 | 28.92711 | | 444894 | 1714706 | 381.07 | -2.04812 | 4.194805 |
| 444897.4 | 1714707 | 377.8764 | -5.58484 | 31.19047 | | 444896 | 1714706 | 381.0718 | -2.04633 | 4.187464 |
| 444899.4 | 1714707 | 377.8471 | -5.61417 | 31.51889 | | 444898 | 1714706 | 381.0771 | -2.041 | 4.165666 |
| 444901.4 | 1714707 | 377.8177 | -5.64354 | 31.8495 | | 444900 | 1714706 | 381.0831 | -2.03501 | 4.141255 |
| 444903.4 | 1714707 | 377.7883 | -5.67295 | 32.18232 | | 444902 | 1714706 | 381.0896 | -2.02852 | 4.114903 |
| 444905.4 | 1714707 | 377.7588 | -5.7024 | 32.51734 | | 444904 | 1714706 | 381.096 | -2.02205 | 4.088697 |
| 444907.4 | 1714707 | 377.7293 | -5.73189 | 32.85457 | | 444906 | 1714706 | 381.1028 | -2.01532 | 4.061498 |
| 444909.4 | 1714707 | 377.6998 | -5.76143 | 33.19403 | | 444908 | 1714706 | 381.1145 | -2.00362 | 4.014493 |
| 444911.4 | 1714707 | 377.6702 | -5.791 | 33.53572 | | 444910 | 1714706 | 381.1337 | -1.98436 | 3.937698 |
| 444913.4 | 1714707 | 377.6406 | -5.82062 | 33.87965 | | 444912 | 1714706 | 381.1553 | -1.96281 | 3.852624 |
| 444915.4 | 1714707 | 377.611 | -5.85028 | 34.22582 | | 444914 | 1714706 | 381.1703 | -1.9478 | 3.793908 |
| 444917.4 | 1714707 | 377.5813 | -5.87999 | 34.57425 | | 444916 | 1714706 | 381.1772 | -1.94088 | 3.767029 |
| 444919.4 | 1714707 | 377.5515 | -5.90973 | 34.92493 | | 444918 | 1714706 | 381.18 | -1.93805 | 3.75602 |
| 444921.4 | 1714707 | 377.5217 | -5.93952 | 35.27788 | | 444920 | 1714706 | 381.1813 | -1.93676 | 3.751053 |
| 444923.4 | 1714707 | 377.4919 | -5.96935 | 35.63311 | | 444922 | 1714706 | 381.1809 | -1.93719 | 3.752708 |
| 444925.4 | 1714707 | 377.462 | -5.99922 | 35.99062 | | 444924 | 1714706 | 381.1793 | -1.93883 | 3.759066 |
| 444927.4 | 1714707 | 377.3551 | -6.10615 | 37.2851 | | 444926 | 1714706 | 381.1797 | -1.9384 | 3.75741 |
| 444929.4 | 1714707 | 377.1975 | -6.26377 | 39.23483 | | 444928 | 1714706 | 381.1852 | -1.93293 | 3.736203 |
| 444931.4 | 1714707 | 377.0397 | -6.42151 | 41.23585 | | 444930 | 1714706 | 381.2001 | -1.91799 | 3.678677 |
| 444933.4 | 1714707 | 376.8819 | -6.57938 | 43.2883 | | 444932 | 1714706 | 381.2263 | -1.89177 | 3.578776 |
| 444935.4 | 1714707 | 376.7239 | -6.73738 | 45.39228 | | 444934 | 1714706 | 381.2602 | -1.85786 | 3.451645 |

| SRTM DEM fishnetsub | | | | | | LiDAR DEM fishnetsub | | | | |
|---|---|---|---|---|---|---|---|---|---|---|
| X-coord (m) | Y-coord (m) | Elevation (m) | diff | diff^2 | | X-coord (m) | Y-coord (m) | Elevation (m) | diff | diff^2 |
| 444937.4 | 1714707 | 376.5657 | -6.8955 | 47.54793 | | 444936 | 1714706 | 381.2959 | -1.82223 | 3.320526 |
| 444939.4 | 1714707 | 376.4075 | -7.05375 | 49.75535 | | 444938 | 1714706 | 381.3285 | -1.78958 | 3.202587 |
| 444941.4 | 1714707 | 376.2491 | -7.21212 | 52.01466 | | 444940 | 1714706 | 381.3591 | -1.75904 | 3.094211 |
| 444943.4 | 1714707 | 376.0906 | -7.37062 | 54.32599 | | 444942 | 1714706 | 381.3888 | -1.72927 | 2.990391 |
| 444945.4 | 1714707 | 375.932 | -7.52924 | 56.68946 | | 444944 | 1714706 | 381.42 | -1.69813 | 2.88365 |
| 444947.4 | 1714707 | 375.7732 | -7.68799 | 59.10518 | | 444946 | 1714706 | 381.4528 | -1.66532 | 2.773282 |
| 444949.4 | 1714707 | 375.6144 | -7.84686 | 61.57327 | | 444948 | 1714706 | 381.4855 | -1.63255 | 2.665217 |
| 444951.4 | 1714707 | 375.4554 | -8.00586 | 64.09386 | | 444950 | 1714706 | 381.5127 | -1.60539 | 2.577272 |
| 444953.4 | 1714707 | 375.2962 | -8.16499 | 66.66706 | | 444952 | 1714706 | 381.5323 | -1.58575 | 2.514604 |
| 444955.4 | 1714707 | 375.137 | -8.32424 | 69.29299 | | 444954 | 1714706 | 381.5558 | -1.56227 | 2.440702 |
| 444957.4 | 1714707 | 375.2411 | -8.22018 | 67.57143 | | 444956 | 1714706 | 381.5823 | -1.53581 | 2.358707 |
| 444959.4 | 1714707 | 375.4541 | -8.00711 | 64.11376 | | 444958 | 1714706 | 381.6072 | -1.51091 | 2.282837 |
| 444961.4 | 1714707 | 375.6673 | -7.79397 | 60.74591 | | 444960 | 1714706 | 381.6387 | -1.47943 | 2.188705 |
| 444963.4 | 1714707 | 375.8805 | -7.58076 | 57.46797 | | 444962 | 1714706 | 381.6791 | -1.43897 | 2.07063 |
| 444965.4 | 1714707 | 376.0937 | -7.3675 | 54.28001 | | 444964 | 1714706 | 381.7274 | -1.3907 | 1.934039 |
| 444967.4 | 1714707 | 376.3071 | -7.15417 | 51.18212 | | 444966 | 1714706 | 381.7872 | -1.33089 | 1.771269 |
| 444969.4 | 1714707 | 376.5205 | -6.94078 | 48.17438 | | 444968 | 1714706 | 381.8628 | -1.25529 | 1.575755 |
| 444971.4 | 1714707 | 376.7339 | -6.72732 | 45.25686 | | 444970 | 1714706 | 381.9556 | -1.16254 | 1.3515 |
| 444973.4 | 1714707 | 376.9474 | -6.5138 | 42.42965 | | 444972 | 1714706 | 382.0686 | -1.04949 | 1.101425 |
| 444975.4 | 1714707 | 377.161 | -6.30022 | 39.69283 | | 444974 | 1714706 | 382.2064 | -0.91167 | 0.831143 |
| 444977.4 | 1714707 | 377.3747 | -6.08658 | 37.04648 | | 444976 | 1714706 | 382.3595 | -0.75862 | 0.5755 |
| 444979.4 | 1714707 | 377.5884 | -5.87288 | 34.49068 | | 444978 | 1714706 | 382.508 | -0.61005 | 0.372161 |
| 444981.4 | 1714707 | 377.8021 | -5.65911 | 32.02551 | | 444980 | 1714706 | 382.6235 | -0.49455 | 0.244578 |
| 444983.4 | 1714707 | 378.016 | -5.44528 | 29.65104 | | 444982 | 1714706 | 382.6892 | -0.42892 | 0.183973 |
| 444985.4 | 1714707 | 378.2299 | -5.23138 | 27.36737 | | 444984 | 1714706 | 382.7111 | -0.40703 | 0.165675 |

| SRTM DEM fishnetsub | | | | | | LiDAR DEM fishnetsub | | | | |
|---|---|---|---|---|---|---|---|---|---|---|
| X-coord (m) | Y-coord (m) | Elevation (m) | diff | diff^2 | | X-coord (m) | Y-coord (m) | Elevation (m) | diff | diff^2 |
| 444987.4 | 1714707 | 378.4188 | -5.04246 | 25.42637 | | 444986 | 1714706 | 382.709 | -0.40908 | 0.167344 |
| 444989.4 | 1714707 | 378.6019 | -4.85934 | 23.61315 | | 444988 | 1714706 | 382.7004 | -0.41769 | 0.174465 |
| 444991.4 | 1714707 | 378.785 | -4.67619 | 21.8668 | | 444990 | 1714706 | 382.6962 | -0.42185 | 0.177956 |
| 444993.4 | 1714707 | 378.9682 | -4.49303 | 20.18734 | | 444992 | 1714706 | 382.6999 | -0.41818 | 0.174873 |
| 444995.4 | 1714707 | 379.1514 | -4.30985 | 18.5748 | | 444994 | 1714706 | 382.7099 | -0.40821 | 0.166633 |
| 444997.4 | 1714707 | 379.3346 | -4.12664 | 17.02919 | | 444996 | 1714706 | 382.7233 | -0.39479 | 0.155856 |
| 444999.4 | 1714707 | 379.5178 | -3.94342 | 15.55055 | | 444998 | 1714706 | 382.7412 | -0.37693 | 0.142079 |
| 445001.4 | 1714707 | 379.7011 | -3.76017 | 14.1389 | | 445000 | 1714706 | 382.7645 | -0.35362 | 0.125046 |
| 445003.4 | 1714707 | 379.8843 | -3.57691 | 12.79425 | | 445002 | 1714706 | 382.7912 | -0.32686 | 0.106839 |
| 445005.4 | 1714707 | 380.0676 | -3.39362 | 11.51664 | | 445004 | 1714706 | 382.8205 | -0.29761 | 0.088572 |
| 445007.4 | 1714707 | 380.2509 | -3.21031 | 10.30608 | | 445006 | 1714706 | 382.8519 | -0.26621 | 0.070867 |
| 445009.4 | 1714707 | 380.4343 | -3.02698 | 9.162599 | | 445008 | 1714706 | 382.8858 | -0.23233 | 0.053979 |
| 445011.4 | 1714707 | 380.6176 | -2.84363 | 8.086218 | | 445010 | 1714706 | 382.9227 | -0.19535 | 0.03816 |
| 445013.4 | 1714707 | 380.801 | -2.66026 | 7.076961 | | 445012 | 1714706 | 382.9623 | -0.15578 | 0.024268 |
| 445015.4 | 1714707 | 380.9844 | -2.47686 | 6.134851 | | 445014 | 1714706 | 383.0018 | -0.11631 | 0.013529 |
| 445017.4 | 1714707 | 381.0614 | -2.39983 | 5.759168 | | 445016 | 1714706 | 383.0388 | -0.0793 | 0.006289 |
| 445019.4 | 1714707 | 381.1285 | -2.3327 | 5.441469 | | 445018 | 1714706 | 383.0707 | -0.04735 | 0.002242 |
| 445021.4 | 1714707 | 381.1957 | -2.26556 | 5.132784 | | 445020 | 1714706 | 383.0969 | -0.0212 | 0.000449 |
| 445023.4 | 1714707 | 381.2628 | -2.19843 | 4.833112 | | 445022 | 1714706 | 383.113 | -0.00511 | 2.61E-05 |
| 445025.4 | 1714707 | 381.3299 | -2.1313 | 4.542453 | | 445024 | 1714706 | 383.1181 | -3.4E-05 | 1.17E-09 |
| 445027.4 | 1714707 | 381.3971 | -2.06417 | 4.260807 | | 445026 | 1714706 | 383.1117 | -0.00637 | 4.05E-05 |
| 445029.4 | 1714707 | 381.4642 | -1.99704 | 3.988174 | | 445028 | 1714706 | 383.0901 | -0.02803 | 0.000786 |
| 445031.4 | 1714707 | 381.5313 | -1.92991 | 3.724554 | | 445030 | 1714706 | 383.0472 | -0.07093 | 0.005031 |
| 445033.4 | 1714707 | 381.5985 | -1.86278 | 3.469948 | | 445032 | 1714706 | 382.9827 | -0.13536 | 0.018321 |
| 445035.4 | 1714707 | 381.6656 | -1.79565 | 3.224354 | | 445034 | 1714706 | 382.9096 | -0.20845 | 0.04345 |

| SRTM DEM fishnetsub | | | | | | LiDAR DEM fishnetsub | | | | |
|---|---|---|---|---|---|---|---|---|---|---|
| X-coord (m) | Y-coord (m) | Elevation (m) | diff | diff^2 | | X-coord (m) | Y-coord (m) | Elevation (m) | diff | diff^2 |
| 445037.4 | 1714707 | 381.7327 | -1.72852 | 2.987774 | | 445036 | 1714706 | 382.8488 | -0.26927 | 0.072505 |
| 445039.4 | 1714707 | 381.7999 | -1.66139 | 2.760207 | | 445038 | 1714706 | 382.817 | -0.30105 | 0.090632 |
| 445041.4 | 1714707 | 381.867 | -1.59426 | 2.541652 | | 445040 | 1714706 | 382.8165 | -0.30157 | 0.090945 |
| 445043.4 | 1714707 | 381.9341 | -1.52713 | 2.332111 | | 445042 | 1714706 | 382.8386 | -0.27947 | 0.078103 |
| 445045.4 | 1714707 | 381.9997 | -1.46157 | 2.136184 | | 445044 | 1714706 | 382.8725 | -0.24564 | 0.060339 |
| 445047.4 | 1714707 | 381.9818 | -1.47939 | 2.188595 | | 445046 | 1714706 | 382.912 | -0.20607 | 0.042466 |
| 445049.4 | 1714707 | 381.964 | -1.49719 | 2.241579 | | 445048 | 1714706 | 382.954 | -0.16407 | 0.026918 |
| 445051.4 | 1714707 | 381.9463 | -1.51497 | 2.295133 | | 445050 | 1714706 | 382.9949 | -0.12323 | 0.015187 |
| 445053.4 | 1714707 | 381.9285 | -1.53273 | 2.349256 | | 445052 | 1714706 | 383.0316 | -0.08644 | 0.007473 |
| 445055.4 | 1714707 | 381.9108 | -1.55047 | 2.403944 | | 445054 | 1714706 | 383.0628 | -0.05527 | 0.003055 |
| 445057.4 | 1714707 | 381.8931 | -1.56818 | 2.459196 | | 445056 | 1714706 | 383.0887 | -0.02942 | 0.000866 |
| 445059.4 | 1714707 | 381.8754 | -1.58588 | 2.51501 | | 445058 | 1714706 | 383.109 | -0.0091 | 8.28E-05 |
| 445061.4 | 1714707 | 381.8577 | -1.60355 | 2.571383 | | 445060 | 1714706 | 383.1254 | 0.007343 | 5.39E-05 |
| 445063.4 | 1714707 | 381.84 | -1.62121 | 2.628313 | | 445062 | 1714706 | 383.1376 | 0.019467 | 0.000379 |
| 445065.4 | 1714707 | 381.8224 | -1.63884 | 2.685798 | | 445064 | 1714706 | 383.1467 | 0.028607 | 0.000818 |
| 445067.4 | 1714707 | 381.8048 | -1.65645 | 2.743836 | | 445066 | 1714706 | 383.1524 | 0.034313 | 0.001177 |
| 445069.4 | 1714707 | 381.7872 | -1.67404 | 2.802424 | | 445068 | 1714706 | 383.1523 | 0.034237 | 0.001172 |
| 445071.4 | 1714707 | 381.7696 | -1.69161 | 2.86156 | | 445070 | 1714706 | 383.1448 | 0.026715 | 0.000714 |
| 445073.4 | 1714707 | 381.7521 | -1.70916 | 2.921242 | | 445072 | 1714706 | 383.132 | 0.013882 | 0.000193 |
| 445075.4 | 1714707 | 381.7406 | -1.72065 | 2.960625 | | 445074 | 1714706 | 383.1158 | -0.0023 | 5.29E-06 |
| 445077.4 | 1714707 | 381.7726 | -1.68869 | 2.851664 | | 445076 | 1714706 | 383.0971 | -0.02098 | 0.00044 |
| 445079.4 | 1714707 | 381.8046 | -1.65669 | 2.744607 | | 445078 | 1714706 | 383.0769 | -0.04115 | 0.001693 |
| 445081.4 | 1714707 | 381.8366 | -1.62464 | 2.639463 | | 445080 | 1714706 | 383.0565 | -0.06159 | 0.003793 |
| 445083.4 | 1714707 | 381.8687 | -1.59256 | 2.536239 | | 445082 | 1714706 | 383.0368 | -0.08127 | 0.006605 |
| 445085.4 | 1714707 | 381.9008 | -1.56043 | 2.434944 | | 445084 | 1714706 | 383.0187 | -0.09941 | 0.009882 |

| SRTM DEM fishnetsub | | | | | | LiDAR DEM fishnetsub | | | | |
|---|---|---|---|---|---|---|---|---|---|---|
| X-coord (m) | Y-coord (m) | Elevation (m) | diff | diff^2 | | X-coord (m) | Y-coord (m) | Elevation (m) | diff | diff^2 |
| 445087.4 | 1714707 | 381.933 | -1.52826 | 2.335586 | | 445086 | 1714706 | 383.0033 | -0.11482 | 0.013183 |
| 445089.4 | 1714707 | 381.9652 | -1.49605 | 2.238172 | | 445088 | 1714706 | 382.9923 | -0.1258 | 0.015827 |
| 445091.4 | 1714707 | 381.9974 | -1.4638 | 2.142711 | | 445090 | 1714706 | 382.9877 | -0.13042 | 0.01701 |
| 445093.4 | 1714707 | 382.0297 | -1.43151 | 2.049211 | | 445092 | 1714706 | 382.9903 | -0.12783 | 0.016342 |
| 445095.4 | 1714707 | 382.0621 | -1.39917 | 1.95768 | | 445094 | 1714706 | 382.9979 | -0.12014 | 0.014435 |
| 445097.4 | 1714707 | 382.0944 | -1.36679 | 1.868126 | | 445096 | 1714706 | 383.0067 | -0.11143 | 0.012417 |
| 445099.4 | 1714707 | 382.1269 | -1.33438 | 1.780557 | | 445098 | 1714706 | 383.0136 | -0.10447 | 0.010915 |
| 445101.4 | 1714707 | 382.1593 | -1.30191 | 1.694981 | | 445100 | 1714706 | 383.0172 | -0.10086 | 0.010172 |
| 445103.4 | 1714707 | 382.1918 | -1.26941 | 1.611407 | | 445102 | 1714706 | 383.0158 | -0.1023 | 0.010465 |
| 445105.4 | 1714707 | 382.2171 | -1.24412 | 1.547836 | | 445104 | 1714706 | 383.0089 | -0.10915 | 0.011914 |
| 445107.4 | 1714707 | 382.2176 | -1.24365 | 1.546675 | | 445106 | 1714706 | 382.9966 | -0.12146 | 0.014752 |
| 445109.4 | 1714707 | 382.2181 | -1.24319 | 1.545515 | | 445108 | 1714706 | 382.9791 | -0.13901 | 0.019324 |
| 445111.4 | 1714707 | 382.2185 | -1.24272 | 1.544356 | | 445110 | 1714706 | 382.9565 | -0.16163 | 0.026125 |
| 445113.4 | 1714707 | 382.219 | -1.24225 | 1.543197 | | 445112 | 1714706 | 382.9289 | -0.18917 | 0.035787 |
| 445115.4 | 1714707 | 382.2195 | -1.24179 | 1.542038 | | 445114 | 1714706 | 382.8972 | -0.22093 | 0.048809 |
| 445117.4 | 1714707 | 382.2199 | -1.24132 | 1.54088 | | 445116 | 1714706 | 382.8643 | -0.25376 | 0.064393 |
| 445119.4 | 1714707 | 382.2204 | -1.24086 | 1.539723 | | 445118 | 1714706 | 382.8368 | -0.28132 | 0.079142 |
| 445121.4 | 1714707 | 382.2208 | -1.24039 | 1.538566 | | 445120 | 1714706 | 382.8223 | -0.29581 | 0.087504 |
| 445123.4 | 1714707 | 382.2213 | -1.23992 | 1.537409 | | 445122 | 1714706 | 382.8275 | -0.29059 | 0.084444 |
| 445125.4 | 1714707 | 382.2218 | -1.23946 | 1.536253 | | 445124 | 1714706 | 382.85 | -0.26813 | 0.071894 |
| 445127.4 | 1714707 | 382.2222 | -1.23899 | 1.535097 | | 445126 | 1714706 | 382.8795 | -0.23862 | 0.05694 |
| 445129.4 | 1714707 | 382.2227 | -1.23852 | 1.533942 | | 445128 | 1714706 | 382.9087 | -0.20935 | 0.043829 |
| 445131.4 | 1714707 | 382.2232 | -1.23806 | 1.532787 | | 445130 | 1714706 | 382.9396 | -0.17852 | 0.031871 |
| 445133.4 | 1714707 | 382.2236 | -1.23759 | 1.531633 | | 445132 | 1714706 | 382.9703 | -0.14781 | 0.021847 |
| 445135.4 | 1714707 | 382.2577 | -1.20354 | 1.448515 | | 445134 | 1714706 | 383.0018 | -0.11633 | 0.013532 |

| SRTM DEM fishnetsub | | | | | | LiDAR DEM fishnetsub | | | | |
|---|---|---|---|---|---|---|---|---|---|---|
| X-coord (m) | Y-coord (m) | Elevation (m) | diff | diff^2 | | X-coord (m) | Y-coord (m) | Elevation (m) | diff | diff^2 |
| 445137.4 | 1714707 | 382.36 | -1.10125 | 1.21275 | | 445136 | 1714706 | 383.0379 | -0.08023 | 0.006436 |
| 445139.4 | 1714707 | 382.4622 | -0.999 | 0.997997 | | 445138 | 1714706 | 383.0752 | -0.0429 | 0.001841 |
| 445141.4 | 1714707 | 382.5645 | -0.89679 | 0.804229 | | 445140 | 1714706 | 383.1056 | -0.01253 | 0.000157 |
| 445143.4 | 1714707 | 382.6666 | -0.79462 | 0.631421 | | 445142 | 1714706 | 383.1385 | 0.020374 | 0.000415 |
| 445145.4 | 1714707 | 382.7687 | -0.69249 | 0.479547 | | 445144 | 1714706 | 383.1798 | 0.061741 | 0.003812 |
| 445147.4 | 1714707 | 382.8708 | -0.59041 | 0.348583 | | 445146 | 1714706 | 383.2235 | 0.105381 | 0.011105 |
| 445149.4 | 1714707 | 382.9729 | -0.48837 | 0.238501 | | 445148 | 1714706 | 383.2649 | 0.146794 | 0.021548 |
| 445151.4 | 1714707 | 383.0749 | -0.38636 | 0.149278 | | 445150 | 1714706 | 383.3054 | 0.187275 | 0.035072 |
| 445153.4 | 1714707 | 383.1768 | -0.28441 | 0.080886 | | 445152 | 1714706 | 383.3474 | 0.229267 | 0.052563 |
| 445155.4 | 1714707 | 383.2788 | -0.18249 | 0.033302 | | 445154 | 1714706 | 383.3923 | 0.274204 | 0.075188 |
| 445157.4 | 1714707 | 383.3806 | -0.08061 | 0.006498 | | 445156 | 1714706 | 383.4383 | 0.32024 | 0.102554 |
| 445159.4 | 1714707 | 383.4825 | 0.021223 | 0.00045 | | 445158 | 1714706 | 383.4806 | 0.362477 | 0.131389 |
| 445161.4 | 1714707 | 383.5843 | 0.123015 | 0.015133 | | 445160 | 1714706 | 383.5134 | 0.395298 | 0.156261 |
| 445163.4 | 1714707 | 383.686 | 0.224766 | 0.05052 | | 445162 | 1714706 | 383.5337 | 0.415577 | 0.172704 |
| 445165.4 | 1714707 | 383.7437 | 0.282463 | 0.079785 | | 445164 | 1714706 | 383.5437 | 0.425579 | 0.181118 |
| 445167.4 | 1714707 | 383.7439 | 0.282618 | 0.079873 | | 445166 | 1714706 | 383.5482 | 0.430073 | 0.184963 |
| 445169.4 | 1714707 | 383.744 | 0.282774 | 0.079961 | | 445168 | 1714706 | 383.5496 | 0.431484 | 0.186179 |
| 445171.4 | 1714707 | 383.7442 | 0.282929 | 0.080049 | | 445170 | 1714706 | 383.5483 | 0.430233 | 0.185101 |
| 445173.4 | 1714707 | 383.7443 | 0.283084 | 0.080137 | | 445172 | 1714706 | 383.5453 | 0.427166 | 0.182471 |
| 445175.4 | 1714707 | 383.7445 | 0.283239 | 0.080225 | | 445174 | 1714706 | 383.5422 | 0.424137 | 0.179892 |
| 445177.4 | 1714707 | 383.7446 | 0.283395 | 0.080313 | | 445176 | 1714706 | 383.541 | 0.422909 | 0.178852 |
| 445179.4 | 1714707 | 383.7448 | 0.28355 | 0.080401 | | 445178 | 1714706 | 383.5431 | 0.424992 | 0.180618 |
| 445181.4 | 1714707 | 383.7449 | 0.283705 | 0.080489 | | 445180 | 1714706 | 383.5479 | 0.429798 | 0.184727 |
| 445183.4 | 1714707 | 383.7451 | 0.283861 | 0.080577 | | 445182 | 1714706 | 383.5552 | 0.437092 | 0.191049 |
| 445185.4 | 1714707 | 383.7453 | 0.284016 | 0.080665 | | 445184 | 1714706 | 383.566 | 0.447895 | 0.20061 |

| SRTM DEM fishnetsub | | | | | | LiDAR DEM fishnetsub | | | | |
|---|---|---|---|---|---|---|---|---|---|---|
| X-coord (m) | Y-coord (m) | Elevation (m) | diff | diff^2 | | X-coord (m) | Y-coord (m) | Elevation (m) | diff | diff^2 |
| 445187.4 | 1714707 | 383.7454 | 0.284171 | 0.080753 | | 445186 | 1714706 | 383.5815 | 0.46336 | 0.214703 |
| 445189.4 | 1714707 | 383.7456 | 0.284326 | 0.080841 | | 445188 | 1714706 | 383.6007 | 0.482594 | 0.232897 |
| 445191.4 | 1714707 | 383.7457 | 0.284482 | 0.08093 | | 445190 | 1714706 | 383.6234 | 0.505329 | 0.255358 |
| 445193.4 | 1714707 | 383.7459 | 0.284637 | 0.081018 | | 445192 | 1714706 | 383.6474 | 0.529331 | 0.280192 |
| 445195.4 | 1714707 | 383.7191 | 0.25789 | 0.066507 | | 445194 | 1714706 | 383.6703 | 0.55222 | 0.304946 |
| 445197.4 | 1714707 | 383.6692 | 0.207947 | 0.043242 | | 445196 | 1714706 | 383.6905 | 0.57243 | 0.327676 |
| 445199.4 | 1714707 | 383.6192 | 0.157984 | 0.024959 | | 445198 | 1714706 | 383.704 | 0.585949 | 0.343336 |
| 445201.4 | 1714707 | 383.5692 | 0.108 | 0.011664 | | 445200 | 1714706 | 383.7029 | 0.584789 | 0.341979 |
| 445203.4 | 1714707 | 383.5192 | 0.057995 | 0.003363 | | 445202 | 1714706 | 383.6813 | 0.563198 | 0.317192 |
| 445205.4 | 1714707 | 383.4692 | 0.007969 | 6.35E-05 | | 445204 | 1714706 | 383.6421 | 0.523983 | 0.274558 |
| 445207.4 | 1714707 | 383.4192 | -0.04208 | 0.001771 | | 445206 | 1714706 | 383.5936 | 0.475521 | 0.22612 |
| 445209.4 | 1714707 | 383.3691 | -0.09215 | 0.008491 | | 445208 | 1714706 | 383.5394 | 0.421261 | 0.177461 |
| 445211.4 | 1714707 | 383.319 | -0.14223 | 0.02023 | | 445210 | 1714706 | 383.4796 | 0.361546 | 0.130715 |
| 445213.4 | 1714707 | 383.2689 | -0.19234 | 0.036996 | | 445212 | 1714706 | 383.4156 | 0.297466 | 0.088486 |
| 445215.4 | 1714707 | 383.2188 | -0.24247 | 0.058793 | | 445214 | 1714706 | 383.3508 | 0.232701 | 0.05415 |
| 445217.4 | 1714707 | 383.1686 | -0.29262 | 0.085629 | | 445216 | 1714706 | 383.2913 | 0.173207 | 0.03 |
| 445219.4 | 1714707 | 383.1184 | -0.3428 | 0.117509 | | 445218 | 1714706 | 383.2425 | 0.124394 | 0.015474 |
| 445221.4 | 1714707 | 383.0683 | -0.39299 | 0.15444 | | 445220 | 1714706 | 383.2114 | 0.093311 | 0.008707 |
| 445223.4 | 1714707 | 383.018 | -0.4432 | 0.196428 | | 445222 | 1714706 | 383.2009 | 0.082852 | 0.006864 |
| 445225.4 | 1714707 | 382.957 | -0.50426 | 0.254281 | | 445224 | 1714706 | 383.2066 | 0.088513 | 0.007834 |
| 445227.4 | 1714707 | 382.8898 | -0.57139 | 0.32649 | | 445226 | 1714706 | 383.2204 | 0.102299 | 0.010465 |
| 445229.4 | 1714707 | 382.8227 | -0.63852 | 0.407713 | | 445228 | 1714706 | 383.2363 | 0.118183 | 0.013967 |
| 445231.4 | 1714707 | 382.7556 | -0.70566 | 0.497949 | | 445230 | 1714706 | 383.2501 | 0.132 | 0.017424 |
| 445233.4 | 1714707 | 382.6885 | -0.77279 | 0.597198 | | 445232 | 1714706 | 383.2603 | 0.142208 | 0.020223 |
| 445235.4 | 1714707 | 382.6213 | -0.83992 | 0.70546 | | 445234 | 1714706 | 383.2669 | 0.148831 | 0.022151 |

| SRTM DEM fishnetsub | | | | | | LiDAR DEM fishnetsub | | | | |
|---|---|---|---|---|---|---|---|---|---|---|
| X-coord (m) | Y-coord (m) | Elevation (m) | diff | diff^2 | | X-coord (m) | Y-coord (m) | Elevation (m) | diff | diff^2 |
| 445237.4 | 1714707 | 382.5542 | -0.90705 | 0.822736 | | 445236 | 1714706 | 383.2697 | 0.151585 | 0.022978 |
| 445239.4 | 1714707 | 382.4871 | -0.97418 | 0.949024 | | 445238 | 1714706 | 383.2688 | 0.150753 | 0.022727 |
| 445241.4 | 1714707 | 382.4199 | -1.04131 | 1.084326 | | 445240 | 1714706 | 383.2666 | 0.148556 | 0.022069 |
| 445243.4 | 1714707 | 382.3528 | -1.10844 | 1.22864 | | 445242 | 1714706 | 383.2637 | 0.145619 | 0.021205 |
| 445245.4 | 1714707 | 382.2857 | -1.17557 | 1.381968 | | 445244 | 1714706 | 383.2602 | 0.142147 | 0.020206 |
| 445247.4 | 1714707 | 382.2185 | -1.2427 | 1.544309 | | 445246 | 1714706 | 383.2539 | 0.1358 | 0.018442 |
| 445249.4 | 1714707 | 382.1514 | -1.30983 | 1.715663 | | 445248 | 1714706 | 383.2465 | 0.128369 | 0.016478 |
| 445251.4 | 1714707 | 382.0843 | -1.37696 | 1.89603 | | 445250 | 1714706 | 383.2385 | 0.120449 | 0.014508 |
| 445253.4 | 1714707 | 382.0171 | -1.4441 | 2.085411 | | 445252 | 1714706 | 383.2296 | 0.11153 | 0.012439 |
| 445255.4 | 1714707 | 381.9751 | -1.48616 | 2.208683 | | 445254 | 1714706 | 383.2186 | 0.100475 | 0.010095 |
| 445257.4 | 1714707 | 381.9416 | -1.5196 | 2.309187 | | 445256 | 1714706 | 383.2049 | 0.086842 | 0.007541 |
| 445259.4 | 1714707 | 381.9082 | -1.553 | 2.411798 | | 445258 | 1714706 | 383.1932 | 0.075077 | 0.005637 |

| SN | Data type / Parameter | SRTM DEM | LiDAR DEM |
|---|---|---|---|
| 1- | Count | 542,050 | 542,050 |
| 2- | Sum | 207,855,164.274 | 207,669,161.459 |
| 3- | Max. (m) | 397.826 | 385.420 |
| 4- | Min. (m) | 372.087 | 380.548 |
| 5- | Variation | 25.739 | 4.872 |
| 6- | Mean | 383.461 | 383.118 |
| 7- | Sum of diff^2 | 2,581,670.290 | 303,701.753 |
| 8- | (Sum of diff^2)/N | 4.7627898 | 0.5602836 |
| 9- | Standard deviation | 2.182 | 0.749 |

**Table No. (A11): Coordinates measured at the field using Garmin GPSMAP60CSx navigator:**

| SN | Latitude | Longitude | y_proj | x_proj | Measured altitude | corrected Alt |
|---|---|---|---|---|---|---|
| 01 | 15.528860 | 32.482175 | 1716888.81 | 444468.48 | 387.59 | 386.94 |
| 02 | 15.528864 | 32.482179 | 1716889.25 | 444468.91 | 386.90 | 386.25 |
| 03 | 15.528984 | 32.482212 | 1716902.52 | 444472.48 | 387.29 | 386.64 |
| 04 | 15.529038 | 32.482222 | 1716908.49 | 444473.57 | 387.29 | 386.64 |
| 05 | 15.529091 | 32.482229 | 1716914.35 | 444474.33 | 387.28 | 386.63 |
| 06 | 15.529138 | 32.482236 | 1716919.55 | 444475.09 | 387.28 | 386.63 |
| 07 | 15.529183 | 32.482244 | 1716924.52 | 444475.96 | 387.28 | 386.63 |
| 08 | 15.529225 | 32.482253 | 1716929.16 | 444476.94 | 387.28 | 386.63 |
| 09 | 15.529264 | 32.482260 | 1716933.48 | 444477.70 | 387.28 | 386.63 |
| 10 | 15.529307 | 32.482272 | 1716938.23 | 444479.00 | 387.28 | 386.63 |
| 11 | 15.529371 | 32.482289 | 1716945.30 | 444480.84 | 387.28 | 386.63 |
| 12 | 15.529429 | 32.482302 | 1716951.72 | 444482.25 | 387.28 | 386.63 |
| 13 | 15.529496 | 32.482320 | 1716959.12 | 444484.20 | 387.28 | 386.63 |
| 14 | 15.529556 | 32.482333 | 1716965.76 | 444485.61 | 387.28 | 386.63 |
| 15 | 15.529707 | 32.482361 | 1716982.45 | 444488.65 | 387.27 | 386.62 |
| 16 | 15.529791 | 32.482380 | 1716991.74 | 444490.71 | 387.27 | 386.62 |
| 17 | 15.529807 | 32.482388 | 1716993.51 | 444491.57 | 387.27 | 386.62 |
| 18 | 15.529861 | 32.482415 | 1716999.47 | 444494.48 | 388.30 | 387.65 |
| 19 | 15.529891 | 32.482439 | 1717002.78 | 444497.07 | 388.30 | 387.65 |
| 20 | 15.529919 | 32.482458 | 1717005.88 | 444499.11 | 388.30 | 387.65 |
| 21 | 15.529956 | 32.482475 | 1717009.96 | 444500.94 | 388.30 | 387.65 |
| 22 | 15.530010 | 32.482499 | 1717015.93 | 444503.53 | 388.46 | 387.81 |
| 23 | 15.530068 | 32.482516 | 1717022.34 | 444505.37 | 388.46 | 387.81 |
| 24 | 15.530096 | 32.482521 | 1717025.44 | 444505.91 | 388.46 | 387.81 |

| SN | Latitude | Longitude | y_proj | x_proj | Measured altitude | corrected Alt |
|---|---|---|---|---|---|---|
| 25 | 15.530164 | 32.482531 | 1717032.96 | 444507.00 | 388.47 | 387.82 |
| 26 | 15.530227 | 32.482545 | 1717039.92 | 444508.52 | 388.37 | 387.72 |
| 27 | 15.530259 | 32.482544 | 1717043.46 | 444508.42 | 388.37 | 387.72 |
| 28 | 15.530293 | 32.482539 | 1717047.23 | 444507.90 | 388.37 | 387.72 |
| 29 | 15.530337 | 32.482537 | 1717052.09 | 444507.69 | 388.37 | 387.72 |
| 30 | 15.530376 | 32.482534 | 1717056.41 | 444507.38 | 388.37 | 387.72 |
| 31 | 15.530466 | 32.482538 | 1717066.36 | 444507.84 | 388.37 | 387.72 |
| 32 | 15.530532 | 32.482542 | 1717073.66 | 444508.28 | 388.37 | 387.72 |
| 33 | 15.530575 | 32.482550 | 1717078.42 | 444509.15 | 388.37 | 387.72 |
| 34 | 15.530693 | 32.482618 | 1717091.45 | 444516.48 | 388.38 | 387.73 |
| 35 | 15.530760 | 32.482676 | 1717098.85 | 444522.71 | 388.37 | 387.72 |
| 36 | 15.530846 | 32.482768 | 1717108.34 | 444532.60 | 388.37 | 387.72 |
| 37 | 15.530878 | 32.482798 | 1717111.87 | 444535.83 | 388.37 | 387.72 |
| 38 | 15.530952 | 32.482857 | 1717120.04 | 444542.18 | 388.37 | 387.72 |
| 39 | 15.531005 | 32.482900 | 1717125.89 | 444546.80 | 388.37 | 387.72 |
| 40 | 15.531146 | 32.482998 | 1717141.46 | 444557.35 | 388.37 | 387.72 |
| 41 | 15.531269 | 32.483100 | 1717155.04 | 444568.32 | 388.37 | 387.72 |
| 42 | 15.531352 | 32.483179 | 1717164.20 | 444576.81 | 388.37 | 387.72 |
| 43 | 15.531411 | 32.483233 | 1717170.71 | 444582.62 | 388.37 | 387.72 |
| 44 | 15.531560 | 32.483326 | 1717187.17 | 444592.63 | 388.37 | 387.72 |
| 45 | 15.531612 | 32.483375 | 1717192.91 | 444597.90 | 388.37 | 387.72 |
| 46 | 15.531646 | 32.483416 | 1717196.66 | 444602.31 | 388.37 | 387.72 |
| 47 | 15.531672 | 32.483461 | 1717199.52 | 444607.14 | 388.37 | 387.72 |
| 48 | 15.531714 | 32.483548 | 1717204.15 | 444616.48 | 388.36 | 387.71 |
| 49 | 15.531796 | 32.483641 | 1717213.19 | 444626.48 | 387.73 | 387.08 |
| 50 | 15.531733 | 32.483569 | 1717206.24 | 444618.74 | 387.59 | 386.94 |
| 51 | 15.531738 | 32.483572 | 1717206.79 | 444619.06 | 387.59 | 386.94 |

| SN | Latitude | Longitude | y_proj | x_proj | Measured altitude | corrected Alt |
|---|---|---|---|---|---|---|
| 52 | 15.531743 | 32.483572 | 1717207.35 | 444619.06 | 387.59 | 386.94 |
| 53 | 15.531745 | 32.483572 | 1717207.57 | 444619.07 | 387.59 | 386.94 |
| 54 | 15.531746 | 32.483574 | 1717207.68 | 444619.28 | 387.59 | 386.94 |
| 55 | 15.531747 | 32.483575 | 1717207.79 | 444619.39 | 387.59 | 386.94 |
| 56 | 15.531749 | 32.483579 | 1717208.01 | 444619.82 | 387.58 | 386.93 |
| 57 | 15.531749 | 32.483579 | 1717208.01 | 444619.82 | 387.58 | 386.93 |
| 58 | 15.531749 | 32.483578 | 1717208.01 | 444619.71 | 387.58 | 386.93 |
| 59 | 15.531742 | 32.483584 | 1717207.23 | 444620.35 | 387.58 | 386.93 |
| 60 | 15.532735 | 32.484098 | 1717316.94 | 444675.74 | 386.37 | 385.72 |
| 61 | 15.532819 | 32.484136 | 1717326.22 | 444679.84 | 386.37 | 385.72 |
| 62 | 15.532873 | 32.484149 | 1717332.19 | 444681.24 | 386.37 | 385.72 |
| 63 | 15.532963 | 32.484152 | 1717342.15 | 444681.59 | 386.38 | 385.73 |
| 64 | 15.533000 | 32.484147 | 1717346.24 | 444681.06 | 386.38 | 385.73 |
| 65 | 15.533110 | 32.484100 | 1717358.42 | 444676.05 | 387.34 | 386.69 |
| 66 | 15.533143 | 32.484093 | 1717362.07 | 444675.31 | 387.34 | 386.69 |
| 67 | 15.533179 | 32.484093 | 1717366.05 | 444675.32 | 387.34 | 386.69 |
| 68 | 15.533212 | 32.484098 | 1717369.70 | 444675.87 | 387.33 | 386.68 |
| 69 | 15.533248 | 32.484109 | 1717373.68 | 444677.05 | 387.33 | 386.68 |
| 70 | 15.533443 | 32.484154 | 1717395.24 | 444681.93 | 386.45 | 385.80 |
| 71 | 15.533554 | 32.484192 | 1717407.51 | 444686.04 | 386.46 | 385.81 |

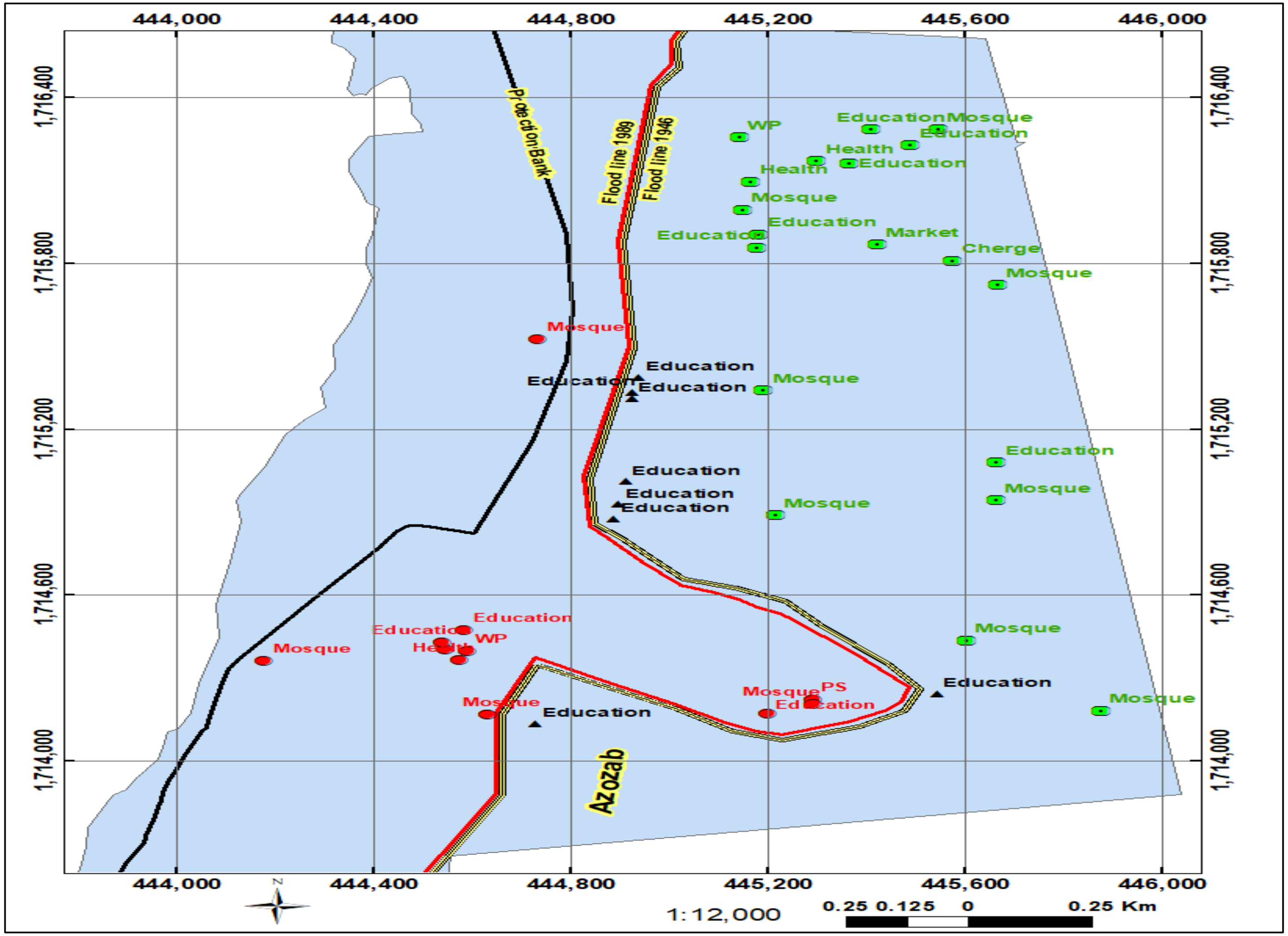


**Figure (4-12): Flood affected services in the study area**

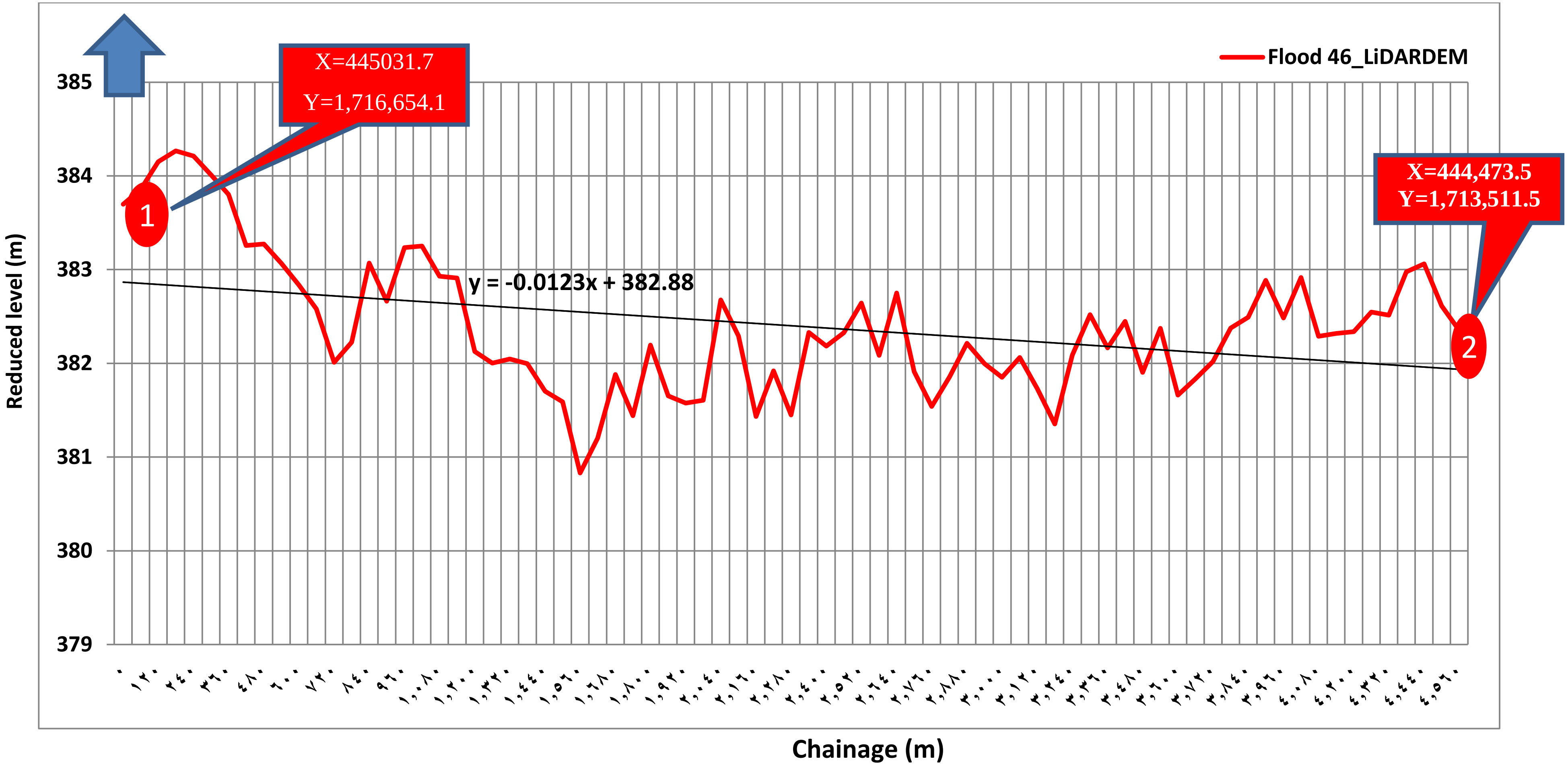


**Figure (4-13): Graph of flood 1946**

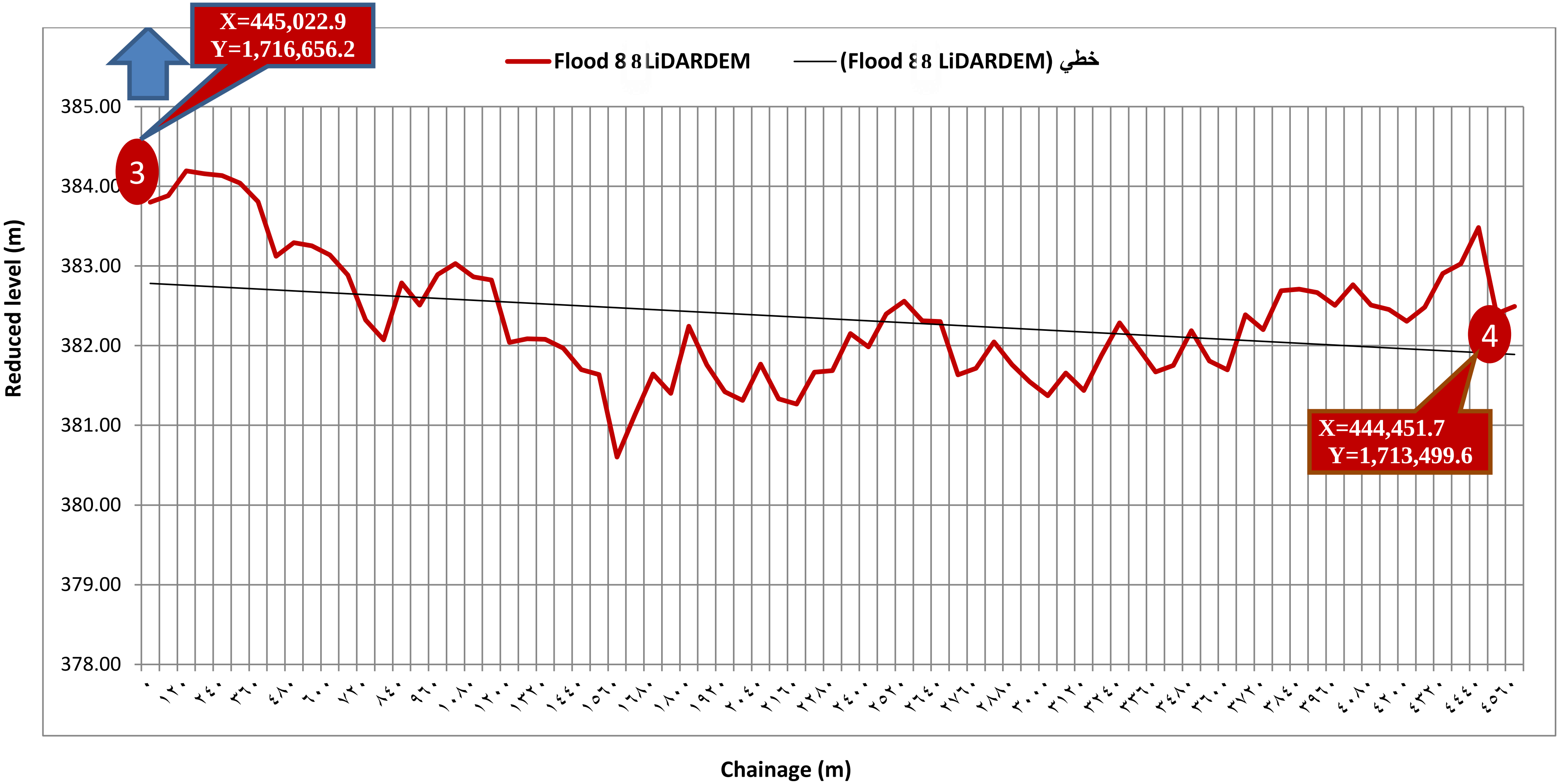


**Figure (4-14): Graph of flood 1988 (LiDAR DEM)**

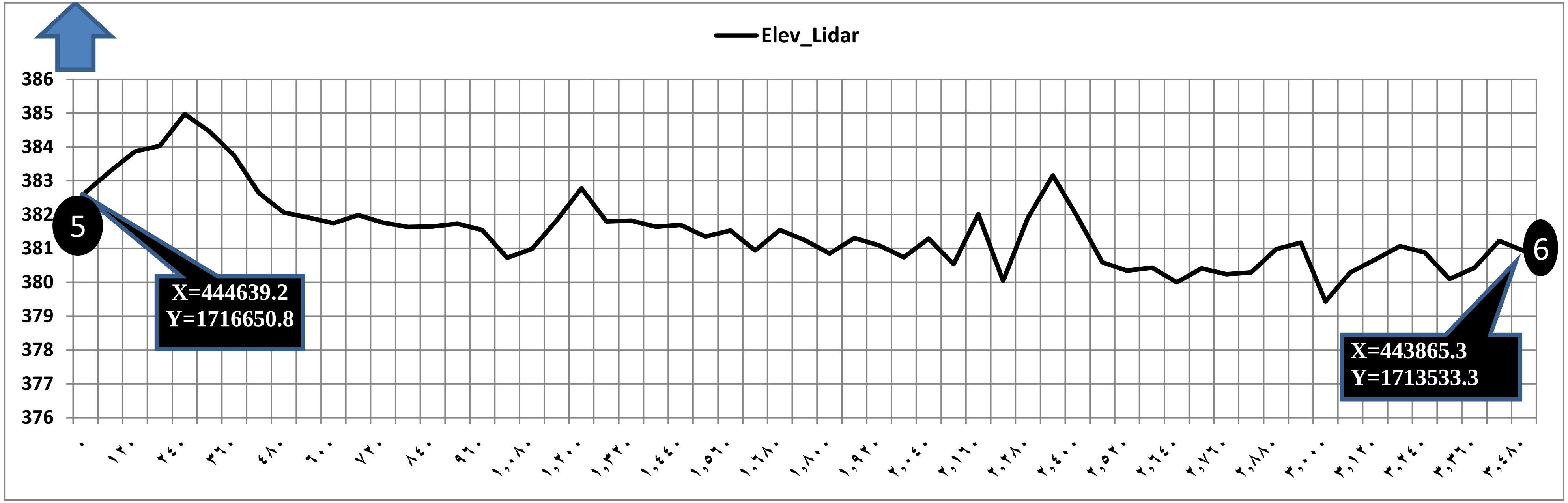


**Figure (4-15): Graph of protection bank (LiDAR DEM)**

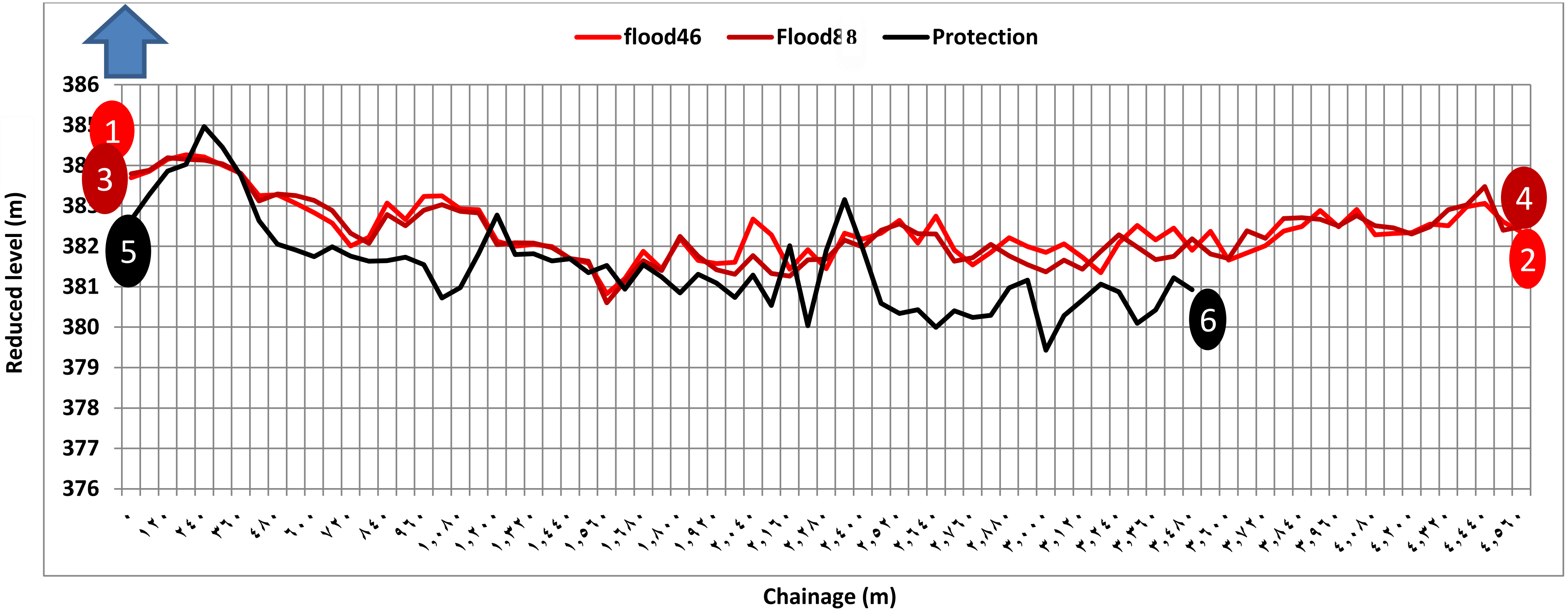


**Figure (4-19): Reduced level of points along the 3 lines from LiDAR DEM**

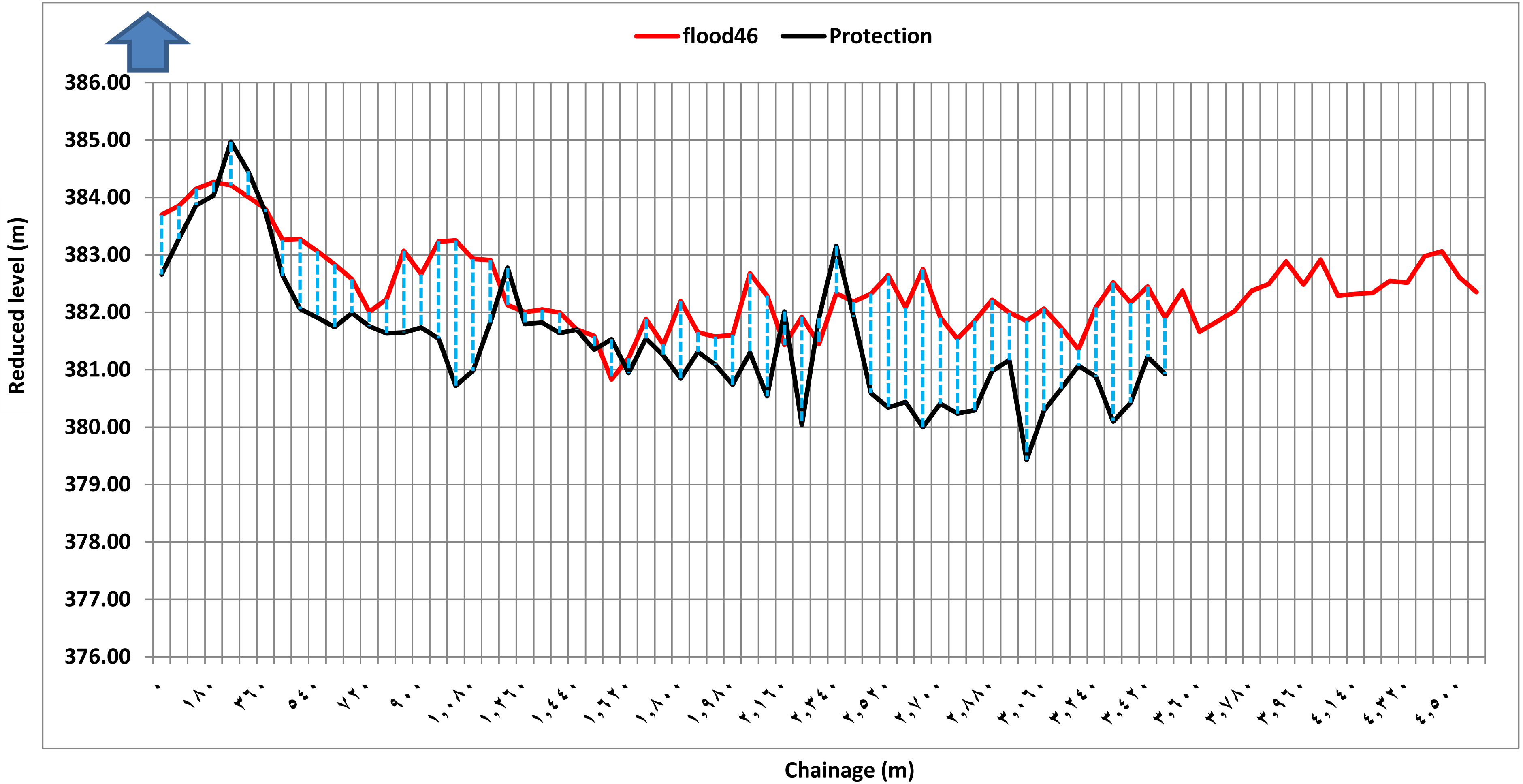


**Figure (4-24): Protection bank height increments (reference is 1946 flood line)**